Geologic Map of the Elephant Butte 7.5-Minute Quadrangle, Sierra County, New Mexico

By

Daniel J. Koning[1], Richard P. Lozinsky[2], and Bruce E. Cox[3]

[1] New Mexico Bureau of Geology and Mineral Resources, 801 Leroy Place, Socorro, NM 87801
[2]Emeritus, Fullerton College, 321 E. Chapman Avenue, Fullerton, CA 92832
[3]737 S. 5th St. W., Missoula, MT 59801

April 2026

New Mexico Bureau of Geology and Mineral Resources
Geologic Map GM 84

Scale 1:24,000

https://doi.org/10.58799/GM-84

This geologic map was funded in part by the USGS National Cooperative Geologic Mapping Program under STATEMAP award number G23AC00578, 2023. Additional support was made possible by the 2023 and 2024 Technology Enhancement Fund provided by the New Mexico Higher Education Department. Funding is administered by the New Mexico Bureau of Geology and Mineral Resources (Dr. J. Michael Timmons, *Director and State Geologist*; Dr. Matthew J. Zimmerer, *Associate Director of Mapping and Hazards*).

New Mexico Bureau of Geology and Mineral Resources
801 Leroy Place, Socorro, New Mexico, 87801-4796

Photograph of the namesake of the quadrangle: a butte resembling an elephant head (which would be looking left in this north-facing view). The butte is only 0.8 km northeast of the cement gravity dam holding Elephant Butte Lake. Geologically, the butte is primarily a basaltic lava plug that upwelled into a throat of a volcano. The upper edifice (cone) of this volcano is now eroded away.

EXECUTIVE SUMMARY

The Elephant Butte 7.5-minute quadrangle encompasses the southern part of Elephant Butte Lake, the town of Elephant Butte, and the eastern part of the town of Truth or Consequences. South of the lake, the Rio Grande flows southwestward for 3 km through a gorge cut into Cretaceous sandstones, which widens into a valley eroded in Santa Fe Group deposits near Truth or Consequences. The arid climate and middle to late Quaternary downcutting of the Rio Grande have resulted in good outcrops throughout the quadrangle, facilitating field-based studies of late Paleozoic, Cretaceous, and late Neogene to Quaternary strata. The Cretaceous section and late Neogene to Quaternary stratigraphy, in particular, are used to interpret a fascinating and relatively complete geologic history for 100 to 60 Ma and 7 Ma to the present.

Paleozoic sedimentary strata record a general progression from dominantly shallow marine (Ordovician, Pennsylvanian) to arid coastal plain (early Permian) and then back to marine conditions around 290 Ma. The earliest strata exposed on the quadrangle are dolomites of the Montoya Formation (Ordovician), which underlie a couple of low knolls in the eastern part of Truth or Consequences. A well-exposed, complete sequence of middle Pennsylvanian to middle Permian strata is preserved on the northern end of the Caballo Mountains. The lowest Pennsylvanian strata include the Gray Mesa and Bar B Formations, differentiated by the Gray Mesa Formation having much more chert-bearing limestone beds. The Bar B Formation contains grayish shales and subordinate limestone, with reddish, fine-grained beds, and sparse conglomerates found near the top. Permian strata include the Abo and overlying Yeso Formations. The Abo Formation was deposited in a fluvial environment on a coastal plain. It has common reddish-brown and brick-red, chunky-textured mudstones interspersed with siltstones and very fine- to fine-grained sandstones, the latter locally filling channel forms. The lower Yeso Group includes the orangish Arroyo Alamillo Formation and the overlying Los Vallos Formation (*sensu* Lucas and Krainer, 2012). Both consist mainly of very fine- to fine-grained sandstones and siltstones, with the Torres Member also containing gypsum beds. The San Andres Formation consists of around 30 m of limestone overlain by intertonguing fine-grained limestone and carbonates.

Cretaceous strata document the arrival and retreat of the Western Interior Seaway between 95 and 89 Ma, followed by a prolonged record of terrestrial deposition that extends into the earliest Paleocene. In the lowest unit, the Dakota Sandstone, mudstones and sandstones (fluvial and near the top possible lagoon or tidal flat) grade upsection into bioturbated, nearshore sandstones. The overlying, lower tongue of the Mancos Shale (the Tokay Tongue of Hook and Cobban, 2015), including the Bridge Creek Limestone Beds, was deposited when the seaway was at its deepest. Progradation of the shoreline resulted in the deposition of the Tres Hermanos Formation, and a brief return of the seaway at 90 Ma deposited the 50-m-thick D-Cross Tongue of the Mancos Shale. Nearshore sandstones, interbedded with offshore marine shales, increase upsection so that they predominate in the Gallup Sandstone.

Terrigenous sediment overlying the aforementioned nearshore strata totals around 1.5 km in thickness. We follow Lucas et al. (2019) in applying the name Flying Eagle Canyon Formation to 300 m of an olive-colored interval of predominately fluvial mudstones and channel-fill sandstones, with coastal swamp sediment occurring near the base. This succession coarsens upward to the Ash Canyon Formation (approximately 200 m thick), which contains a subequal to dominant proportion of sandstones and local petrified wood. The Ash Canyon Formation is overlain by the McRae Group, which was deposited in an actively subsiding basin during Laramide tectonism. The oldest (lowest) formation of the McRae Group is light-grayish to light-greenish sandstones and siltstone-rich, fine-grained deposits of the José Creek Formation. Conglomerates in the José Creek Formation contain predominately andesitic clasts, and these coarsen and become more abundant to the southwest. In contrast, the Hall Lake Formation is mostly composed of reddish-brown mudstones with sparse sandstone channel fills. In the northeast corner of

the quadrangle, the recently recognized Double Canyon Formation (Lucas et al., 2019) consists of a higher proportion of sandstone and pebbly sandstone (compared to the Hall Lake Formation), where the pebbles consist of chert and granite clasts.

Except for dikes, strata are missing for the time period between about 60 Ma and about 20 Ma. Strata younger than 20 Ma were deposited in the Engle basin, created by the eastward tilting of a half graben bounded on its east side by the linked Walnut Canyon and Hot Springs faults. The Engle basin is one of many basins of the Rio Grande rift, whose subsidence during rifting allowed for the accumulation of clastic deposits of the Santa Fe Group. The lower Santa Fe Group is assigned to the Rincon Valley Formation, which represents deposition in a closed basin. The lowest part of the Rincon Valley Formation is not exposed, but associated well data indicate it consists of approximately 100 m of reddish, interbedded sequence of sandstones and reddish-brown mudstones. This sequence is overlain by 220 m of reddish-brown, claystone-dominated strata that probably represent a playa-lacustrine lake in the Engle basin. The uppermost strata of this playa lake grade upward into quartz-rich, axial-fluvial sediment of the Palomas Formation. The axial-fluvial sediment of the Palomas Formation has a lower, coarser-grained interval (approximately 80 m thick) that intertongues with a relatively extensive, coarse-grained alluvial fan associated with a paleo Mescal Canyon. This fan shrank, and the axial-fluvial system widened by the middle Pliocene. In the early Pleistocene (after 2.6–2.5 Ma), western piedmont deposits (sourced from the Sierra Cuchillo and the Black Mountains) prograded eastward, shifting the axial-fluvial system eastward. Profuse basaltic volcanism occurred near the Pliocene–Pleistocene transition. Basaltic magmas upwelling through saturated, sandy axial-fluvial sediment caused groundwater to explode into steam, resulting in numerous maar deposits. Two basaltic intrusions associated with the Rattlesnake Island maar returned a weighted mean age of 2.495±0.016 Ma (2-sigma) and an MSWD = 1.85.

Noteworthy structures on the Elephant Butte quadrangle include faults and folds. The faults are primarily normal and can be categorized into two sets: (1) north-northeast-trending faults with traces generally longer than 1.5 km and (2) randomly trending faults with traces generally shorter than 1.5 km and throws less than 30 m. The most prominent structure is the Hot Springs fault, which trends N20–30°E, dips about 70–80° to the west, and extends across the entire quadrangle. This fault separates Cretaceous and older bedrock from the Santa Fe Group. Although it exhibited normal, west-side-down displacement during rifting (at least 500 m), fault plane kinematic features and stratigraphic relations indicate 0.5 to possibly 26 km of earlier, right-lateral offset (Lozinsky, 1986; Harrison and Cather, 2004), during the Laramide orogeny. We interpret that the Hot Springs fault acted as a right-oblique reverse fault during the Laramide and prefer the interpretation of <5 km of right-lateral slip. Uplift of its western side induced erosion of the majority of the Cretaceous section there. Subsequent movement along the Hot Springs fault deformed Rincon Valley and lower Palomas Formation strata during the late Miocene–early Pliocene. At Rattlesnake Island, the aforementioned 2.5 Ma maar deposits are not offset by the fault, so the fault has been inactive in the quadrangle since 2.5 Ma.

Downcutting of the Rio Grande and its tributaries commenced shortly after the formation of the Cuchillo geomorphic surface, which is thought to be around 800 ka (Mack et al., 1998b; McCraw and Love, 2012). Due in large part to the eastward progradation of the western piedmont and axial-fluvial system, the Rio Grande onlapped eastward onto planated bedrock on the footwall of the Hot Springs fault. When it incised, it more or less kept its position and incised into bedrock, forming the gorge that now hosts the Elephant Butte dam. The Rio Grande and its tributaries progressively incised through bedrock and the Santa Fe Group during the middle and late Pleistocene. However, the fluvial system periodically aggraded or experienced sufficient base-level stability to form a suite of five general terrace levels.

INTRODUCTION

Building on earlier work by Lozinsky (1986), this report summarizes the stratigraphy and structure of the Elephant Butte 7.5-minute geologic map. Special emphasis is placed on the Santa Fe Group and maar deposits, a focus of most of the field work for this effort. We review the geologic history of the quadrangle, summarize mineral resources, and comment on hydrogeologic features relevant to the town of Elephant Butte. For more detail on the stratigraphy of the upper Paleozoic and Cretaceous bedrock, refer to Seager and Mack (2003), Lucas and Krainer (2012), and Lucas et al. (2012a, 2012c, 2019). Note that Truth or Consequences is commonly abbreviated as TorC.

This report generally uses metric units. To convert meters to feet, multiply by 3.281. To convert kilometers to miles, divide by 1.61. The conversion of Celsius to Fahrenheit uses this formula: (Celsius x 9/5) + 32. An exception is well depths, which are listed in feet on the original logs, and we retain imperial units (feet) to facilitate comparison with wireline and cuttings logs.

Geography and topography

The Elephant Butte 7.5-minute quadrangle lies in the southern Engle basin in south-central New Mexico (Fig. 1). The Engle basin is flanked by the San Mateo Mountains to the northwest, the Fra Cristobal Mountains to the east that continue southward as low hills, the Cutter sag to the southeast, the Caballo Mountains to the south, and the Mud Springs Mountains to the southwest (Fig. 1). The west-down Mud Springs fault separates the Palomas basin from the Engle basin. Both basins are east-tilted half grabens whose master faults correspond to the Mud Springs fault (Palomas basin) and the Walnut Springs and Hot Springs faults (Engle basin).

The quadrangle encompasses the southern part of Elephant Butte Lake, the town of Elephant Butte, and the eastern part of the town of Truth or Consequences (Fig. 2). The cement dam holding Elephant Butte Lake was constructed in 1916 in a gorge carved in Cretaceous sandstones. It is actually a cement gravity dam, where blocks of sandstone are encased in cement. South of the lake, the Rio Grande flows southwestward for 3 km through this gorge, which eventually widens into a valley near Truth or Consequences (population 6,052; U.S. Census Bureau, 2022). The town of Elephant Butte (population 1,447; U.S. Census Bureau, 2022) is located 4.5 km west of the dam. The Cutter sag region east of the lake and the Rio Grande is characterized by a few basalt-capped mesas (elevation 1465–1490 m; 4,800–4,900 ft) that stand over badlands developed in Cretaceous sandstones and mudstones. These badlands are characterized by rugged slopes and shallow canyons with up to 60 m of local relief. To the west of the lake and river, erosion of Santa Fe Group strata has formed a badland landscape with similar local relief. Near the western quadrangle boundary, extensive gravels underlie broad mesa tops of the Cuchillo surface (McCraw and Love, 2012) that become more continuous to the west and northwest.

Climate and vegetation

An arid climate and a Chihuahuan Desert scrub vegetation community typify the study area. Annual precipitation is around 25 cm, most of which comes in June through October via summer, monsoonal thunderstorms (Climate-Data.org, 2025). Average daily temperatures range from 0° to 16°C from December to February and 32° to 34°C from June to August. Sparse vegetation is dominated by creosote brush, mesquite, and variable yucca. Locally on the west side of the lake, north-facing slopes and well-drained soils allow sparse juniper trees to grow as low as 1,340 m (4,400 ft) elevation.

PREVIOUS WORK

Two noteworthy earlier investigations include Kelley and Silver (1952) and Lozinsky (1986). The former investigated the stratigraphy and structure of the Caballo Mountains and the Truth or Consequences area. Lozinsky (1986) published a geologic map that included the entire Elephant Butte quadrangle as well as the eastern part of the Cuchillo 7.5-minute quadrangle and about 1.5 km of the southern portion of the Black Bluffs 7.5-minute quadrangle to the north. A thorough review of the geology of the quadrangle, with particular emphasis placed on the late Cenozoic history, accompanied the geologic mapping of Lozinksy (1986).

Lozinsky published several other papers relevant to the Elephant Butte area. These include a formal definition of the Palomas Formation(Lozinsky and Hawley, 1986) and the construction of a cross-section across the Jornada del Muerto, Cutter sag, Engle basin, and northern Palomas basin (Lozinsky, 1987). Dinosaur fossil discoveries in the McRae Group are described in Lozinsky et al. (1984), Wolburg et al., (1986), and Gillette et al. (1986).

A wide variety of other geologic investigations were conducted prior to Lozinsky (1986). Lee (1907a) described the geology of the area and produced a very generalized geologic map. Bushnell (1953) focused on the stratigraphy of the post-Mancos, terrigenous rocks. Three student theses—Doyle (1951), Melvin (1963), and Mason (1976)—describe and map Paleozoic and Cretaceous units in the northern Caballo Mountains. Thompson (1961) investigated the geology of the southern Fra Cristobal Mountains. Several articles about this area are contained in the sixth field conference guidebook of the New Mexico Geological Society (Fitzsimmons, 1955). Cenozoic sedimentary deposits between Truth or Consequences and the Mud Springs Mountains were mapped by Wells and Granzow (1980). Other reports relevant to the geology of the Elephant Butte area include Lee (1905, 1907b), Darton (1922), Harley (1934), and Bryan (1938).

Publications since Lozinsky (1986) include detailed geologic mapping and stratigraphic investigations, work regarding the structure of the Hot Springs fault and Cutter sag, and studies of plant fossils in the Cretaceous strata. Detailed geologic maps of the quadrangles to the east (Engle) and south (Palomas Gap) of the Elephant Butte 7.5-minute quadrangle were produced by Mack and Seager (1993) and Seager (2015), respectively. Geologic maps of the quadrangles west (Cuchillo) and north (Black Bluffs) of the Elephant Butte quadrangle were produced by Koning et al. (2018b) and Cikoski et al. (2017), respectively. Mapping and stratigraphic work by Foster (2009) and Mack et al. (2012) allow refinement of the stratigraphic architecture of the Palomas Formation in the western Truth or Consequences area. The lower part of the Cretaceous section in Mescal Canyon is detailed in Hook et al. (2012). Seager and Mack (2003) provide a thorough summary of the stratigraphy, structure, and geologic history of the Caballo Mountains. Stratigraphic refinement and description of the Pennsylvanian and Permian strata of the Caballo Mountains are found in Lucas et al. (2012a, 2012b) and Lucas and Krainer (2012). Lucas et al. (2019) provide a report on the Cretaceous stratigraphy in central Sierra County, in which they propose revisions to the stratigraphic nomenclature (see below). The role the Cutter sag plays in relaying extensional strain is interpreted by Mack and Seager (1995). Right-strike-slip faulting on the Hot Springs fault is detailed by Harrison and Cather (2004). Estrada-Ruiz et al. (2012a, 2012b, 2018) describe fossil plants in fluvial Cretaceous strata.

Geochronologic investigations have refined our understanding of the geologic history of the area. Dating of basalt flows correlative to those in the southeastern part of the quadrangle was conducted by Bachman and Mehnert (1978). Amato et al. (2012) dated a flow on the eastern margin of this quadrangle and investigated the age of unique xenoliths in the lava. Species-level identification of paleofauna west of Elephant Butte Lake provides age control for the Santa Fe Group (Lucas and Oakes, 1986; Morgan and Lucas, 2012). A tephra bed at about the same stratigraphic level as this fauna correlates to a 3.1 Ma pumice bed at Hatch Siphon (Mack et al., 2009). Amato et al. (2017) used U-Pb dating to determine an age of approximately 75 Ma for the lower José Creek Formation (lowest unit of the McRae Group), and ongoing work has improved age control for the upper McRae Group (Schantz et al., 2024).

STRATIGRAPHY

Stratigraphic units fall into four general groupings. The oldest is Paleozoic strata, which are mainly Upper Pennsylvanian through Permian except for a few outcrops of the Ordovician Montoya Formation (Fig. 3). The second-oldest is a relatively complete sequence of marine and terrestrial, clastic rocks extending from the Upper Cretaceous rocks into the Paleocene. The third group is the Neogene to Quaternary strata of the Santa Fe Group, including maar eruptive deposits and flows. Post-Santa Fe Group (post-early Pleistocene) terrace deposits and valley fills make up the youngest group. Detailed descriptions of the map units are provided in Appendix 1.

Ordovician

The oldest stratigraphic unit exposed on the Elephant Butte quadrangle underlies two knolls in the eastern Truth or Consequences area. It consists of a thinly bedded to massive, gray dolomite with scattered brown chert nodules and lenses. This rock was correlated to the Montoya Group by Lozinsky (1986), but we downgrade it to a formation-rank status to be consistent with usage by Seager and Mack (2003) and Lucas et al. (2012c).

Pennsylvanian

Pennsylvanian strata are well exposed and located on the western front of the north end of the Caballo Mountains. Lower Pennsylvanian strata, including the Red House Formation, are cut out by the Hot Springs fault. The reader is referred to detailed descriptions and interpretations by Seager and Mack (2003) and Seager (2015), which is the source of these descriptions. Figure 3 illustrates the lithology and thicknesses of the stratigraphic units described below.

Gray Mesa Formation

The lowest Pennsylvanian unit, the Red House Formation, is not exposed on the quadrangle. The overlying Gray Mesa Formation lies immediately east of the Hot Springs fault and is 190 m thick. This same interval has previously been called the Nakaye Formation, but Lucas et al. (2012a, 2012c) extends the Gray Mesa into this area and the USGS Geolexicon notes that usage of the Nakaye has been replaced by the Gray Mesa Formation. The Gray Mesa Formation is a 190-m-thick succession dominated by ledge-forming, very thick-bedded, cherty limestones (1–15 m thick). The limestones are gray (weathering gray to tan), bioturbated, and fossiliferous and include packstones and grainstones. Covered, slope-forming intervals correspond to thin-bedded limestones and reddish, green, or gray shale. The Gray Mesa Formation was deposited in an open-marine environment below the normal wave base (Seager and Mack, 2003) during the first half of the Desmoinesian (Lucas et al., 2012a).

Bar B Formation

The highest Pennsylvanian unit is the Bar B Formation, which is around 120 m thick and distinguished from the Gray Mesa Formation by its lower proportion of cherty limestone and higher proportion of shales. The Bar B Formation is composed mainly of shale with subordinate limestone and dolomite. The shale is gray to purplish-gray and a slope former. Limestone intervals are 1–5 m thick and micritic and range from gray to tan to orange. The upper 50 m of the formation consists of interbedded purplish and red siltstone, shale, limestone, and limestone-pebble conglomerate. Deposition of the Bar B Formation occurred in a marine environment that was somewhat more restricted than that of the Nakaye Formation (Seager and Mack, 2003). Its age ranges from Desmoinesian to Missourian, although some locales preserve strata of Virgilian age (Verville et al., 1986; Singleton, 1990; Lawton et al., 2002). The occurrence of limestone-clast pebble conglomerates and inferred unconformities in the upper 50 m of the unit suggest that tectonism occurred in the region and facilitated the erosion of nearby uplifts between 310 and 300 Ma (Singleton, 1990; Lawton et al., 2002). Indeed, Lucas et al. (2012a) also invoke Pennsylvanian tectonism to explain differences in thickness and lithology between Pennsylvanian stratigraphic sections in the Mud Springs, Fra Cristobal, and Caballo Mountains, which are particularly evident in the Bar B Formation.

Permian

Abo Formation

The distinctive Abo Formation is reddish-brown to brick-red and composed of an approximately 150-m-thick succession of mudstone, shale, siltstone and fine-grained sandstone (Fig. 3; Seager and Mack, 2003; Lucas et al., 2012b). The dominant lithologic type is mudstone followed by sandstone (71–80% versus 19–27% per Lucas et al., 2012b). Minor lithologies include shale, siltstone, and sparser limestone interbeds. The mudstone has a blocky texture and commonly displays slickensides; in some mudstone beds, calcic nodules are locally observed. Siltstones and very fine-grained sandstones are commonly in thin (<1 m) beds and exhibit ripple cross laminae (including distinctive climbing ripples) or horizontal-planar laminae. The upper parts of siltstone and very fine-grained sandstone beds may have desiccation cracks or bioturbation features. Very fine- to fine-grained sandstones occupy paleochannels or are in sheet forms; these locally exhibit small-scale trough cross-beds. In the lower part of the unit are sparse, thin (<0.5 m) beds of intraformational conglomerate that fill broad, shallow paleochannels. These paleochannels are relatively devoid of sedimentary structures or may exhibit small-scale trough cross-beds; intraformational clasts consist of shale, siltstone, and carbonate.

Architectural elements associated with specific depositional environments include (1) floodplain deposits (mudstones with calcic paleosols); (2) broad, laterally accreting, sinuous channels where siltstone to very fine-grained sandstone sheets were deposited, locally on top of lags of rip-up-clast conglomerate; (3) sheets of siltstone and very fine-grained sandstone deposited by unchannelized flow, including crevasse splays; and (4) ribbon channel forms that infilled vertically (Seager and Mack, 2003; Lucas et al., 2012c). At Palomas Gap, estuarine facies were interpreted by Lucas et al. (2012a).

Yeso Group

We agree with Lucas et al. (2005) that the lithologic distinctness of two units within the Yeso, the Arrroyo de Alamillo and the Los Vallos, allow them to be formation-rank units and therefore the Yeso can be raised to a Group status. The 180- to 210-m-thick Yeso Group is differentiated from the underlying Abo Formation by its color (more orange and containing some greenish/pastel intervals) and its slightly more ledgy (step-case) outcrop character (Fig. 3). Descriptions for the Yeso Group are from Seager and Mack (2003) and Lucas et al. (2012a). Although mapped as an undivided unit on this quadrangle, within the Yeso Group there is a lower and upper unit: the lower unit is the Arroyo de Alamillo Formation (*sensu* Lucas et al., 2005, and Lucas and Krainer, 2012) the upper unit is theLos Vallos Formation. The Los Vallos Formation on this quadrangle primarily consists of the Torres Member; the medial, gypsum-dominated Cañas Member is not too thin and/or concealed (by colluvium) to be a distinctive unit. The Arroyo de Alamillo Formation primarily consists of orange, very fine- to fine-grained, well-sorted sandstone. There are subordinate beds of medium-grained sandstone and siltstone (Seager and Mack, 2003). The sandstone exhibits millimeter- to centimeter-scale, horizontal or low-angle lamination. Shale and mudstone are sparse and restricted to the top of the member. Several distinct, white to light-green, fine-grained sandstone beds exhibit symmetrical ripple marks, salt casts, and burrows (Seager and Mack, 2003).

In the overlying Los Vallos Formation, there are three ledge-forming limestone-dolomite units, each about 10–15 m thick, within a sequence of interbedded, massive or thinly bedded gypsum, thin-bedded limestone, and red to yellow sandstone and siltstone (Seager, 2015). The sandstone and siltstone are similar to that seen in the Arroyo de Alamillo Formation. Flowage of the gypsum resulted in contortion of bedding and thinning and thickening of the Torres Member. The upper contact of the Los Vallos Formation appears to be conformable with the overlying San Andres Formation according to Seager and Mack (2003), but Lucas and Krainer (2012) interpret an unconformity.

The Yeso Group was deposited in an arid setting in the interface between coastal plain and shallow marine (Mack and Suguio, 1991; Mack and Dinterman, 2002; Seager and Mack, 2003). The Arroyo de Alamillo Formation is interpreted to represent deposition primarily as an eolian sand sheet. Strata of the Los Vallos Formation were deposited in upward-shallowing cycles in settings ranging from shallow-marine, lagoonal or tidal flat, and eolian. Limestones in the Los Vallos Formation represent shallow-marine conditions, and dolomites are probably associated with tidal-flats or lagoons.

San Andres Formation

We apply the name San Andres Formation (*sensu* Kelley and Silver, 1952) for the two informal lithologic units recognized by Seager and Mack (2003): a lower limestone member and an upper sandstone-limestone member. We use descriptive data of Seager and Mack (2003) in the following. The lower limestone is 30 m thick and forms a topographic hogback. It consists of a medium-bedded, fossiliferous, dark-gray to black, packstone limestone with only a few chert nodules (Seager and Mack, 2003). There are minor, thin-bedded intervals of dark-gray shale as well as lenticular sandstones. Fossils include brachiopods, gastropods, bryozoans, corals, and pelecypods. The overlying upper sandstone-limestone interval consists of around 200 m of intercalated carbonates and sandstones, with local beds of gypsum. The carbonates consist of medium-bedded, fossiliferous limestone and dolomite. The sandstones are yellow to red, very fine- to fine-grained, and similar to those found in the lower Yeso Formation. The 30-m-thick lower unit is interpreted to have been deposited in open-marine conditions (Mack and Dinterman, 2002), while the middle-upper San Andres Formation represents deposition in alternating marine and coastal (e.g., tidal flats, lagoons, sabkha, or eolian) environments (Seager and Mack, 2003).

It should be noted that, for the upper Permian, we elected to follow the stratigraphic concepts of Kelley and Silver (1952) in assigning the San Andres Formation to the stratigraphic interval called the upper

Yeso Formation by Seager and Mack (2003) and Seager (2015). Seager and Mack (2003) base their correlations on maintaining thickness consistency of the Yeso Group here compared to other locales, and also on the similarities of the reddish sandstones in the upper San Andres Formation with those in the underlying Yeso Formation. Such a scheme would require complete removal of the San Andres Formation in the map area. However, about 160 m of the San Andres Formation is confidently identified in the southern Fra Cristobal Mountains, only 20 km away (Nelson et al., 2012). Having 160 m of erosion of the San Andres Formation over only 20 km seems unrealistic, and lateral facies changes (to explain the sandstone tongues in the middle to upper San Andres Formation) seems a better alternative.

Upper Cretaceous

Upper Cretaceous strata are the most widespread stratigraphic group in the Elephant Butte quadrangle. Because they are well exposed here and to the northeast, these strata have received much attention over the last century (e.g., Lee, 1905; Bushnell, 1953; Melvin, 1963; Lozinsky, 1986; Mack and Seager, 1993; Seager and Mack, 2003; Hook et al., 2012). The Upper Cretaceous can be divided into a lower and upper succession. The lower succession (340 m thick) includes the basal Dakota Sandstone that is overlain by dominantly marine strata of the Western Interior Seaway. These marine strata include the Tokay Tongue of the lower Mancos Shale, the base and top of the Tres Hermanos Formation, the D-Cross Tongue of the Mancos Shale, and the Gallup Sandstone. Note that there is a tongue of terrestrial sediment within this marine package called the Carthage Member of the Tres Hermanos Formation (*sensu* Seager and Mack, 2003; Hook et al., 2012). The thicker upper succession of Cretaceous strata represents fluvial deposition on a coastal plain (Flying Eagle Canyon and Ash Canyon Formations), followed by deposition of the McRae Group in the Laramide-age Love Ranch basin. The McRae Group includes the following units: José Creek, Hall Lake, and Double Canyon Formations. Except where noted, the descriptions below represent a synthesis of those in Seager and Mack (2003) and Lucas et al. (2019).

Lower part of Upper Cretaceous (dominantly marine strata)

Dakota Sandstone

The lowest Cretaceous unit is the Dakota Sandstone (Seager and Mack, 2003; Lucas et al., 2019), whose basal contact corresponds to a regional unconformity (Cather, 2012). It consists of a basal and upper sandstone separated by a 15–27 m thick, medial fine-grained unit. The lower sandstone is 6–8 m thick and trough cross-bedded to horizontally laminated. There are some pebbly conglomerate lenses. Common oxidized fossil plant debris is present. We note that this basal contact was difficult to map in many places because the predominately medium-grained sandstone of the basal Dakota Sandstone was similar to sandstone assigned to the underlying San Andres Formation by previous workers (e.g., Lozinsky, 1986; Seager, 2015). The medial unit is dominated by sandy shale and gray mudstone. It has relatively thin sandstone beds or lenses (mostly <0.2 m, with some up to 1 m) that exhibit cross-bedding (including ripple marks) or are bioturbated; scattered carbonaceous debris is observed. The upper sandstone is about 5 m thick and trough cross-bedded or horizontal-planar laminated. It contains burrows of *Ophiomorpha* and *Thalassinoides.* Capping the upper sandstone is a pebbly transgressive lag related to the advance of the Western Interior Seaway.

The Dakota Sandstone represents a mix of fluvial, lagoonal to tidal flat, and deltaic environments (Seager and Mack, 2003). The lower sandstone corresponds to a fluvial channel fill, and the medial, fine-grained unit contains features suggestive of floodplains, lagoons, or tidal flats (Mack et al., 1998a).

Ophiomorpha burrows indicate that the upper sandstone is marine, with the specific depositional environment interpreted as a flood-tidal delta (Bauer, 1989; Mack et al., 1998a).

Tokay Tongue of the Mancos Shale

A 130–160 m thick interval dominated by shale overlies the Dakota Sandstone. We follow Hook and Cobban (2015) in assigning this to the Tokay Tongue of the Mancos Shale. Strata are composed of dark-gray, calcareous shale and siltstone with some sandstone and thin, intercalated limestone in 3–30 cm thick beds (Fig. 4). Shale weathers greenish gray or olive gray and is silt-free to slightly silty in the lower and medial part of the unit. Limestone beds are most common in an approximately 10 m interval located 60 m above the base of the Mancos Shale and assigned to the Bridge Creek Limestone by Hook et al. (2012). However, Lucas et al. (2019) interpret that the limestone-rich interval occurs much lower (12–25 m), and they call it the Greenhorn Member of the Mancos Shale. We agree that the limestone is concentrated 60 m above the base. In the lower 60 m, there are 64 bentonites. Silty shale and siltstone increase upsection above the medial limestone interval. The sandstones in the upper part are commonly hummocky cross-stratified or horizontally laminated; sandstone occurs mainly as thin beds (<0.2 m thick) and less commonly as 0.5–3 m thick beds. These strata were deposited in Molenaar's (1983) T1 transgression and the early part of the R1 regression of the Western Interior Seaway (Hook et al., 2012; Mack et al., 2015).

Tres Hermanos Formation

The Tres Hermanos Formation is assigned to a relatively resistant, 70–75 m thick interval (Fig. 5) subdivided into a basal sandstone (Atarque Member), medial mudstone-dominated interval (Carthage Member), and upper sandstone (Fite Ranch Member). Descriptions of this formation at Mescal Canyon are presented in Mack et al. (1998a), Seager and Mack (2003), Hook et al. (2012), Mack et al. (2015), and Lucas et al. (2019). We employ the stratigraphic terminology and thicknesses of Hook et al. (2012), Mack et al. (2015), and Seager (2015). The Atarque Member is 13–14 m of sandstone and minor shale. The sandstone is trough cross-bedded, horizontally laminated, or massive (Seager and Mack, 2003; Lucas et al., 2019). The sandstone is commonly fine- to medium-grained, subangular to subrounded, well-sorted, and composed of quartz and minor potassium feldspar, plagioclase, and chert; there are rare lithic grains composed of fine-grained volcanic and metamorphic fragments and opaque grains (Lucas et al., 2019). The Atarque Member is very calcareous and weathers to large, rounded, concretionary forms. The Carthage Member is 50 m thick and composed of olive-gray, non-fissile mudstone and siltstone with minor thin (<1 m thick) fine-grained sandstone beds (Seager and Mack, 2003; Lucas et al., 2019). Some mudstone layers are carbonaceous. There are also some ledge-forming, fine- to medium-grained sandstone tongues up to 3 m thick; these are are trough-cross-bedded, planar cross-bedded, ripple-laminated, or massive to bioturbated. The Fite Ranch Member consists of 3–5 m of fine-grained sandstone that is in thick beds that are massive or display hummocky cross-stratification; the upper 0.5 m consists of a calcareous, granular, medium-grained sandstone with shell fragments and shark teeth (Seager and Mack, 2003). The upper sandstone is underlain by offshore marine shale, locally with boulder-sized calcareous concretions and ammonites, and weathers to form a hummocky outcrop (Seager and Mack, 2003; this effort).

Workers agree that the Tres Hermanos Formation was deposited in the upper part of the R1 regression and the lower part of the T2 transgression of Molenaar (1983). The Atarque Member represents nearshore deposition of a regressive shoreline, characterized by barrier islands, at the end of R1, and the Fite Ranch Member represents the transgressive nearshore facies at the beginning of T2.

Seager and Mack (2003) interpret that a brown, granular sandstone at the top of the Fite Ranch Sandstone as a transgressive lag. The medial Carthage member represents fluvial deposition and, near its base, lagoonal and swamp environments (Lucas et al., 2019; Seager and Mack, 2003). Differences of specific lithofacies interpretations exist between Seager and Mack (2003) and Lucas et al. (2019), and these are outlined in Lucas et al. (2019, p. 15).

D-Cross Tongue of the Mancos Shale

The D-Cross Tongue of the Mancos Shale is a coarsening-upward sequence characterized by shale in the lower 30 m that transitions upward to about 20 m of interbedded shale, siltstone, and sandstone (Seager and Mack, 2003; Lucas et al., 2019). In our mapping, the base of the overlying Gallup Sandstone is placed at the sandstone bed above which sandstones are dominant. The D-Cross Tongue shale is dark gray weathering to olive gray. It is calcareous in the lower part and becomes silty upsection. There are distinctive dark-brown concretions composed of dark-gray, dolomitic and micritic limestone that weathers rusty orange (0.2–1.2 m diameter). Ammonites and other marine fossils are present. This unit was deposited in a prodelta to delta front environment (Seager and Mack, 2003) and includes the upper part of the T2 transgression and the lower part of the R2 regression of Molenaar (1983).

Gallup Sandstone

The 40 m thick Gallup Sandstone conformably and gradationally overlies the D-Cross Tongue. Seager and Mack (2003) recognize three subunits in the Gallup Sandstone, and this description is from their work. The lower subunit (approximately 10 m thick) is characterized by two parasequences containing interbedded very fine- to fine-grained sandstone and gray, silty shales, but there is a systematic upsection increase in the number and thickness of sandstone beds. Shale is absent in the upper part of the lower subunit, and there the sandstone is tan to light brown and thin- to medium-bedded. These beds exhibit horizontal-planar lamination, hummocky cross-stratification, ripple marks, and numerous burrows (mostly horizontal). The middle subunit of the Gallup is a 10 m thick, ledge-forming sandstone that is fine- to medium-grained, contains plant debris and oyster shells (our observation), and is thick-bedded to massive; this sandstone has sparse cross-bedding, horizontal-planar lamination, and ripple marks. The upper subunit (approximately 20 m thick) has dark-gray, argillaceous sandstone at its base (with numerous burrows and oyster shells) capped by a sandstone channel fill that is trough cross-bedded and oyster-bearing; this channel fill has a shell lag at its base. The upper part of the upper subunit consist of gray, thin-bedded, heavily bioturbated, very fine- to fine-grained sandstone capped by a sandstone that exhibits channel morphology and is trough cross-bedded. This capping sandstone is overlain by thin coal that marks the base of the Flying Eagle Canyon Formation.

The lower and middle parts of the Gallup Sandstone are interpreted to represent delta front and distributary mouth bar environments, respectively. In the upper subunit, the lower, dark, argillaceous sandstone is interpreted as a brackish bay on the delta coastline, overlain by delta front sandstones; the two trough cross-stratified sandstones in the upper subunit may represent distributary channels or tidal channels. More information regarding justification of a deltaic environment is presented in Seager and Mack (2003).

Upper part of Upper Cretaceous: Lower sequence of terrestrial strata

Flying Eagle Canyon Formation

The approximately 300 m thick Flying Eagle Canyon Formation (*sensu* Lucas et al., 2019) has a notably olive to brown color and consists of ledge-forming sandstones interbedded with slope-forming intervals of mudstone and thin sandstones. This description is from Lucas et al. (2019). At the base of the unit are two thin coal beds; another coal is found about 220 m above the base. The ledge-forming sandstones are sheet-like to lenticular or ribbon-like and range from 1–13 m thick. These sandstones are mainly fine- to medium-grained, typically single-story, and gray, tan, or greenish brown. The sandstone is composed of abundant quartz and much pinkish feldspar. The sandstone bases are sharp and erosional, but the upper contacts are commonly gradational. Cross-stratification is common within the sand bodies (mostly trough cross-bedding), but there is also lesser horizontal-planar lamination in addition to minor asymmetrical ripple cross-laminae and intraformational conglomerates (with mudstone rip-ups). The slope-forming mudstones are interbedded with thin (<1 m thick) sandstones that are very fine- to fine-grained and massive (with variable root traces), but may exhibit horizontal laminations or sparse ripple marks. The mudstones are brown, gray, olive gray, and greenish gray and weather into blocky fragments. There are local (2–3 m across) sandstone concretions that weather dark brown. These strata represent fluvial deposition on a coastal plain flanking the southwestern margin of the Western Interior Seaway, consistent with general northeast-directed paleoflow from cross-stratification (Wallin, 1983).

Ash Canyon Formation

The Ash Canyon Formation (description and formation-rank usage is from Lucas et al., 2019) differs from the Flying Eagle Canyon Formation by having abundant, resistant and ledge-forming, tan, medium-grained, quartzose sandstones that form multistory sheets. It is about 215 m thick at its principal reference section, corresponding to the Mescal Canyon C section of Lucas et al. (2019). Thickness elsewhere is up to 360 m (Mack and Seager, 1993). Petrified wood is locally abundant. Sandstone intervals are typically several meters (up to 15 m) thick and laterally continuous over 100–800 m. Mudstone and siltstone intervals, similar to those described for the Flying Eagle Canyon Formation, are subordinate to these sandstones. Sandstones are light gray to pale yellow on fresh surfaces, weathering to light brownish, yellowish, and pinkish gray. There is extensive cross-stratification (with common trough forms and tangential foresets), but horizontal-planar laminations and massive beds are locally present. Grain size ranges from very fine to very coarse but is mostly medium-grained. Based on hand lens inspection, composition is estimated to be 50–90% quartz, 10–30% feldspar, and <10% lithic fragments. Pebbly sandstone and pebble-conglomerate are composed of rounded clasts of chert, quartz, quartzite, siltstone rip-ups, and 1–5% siliceous volcanic rocks (aphanitic and gray). Conglomerate is trough cross-bedded or rarely massive. These strata represent fluvial deposition by sand-dominated fluvial systems.

Upper part of Upper Cretaceous: McRae Group, the upper sequence of terrestrial strata

The McRae Formation was proposed by Kelley and Silver (1952) for exposures around the historic Fort McRae. It is a greater than 1-km-thick succession containing tongues of volcaniclastic conglomerates and, higher up, abundant reddish mudstones. The McRae Formation was divided into the José Creek (lower) and Hall Lake (upper) Members by Bushnell (1953, 1955b). We agree with Lucas et al. (2019) that the lithologic distinctness of these two units and their ability to be mapped at 1:24,000 scale justifies their elevation to formation-rank status and that the McRae Formation should be raised to group status. We also adopt usage of the Double Canyon Formation for uppermost McRae strata, as proposed by Lucas et al. (2019). The contact between the McRae Group and the underlying Ash Canyon Formation was thought to be an unconformity by most workers (e.g., Bushnell 1953; Lozinsky, 1986; Seager and Mack, 2003). However, Lucas et al. (2019) interpret that the contact is conformable based on an exposure 2.3 km northeast of Kettle Top Butte.

José Creek Formation

The José Creek Formation is brown to greenish-gray to olive-gray and composed of sandstone, siltstone and mudstone, and intermediate-volcaniclastic conglomerates. It is about 200 m thick in the east-central Elephant Butte Lake quadrangle and 120 m thick near the south end of Elephant Butte Lake, continuing to thin southward until it pinches out east of the central Caballo Mountains. Reddish-brown mudstones are nonexistent or very sparse, in contrast to the overlying Hall Lake Formation, and conglomerates are composed mainly of intermediate-type volcanic clasts. Descriptive data for this formation comes primarily from Lucas et al. (2019).

Fine-grained strata are about 40–70% in proportion relative to sandstones and conglomeratic sandstones. Mudstone and siltstone are mostly olive, dark green, and brownish gray. Mudstone and siltstone strata range from 1–15 m thick and commonly contain thin (<1 m thick) interbeds of very fine- to fine-grained sandstone. Mudrocks are massive and exhibit paleosols. Sandstones are grayish to brown and typically are in 2–9 m thick bodies that are continuous over tens to hundreds of meters. Bedding within these bodies is lenticular to tabular and thin to thick. Cross-bedding, scour and fill features, and horizontal-planar lamination (and lesser ripple marks) are observed. Sand is mainly composed of volcanic grains and feldspar with little to no quartz. Conglomeratic sandstones are 1–10 m thick and massive to trough cross-bedded and extend laterally a few hundred meters to 1 km. These sandstones contain granules and pebbles composed mainly of intermediate rocks (i.e., porphyritic andesites) as well as intraformational clasts of siltstone, sandstones, and carbonate. Less common clasts include mafic clasts and chert pebbles (the latter locally present near the base of the formation). Conglomerates make up only 5% of strata north of McRae Canyon. But the overall proportion and size of clasts in conglomerate of the José Creek Formation increases southward so that, at the south end of Elephant Lake, cobbles and boulders are abundant (Bushnell, 1953, 1955a, 1955b). $^{40}Ar/^{39}Ar$ dating of tuff beds in the lower part of the José Creek returned ages of about 75 Ma (Amato et al., 2017). Sparse, laterally continuous, thin (0.3–1 m thick) beds of siliceous tuffs are mainly observed in the upper half of the unit. Leaf fossils and petrified wood are observed throughout the José Creek Formation (Upchurch and Mack, 1998; Estrada-Ruiz et al., 2012a, 2012b, 2018). Although a sauropod femur was purported to have been collected from the José Creek Formation (e.g., Lozinsky et al., 1984, fig. 6), Lucas et al. (2019) argue this femur actually belongs to the Hall Lake Formation.

The depositional environment of the José Creek Formation was fluvial. The thicker sandstone units and conglomerates were deposited in major channels, and the mudstone-siltstone lithofacies represent floodplain deposits. Thin sandstone beds within the fine-grained facies were deposited as sheetflood deposits, including crevasse-splay processes, and small channel fills (Seager and Mack, 2003; Lucas et al., 2019). The river flowed northeastward into the subsiding Love Ranch basin from volcanoes to the southwest (Lucas et al., 2019). These volcanoes are likely buried by the Santa Fe Group, but the field may include the volcanic complex mined immediately northeast of Hillsboro. The nature of the paleosols indicates deposition under subhumid paleoclimates (Buck, 1992; Levron, 1995; Seager and Mack, 2003).

Hall Canyon Formation

Reddish-brown to maroon mudstones typify the Hall Canyon Formation. These are interbedded with subordinate, lenticular sandstone tongues and sparse conglomeratic beds. Total thickness is probably about 700 m (Lucas et al., 2019). The formation has conformable upper and lower contacts. Mudstones exhibit blocky structure and slickensides and contain calcisols and vertic calcisols according to Buck and Mack (1995). Sandstones are mostly reddish gray to gray, single- to multistory, and up to 4–6 m thick and extend laterally 20–150 m (Cikoski et al., 2017). Sand is fine- to very coarse-grained and a feldspathic litharenite. Hunter (1986) shows a composition of 43–66% lithic grains, 13–30% feldspar, and 15–27% quartz. Lucas et al. (2019) note that coarse-grained sandstones are dominated by quartz with subordinate feldspars (plagioclase and potassium feldspars) and volcanic rock fragments (the average composition being $Q_{45}F_{24}L_{31}$) and are mainly a lithic arenite to feldspathic litharenite. Although lithic grains are mostly volcanic, metamorphic and plutonic rock fragments are more abundant relative to José Creek Formation strata. Conglomeratic strata are up to about 2 m thick and massive or trough cross-bedded. There is a basal conglomerate that contains cobbles as large as 30 cm, whose clast composition includes quartzite, rhyolite, granite, and intermediate volcanic rocks. In overlying strata, intermediate volcanic clasts dominate the conglomerate clast assemblage, but red to pink granite, chert, quartzite, and quartz increase in proportion upsection (Lucas et al., 2019); intraformational conglomerates are also observed.

The age of the Hall Lake Formation was thought to be latest Cretaceous based on dinosaur fossils, within the Maastrichtian stage and Lancian North American fauna age (68–66 Ma). Ongoing geochronologic work has interpreted an age range of 74–63 Ma (Schantz et al., 2024). The 74 Ma age comes from a tuff about 15 m above the base of the unit. These ages, in turn, provide biostratigraphic constraints for dinosaur fossils found in the Hall Lake Formation. These dinosaurs include *Tyrannosaurus rex*, *Torosaurus* or *Triceratops*, ankylosaur, and *Alamosaurus* (Lucas et al., 2019; Lozinsky et al., 1984; Wolberg et al., 1986; Gillette et al., 1986).

The interpreted depositional environment is fluvial, with extensive floodplains and braided to anastomosing channels (Hunter, 1986; Seager and Mack, 2003; Lucas et al., 2019). Tectonic subsidence of the intraforeland Love Ranch basin allowed the thick accumulation of sediment (Seager et al., 1997). Red mudstones and common calcic horizons indicate deposition under a relatively dry paleoclimate (Buck, 1992; Buck and Mack, 1995; Seager and Mack, 2003).

Double Canyon Formation

The type section for the Double Canyon Formation was measured and described 1.5 km northeast of Kettle Top, where it is about 130 m thick (Lucas et al., 2019). North of here, its thickness is likely greater than 400 m (Cikoski et al., 2017). In the type section, the Double Canyon Formation is a light-colored succession of interbedded mudstone, siltstone, sandstone, conglomerate, and minor bedded chert. Sandstone and pebbly sandstone are light gray, light brownish gray, or greenish gray; mudstone and siltstone are typically olive-colored to gray, contrasting with the underlying reddish mudstones of the Hall Canyon Formation. Thin sandstone interbeds are common in the fine-grained strata. Amalgamated (multistory) channel-fill complexes are several meters thick and cross-bedded (commonly trough cross-stratified) or horizontal-planar laminated. Sand is fine- to coarse-grained, subangular to subrounded, and composed of feldspar, quartz, and minor volcanic grains; the average composition per Lucas et al. (2019) is $Q_{55}F_{19}L_{26}$. Lithic grains consist of volcanic rock fragments and volcanic chert grains, with less common granitic rock fragments.

The Double Canyon Formation was deposited in the Paleocene (Schantz et al., 2014) in a fluvial depositional environment (Lucas et al., 2019). Discharge in channels carried coarser sediment than in the underlying Hall Canyon Formation. The age of the Double Canyon Formation spans the Paleocene based on recent dating of tuffs in the type section using U-Pb techniques on zircons (Schantz et al., 2024). Tuffs near the base of the unit each yield 60.6 ± 1.2 Ma, and maximum depositional ages of sandstones (from detrital zircon) near the middle of unit are 58–56 Ma.

Paleogene–Neogene

Eocene through Oligocene strata are not exposed on the quadrangle, nor are they penetrated by well data in the southern Engle basin (Lozinsky, 1987). However, prominent andesite dikes on the quadrangle are likely of that age. These dikes are up to 8 m thick and trend mainly northwest. The longest dike is 9 km and strikes 350°. The next longest is 6 km and strikes 320°. The dike rock is a gray, porphyritic, fine- to medium-grained andesite that weathers brown or dark gray. Phenocrysts are composed mainly of plagioclase. Constraining their age through radiometric dating would be important for constraining structural events (see below).

Neogene–Quaternary

Neogene to early Quaternary Santa Fe Group strata, a term applied to clastic strata and interbedded volcanic rocks that accumulated in the Rio Grande rift (Spiegel and Baldwin, 1963), extend across the quadrangle west of the Hot Springs fault. Earliest exposed Neogene strata belong to the Rincon Valley Formation (late Miocene). Greater than 95% of Santa Fe Group exposures on the Elephant Butte quadrangle consist of the latest Miocene through early Pleistocene-age Palomas Formation (Lozinsky and Hawley, 1986). Due to incision of the Rio Grande during the middle to late Quaternary, dissection of the Santa Fe Group provides extensive exposures of the upper Palomas Formation. Based on these exposures and previous geologic mapping (e.g., Lozinsky, 1986; Jochems, 2015; Jochems and Koning, 2015; Koning et al., 2015, 2018b), we differentiate six stratigraphic units in the Palomas Formation. Another geologic feature are maar complexes that are likely 2.6–2.4 Ma. Three stratigraphic units are mapped to represent these maar deposits and related intrusions.

Rincon Valley Formation

The Rincon Valley Formation is applied to pinkish to light reddish-brown strata underlying the light-colored, tannish to light-gray axial-fluvial facies and the brownish eastern piedmont facies of the Palomas Formation. The most detailed and complete record of these strata comes from the Getty No. 2 West Elephant Butte Federal Well, drilled 2.5 km northwest of downtown Elephant Butte. A summary of the main units of this well is given in Table 1, and cuttings and wireline data for the well are housed in the New Mexico Bureau of Geology Subsurface and Core Library. In this well, the Rincon Valley Formation disconformably overlies Cretaceous strata correlative to the Gallup Sandstone or basal Flying Eagle Canyon Formation. Depending on the location within the Engle basin, the particular underlying Cretaceous unit will probably vary. Three stratigraphic intervals of the Rincon Valley Formation are interpreted using data from the Getty No. 2 West Elephant Butte Federal Well, informally referred to here as the lower, middle, and upper units.

Lower unit

The lower 350 ft of the Rincon Valley Formation in the well (1,330–1,680 ft depth) consists of clayey, very fine- to fine-grained sand, where sand is mostly composed of rounded quartz grains (Table 1). The lowest 70 ft (1,610–1,680 ft depth) is a clear-white, very fine-grained, subrounded to rounded sand. Quartzose, very fine-grained sandstones typify Yeso Group strata in bedrock strata (see above). Consequently, the lowest Rincon Valley Formation unit is inferred to represent clastic deposits eroded from Yeso Group strata that once capped the Mud Springs Mountains. Furthermore, the depositional environment at the site of the well may have corresponded to a distal piedmont sloping northeastward away from the Mud Springs Mountains. A playa lake likely existed northeastward of the well in the Engle basin.

Middle unit

The middle stratigraphic unit is assigned to 616–1,330 ft depth in the Getty No. 2 West Elephant Butte Federal Well. It is composed mainly of reddish-clay with minor very fine- to fine-grained sand. The clay-rich nature is manifested by an expanded borehole measured below the base of the casing (commonly >20 inches below the casing base of 1,000 ft), relatively high gamma-ray values, and driller cuttings reports of gummy, red-bed clay with only trace very fine quartz and feldspar grains (Appendix 1). The driller log noted that the clay swelled when wet but dried very hard. This interval reflects deposition in a playa lake that expanded or shifted westward after deposition of the lower unit. It is likely that tongues of sandy distal piedmont sediment episodically extended (prograded) into the playa lake, but the complications of reading the well log due to the washouts hampers identification of these tongues.

Upper unit

The upper stratigraphic unit of the Rincon Valley Formation is characterized by a progressive gamma ray decrease up-section from 616 to 511 ft depths. Inspection of the cuttings housed by the New Mexico Bureau of Geology (by Daniel Koning) indicated around 15% lower-fine to upper-fine-grained sand mixed with light reddish-brown to pink clay; the sand was composed of felsic-volcanic grains with subordinate to subequal quartz. Although much of this sand is likely slough, the decreasing upsection gamma-ray signal indicates a decreasing clay component going upsection between 511–616 ft, probably corresponding to an upsection increase in silt and sand. Minor (20–30%) sand consistent with that of the Rio Grande (c.f. unit QNpa) is noted in the driller cuttings description for the upper part of the 511–616 ft depth interval, with reddish claystone for the lower part of that interval.

There are two map units that correlate to the upper interval described in the Getty No. 2 West Elephant Butte Federal Well. One is pebbly sandstone and conglomerate adjoining the west side of the Hot Springs fault south of the earthen auxiliary dam (Nrpe). This unit consists of medium to thick, tabular to lenticular beds that are mostly internally massive (Fig. 6); these are probably laid down, at least in part, by debris flows or hyperconcentrated flows. Pebbles are angular to subangular, poorly sorted, and composed of intermediate-volcanic rocks that has abundant plagioclase phenocrysts and minor green sandstone (Fig. 7). The sand is mostly upper-fine to upper-medium in grain size, subrounded to subangular, and composed of quartz, lesser feldspar, and 5–20% volcanic lithic grains. The dominance of volcanic clasts suggests a more extensive cover of José Creek Formation to the east than exists today and contrasts markedly with the sediment-clast dominated nature of the younger Nppe unit.

The other map unit associated with the upper interval of the Rincon Valley Formation occurs in outcrops along the southern quadrangle boundary, illustrated by the Boyd stratigraphic section (Fig. 8). There, the upper Rincon Valley Formation mainly consists of interbedded clay, silt, and very fine- to fine-grained sand (unit Nrpd). Locally, these strata overlie a lower subunit of clayey piedmont-slope conglomeratic sandstone that is included in the upper interval of the Rincon Valley Formation (but too small to map at 1:24,000 scale). It is possible that fine-grained strata similar to the upper unit underlie the conglomeratic sandstone farther down in the subsurface.

In the fine-grained upper subunit (Nrpd), clay is reddish brown to brown and the silt is yellowish brown. Both are in very thin to medium, tabular beds that are massive to horizontal-planar laminated. Sand tongues may increase upsection (Fig. 8). These tongues are up to a few meters thick and consist of lower-very fine to upper-fine-grained sand that is distinctly micro-laminated. Laminae are commonly <3 mm thick and include interstratified clayey sand and silt laminae (Fig. 9). The laminated sedimentary structures are horizontal-planar, cross-stratified (up to 10 cm thick), or ripple-marked. The well-sorted sand is dominated by quartz grains. The reddish-brown, clayey lithologic unit becomes more sandy to the east (becoming mostly a very fine- to fine-grained sand), and calcium carbonate nodules also become more abundant in that direction (Fig. 9). Intertongues of the quartz-rich and light-colored sands appear to decrease to the east.

The lower subunit (of the upper Rincon Valley unit) consists of sandy pebble-conglomerate and pebbly sandstone in very thin to medium, tabular to lenticular beds. This lower subunit is present at the base of the stratigraphic section in Figure 8. The pebbles are subangular to angular and composed of reddish siltstones to fine-grained sandstones (similar to Abo and Yeso Formation strata), light-gray limestones (similar to Pennsylvanian strata), and greenish sandstones (similar to those in the Flying Eagle Canyon Formation). Some beds contain up to 5% granite and 1% felsic volcanic clasts. Sand is reddish brown to reddish yellow, fine- to very coarse-grained, and angular to subrounded and includes some clay (up to approximately 10% estimated). The sand composition is mainly lithic-dominated, with 15–20% quartz and 15–20% feldspar. Lithic grains are similar to those listed for the conglomerate clasts. Paleoflow data are to the southwest (Fig. 8).

Outcrop data for the upper stratigraphic unit of the Rincon Valley Formation are interpreted to indicate a transition from an ephemeral, fluvial system on the basin floor, flanked by alluvial fans, to a playa lake environment with fluvio-deltaic tongues of the ancestral Rio Grande. The sand and pebbles in the lower subunit of the Boyd section are notably quartz-poor and angular. Their compositions are consistent with input primarily from Cretaceous and Permian bedrock currently exposed in the Cutter Sag and headwaters of Mescal Canyon. However, the minor proportion of granite and felsic volcanics indicates that the drainage extended northward to the Engle basin, since granite is only exposed on the western front of the Fra Cristobal Mountains and the nearest source of felsic volcanics (in an upstream direction) is in the southeastern Fra Cristobal Mountains (for more information on gravel lithologies and provenance, see Koning et al. [2016]). In the upper subunit, a playa lake environment is consistent with the reddish-brown to brown claystones, slightly more yellow siltstones, and light-colored, very fine- to fine-grained sandstones. The well-sorted, quartz-dominated sand stands in stark contrast to the conglomeratic sandstone of the lower subunit. It is interpreted to have been deposited as terminal Rio Grande deltaic bars in relatively shallow water. The eastward trend to more sandy textures and carbonate nodules is consistent with sand being inputted onto the eastern playa by local drainages of the western front of the northern Caballo Mountains; prolonged periods of subaerial exposures are indicated by the presence of calcium carbonate nodules (Fig. 10). Interbedding of reddish-brown playa lake clays with quartz-rich, fine sand is interpreted for the 616–511 ft depth interval in the Getty West Elephant Butte No. 2 Federal Well, but the clayey, conglomeratic sandstone is apparently absent. We similarly interpret playa lake and fluvial-deltaic depositional environments for the Getty well location in the upper Rincon Valley Formation.

Palomas Formation

The Palomas Formation was applied to relatively coarser sediments that characterize the upper Santa Fe Group in the Palomas, Engle, and San Marcial basins of the Rio Grande rift (Lozinsky and Hawley, 1986). The term "Palomas gravel" was used early in this century for gravelly deposits at approximately this stratigraphic level (Gordon and Graton, 1907; Gordon, 1910; Harley, 1934). However, it was formally defined by Lozinsky and Hawley (1986). The Palomas Formation is characterized by relatively broad piedmont deposits (i.e., alluvial fan and coalescing alluvial fan deposits) and a relatively narrow belt of axial-river deposits. It overlies closed-basin deposits that locally contain playa lake facies (e.g., unit Nrpd, Nrp). Geologic mapping efforts in the Palomas basin to the west and southwest (Jochems, 2015; Jochems and Koning, 2015; Koning et al., 2015, 2018b) divided the Palomas Formation into various lithologic units based on texture and composition, which we apply to this quadrangle. The divisions can be informally categorized as the lower, middle, and upper Palomas Formation (Fig. 11), although in reality there is some vertical overlap between the three. Note that we use the terms conglomerate, sandstone, siltstone, and claystone for the lower Palomas Formation due to its relatively strong cementation. However, strata in the middle and upper Palomas Formation are generally not cemented, so for those intervals we use the terms gravel, sand, silt, and clay.

Lower

The lower Palomas Formation is relatively coarse-grained and has two stratigraphic components on this quadrangle. To the east lie relatively cemented, yellowish-brown to light olive-brown, conglomeratic strata (Fig. 12) associated with paleofans of drainages sourced in the northern Caballo Mountains and Cutter sag, including Mescal Canyon (unit Nppe). Beds are primarily tabular to lenticular, with ≤10% cross-stratification. The gravel is sand- to clast-supported, subrounded to angular, and poorly to moderately sorted within a bed and consist of pebbles and about 5–15% cobbles. Clasts are composed of 50% greenish sandstone (matching the Flying Eagle Canyon Formation and especially abundant in the finer pebble fraction), 10–45% light-gray limestone (upper Paleozoic source), 1–5% reddish very fine- to fine-grained sandstones and siltstones (inferred Permian strata source), and 0–1% granite. Paleoflow data are westward. The sand associated with conglomeratic strata is fine- to very coarse-grained. Medium sand is mostly composed of quartz, whereas coarse- to very coarse-grained sand is composed of sedimentary lithic fragments. There are minor tongues (<3 m thick) of pebbly, very fine- to fine-grained sand with an estimated 1–10% content of silt–clay. Strata have 10–50% calcium carbonate cementation in the form of nodules and irregular masses. Locally, beds are 1–3 m thick, matrix-supported, and internally massive; these are interpreted as debris flow deposits. The presence of debris flows, the lack of cross-stratification and relatively tabular bedding, the paleoflow direction, and the gravel composition indicate deposition of an alluvial fan sourced from a paleodrainage approximating Mescal Canyon and possibly Ash Canyon.

This eastern fan complex transitions southward to locally derived, well-cemented paleo-alluvial fan deposits at the mouths of small canyons draining the western flank of the northern Caballo Mountains, which make up map unit Nppes. These deposits are sandy conglomerate and conglomeratic sandstone in medium to thick (minor thin), tabular to broadly lenticular beds that are internally massive (Fig. 13). Gravel is angular to subrounded (mostly subangular) and composed of reddish siltstones–fine sandstones to the north, but along the southern quadrangle boundary clasts are mainly light-gray limestones; 1–3% monolithic, subangular chert is also observed. The matrix between clasts is silty-clayey, very fine- to very coarse-grained sand. The coarse to very coarse sand is composed of angular to subangular, Paleozoic-sedimentary lithic grains.

The eastern fan complexes (Nppe and Nppes) disconformably overlie the Rincon Valley Formation near the southern border of the quadrangle (Fig. 8), but the contact may be conformable in the subsurface to the north. These conglomeratic, alluvial fan units intertongue westward with relatively coarse-grained, axial-fluvial strata, as illustrated in the cross section. The coarse-grained, axial-fluvial strata are not exposed on this quadrangle, but on the Cuchillo Negro quadrangle they correspond with unit Tpal2 and Tpal1 (Koning et al., 2018b).

An inspection of cuttings from the Getty West Elephant Butte No. 2 Federal Well by Daniel Koning indicates relatively coarse strata from 350 to 511 ft, which we assign to the Npal2 map unit. Pebbles are broken and up to 12 mm long. These clasts are composed of subangular to subrounded felsic volcanic rocks, likely derived from the San Mateo Mountains and/or Alamosa Creek (c.f. Koning et al., 2016). The pebble size and abundance increase downsection. Trace clear-green, quartz-rich sandstone clasts are noted at 460–470 ft and 480–490 ft (Table 1). The sand is mostly coarse to very coarse and composed of quartz in addition to 30–50% volcanic lithic grains, 5-20% potassium feldspar, variable granite, and 1% chert. The abundance of quartz grains is similar to the quartz-rich axial-fluvial deposits mapped and described higher in the axial-fluvial facies of the Palomas Formation (e.g., unit QNpa). Volcanic grains and potassium feldspar clasts are consistent with a provenance in the southern San Mateo Mountains and western Fra Cristobal Mountains, respectively (Koning et al., 2016). The clast composition and quartz-rich character of the sand in the well compare well with older axial-fluvial deposits noted on the southwestern Cuchillo Negro quadrangle (unit Tapl2 in Koning et al. [2018b]). The preponderance of volcanic gravel and relative lack of sedimentary gravel, in contrast to that seen in correlative Tpal2 and Tpal1 exposures on the southeastern corner of the Cuchillo quadrangle (Koning et al., 2018b), indicate that the Getty West Elephant Butte No. 2 Federal Well was mainly north of the Mescal-Ash Canyon paleofan.

Below the Npal2 unit lies a 105 ft-thick (32 m-thick) transitional zone with the Rincon Valley Formation, which we assign to unit Npal1. It is composed reddish clay and fine- to medium-grained, quartz-rich sand. Higher in the unit are subrounded to broken pebbles composed of felsic volcanic rocks, 1–5% greenish (Mesozoic?) sandstone, and 1–3% quartz.

Middle

Map units QNpa, QNpf, and QNpt, which correspond to axial-fluvial sand and floodplain-margin deposits, make up the middle interval of the Palomas Formation. Axial-fluvial sand (QNpa) progrades eastward over the underlying eastern alluvial fan complexes (Fig. 11; Nppe), and in outcrop, the base of the axial-fluvial sand is locally observed as intertonguing with these underlying, coarser-grained fan deposits. The axial-fluvial sand is white to light gray to pale brown and contains 1–15% pebbly sand (Fig. 15). In general, sandy strata are in tabular to broadly lenticular, 0.5–3 m-thick beds. Within these beds, sand is horizontally laminated with variable, but typically minor, cross-stratification <1 m thick (Figs. 15 and 16). Pebble beds are very thin to medium and lenticular. Clasts are mostly very fine to medium pebbles, with minor coarse to very coarse pebbles and up to 3% fine cobbles. Gravel composition is dominated by felsic volcanic rocks and intraformational clasts (mainly calcium carbonate nodules plus cemented sandstone and siltstone) and includes the following accessory lithologic types: 5–20% granite, 0–3% gneiss, 3–30% greenish sandstone (generally resembling those in the Flying Eagle Canyon Formation [Kfe]), trace to 5% limestone, 1–5% chert, 1–2% reddish Permian clasts, and 1–20% intermediate volcanic rocks. The proportion of extra-basinal (exotic clasts) markedly increases in the upper 10–30 m of the deposit, where there are 15–

20% brown and black cherts, trace petrified wood, and 1–5% quartzite. Sand is mostly lower-medium to lower-coarse-grained, but ranges from fine- to very coarse-grained, and is composed of quartz with subordinate sanidine and plagioclase, 5–15% orangish grains (potassium feldspar, stained quartz, minor chert), about 10–15% yellow-stained quartz, 7–20% dark lithic grains dominated by volcanic rocks, and 1–5% mafic grains. In the Getty No. 2 West Elephant Butte Federal Well, the proportion of granite fragments is 5–10% in the upper 280 ft, but is notably less (1–3%) at 280–370 ft (Table 1).

Fine-grained strata of the middle Palomas Formation (unit QNpf) intertongue laterally with the axial-fluvial unit and also prograde over it. These fine-grained strata contain <5% gravelly tongues and are mostly tabular-bedded (Figs. 17 and 18). Their color is mainly light brown to brown to pinkish gray, with some light reddish brown (Figs. 17–19). Beds are medium to thick and internally massive. Sediment consists of silt, very fine- to fine-grained sand, silt-clay, and subordinate clay to clayey fine-grained sand. These fine-grained strata have minor (1–3%), 10–30 cm thick intervals with abundant in situ calcium carbonate nodules mostly inferred to be related to shallow groundwater carbonate. There are also 0.5–5% strongly cemented, very fine- to fine-grained sandstone beds inferred to be authigenic groundwater carbonates (*per* Seager and Mack, 2003). There are sparse (1–10%) paleosols where illuviated clay horizons overlie calcic horizons, or these features are combined in one soil horizon (e.g., Fig. 18). The sparse gravelly tongues are narrower than in overlying strata and up to 2 m thick. The sand in these tongues lacks clay and is commonly grayish. Fine- to medium-grained sand is mostly feldspar with minor dark lithic (volcanic) grains, and 5–20% quartz, but coarser sand is composed of volcanic lithic grains. Pebbles are subrounded and composed of felsic volcanic rocks (containing abundant Vicks Peak Tuff) with minor (10–20%) intermediate types, 1–2% Kneeling Nun Tuff, 0–0.5% reddish siltstones and very fine-grained sandstones (eroded from Permian strata). The mix of Vicks Peak Tuff and the presence of Permian clasts indicate a mix of inputs from Cuchillo Negro Creek and Alamosa Creek (Koning et al., 2016). Application of Walther's Law (considering the fact that axial-fluvial sediment lies below and western piedmont sediment lies above), the paucity of clay beds and axial-fluvial sand, and the lower gravel content, indicates that deposition of the fine-grained unit occurred on the outer margin of the paleo floodplain of the axial valley. Here, deposition occurred on a gently sloping surface, probably via sheetfloods debouching off of the toe of coalesced alluvial fans associated with the lower part of the western piedmont.

A notable increase in gravel beds, plus slightly more reddish-brown colors, occupies a 3–10 m thick transitional zone overlying unit QNpf (Fig. 20). This transitional zone is brownish (7.5YR), with minor reddish-brown beds that increase in abundance upsection. The sand in the gravelly tongues is clay-free and gray to brownish and fine- to very coarse-grained. The base of Qpt is mapped where, in a downsection direction, gravelly strata are <5%. The top of Qpt is mapped at the top of the zone of slightly more abundant gravels, near which (± 5 m) reddish-brown and light reddish-brown (5YR) beds become relatively common upsection.

Upper

The upper Palomas Formation unit, represented as map units Qppw and Qppwc, represents deposition on the distal piedmont slope, where alluvial fans associated with western-sourced drainages coalesced to form a relatively smooth, southeastward-sloping landform west of the floodplain margin associated with unit QNpf. It is characterized by tabular-bedded, very fine- to fine-grained sand and clayey-silty sand interbedded with 15–35% gravel tongues (Fig. 21). There are fewer proportions of clay–silt beds. These fine-grained beds are internally massive to vaguely horizontal-planar laminated (Figs. 21 and 22). Also, many of the finer-grained beds contain 1–5% scattered, outsized (coarser) grains and trace to 5% pebbles

(Fig. 22c). Most of the fine-grained strata are a light reddish brown to reddish brown or light brown to brown, with browner colors more common in the lower part. There are numerous weakly developed paleosols characterized by ped development, with a subordinate proportion of these exhibiting illuviated clay and calcic horizons (Figs. 22d and 22e). There are sparse (approximately 1%) sand beds that are fine- to medium-grained and lack silt and clay.

The proportion of gravelly tongues increases upsection in most exposures, although such a trend is not universal (Fig. 11). Typically, the upper third to half of the unit has up to 50% gravelly bodies and the lower half to two-thirds has 10–20% gravelly bodies. Gravelly strata are in tabular to broadly lenticular, single-story intervals 1–4 m thick (Figs. 21 and 22). These gravel tongues have scoured bases and relatively sharp to abrupt (i.e., gradation occurs over <3 cm), planar to slightly wavy tops. Within these tongues are thin to thick, tabular to broadly lenticular beds with only minor (<5%) cross-stratification. Gravelly strata also occur as narrower, single-story, broadly U-shaped or wedge-shaped paleochannels 0.1–1.5 m thick. Gravel clasts consist of pebbles with <10% cobbles that are subrounded, poorly to moderately sorted, and clast-supported. Gravels are composed predominantly of intermediate and felsic volcanic rocks, the latter ranging from 30 to 70%. Gravels have trace to 0.5% reddish siltstone to very fine sandstone clasts (eroded from Permian strata), trace to 0.5% coarse-grained Kneeling Nun Tuff, and about 1% monzonite-diroite, phaneritic clasts. This clast composition is broadly consistent with Cuchillo Negro Creek provenance, although some input from Arroyo Alamosa is allowable (see Koning et al., 2016). The gravel matrix consists of brown, reddish-brown, or light reddish-brown sand that is mainly medium- to very coarse-grained and subrounded. Coarse to very coarse-grained sand is composed of volcanic lithic grains, whereas medium-grained sand is composed of volcanic lithics, feldspar, and quartz. Interstitial clay (1–5%) is relatively common, typically as films on clasts and grains.

The top of the upper unit (Qppw) is capped by a 2–15 m thick interval where sandy gravel is dominant (Qppwc). There are minor interbeds of fine-grained sediment similar to those in unit Qppw. Like those in the underlying Qppw strata, the gravels are clast-supported, subrounded, and have medium- to very coarse-grained sand constituting the gravel matrix; this sand is a lithic arenite and has minor clay (1–10%). In contrast to underlying gravels, these are coarser (contain 10–20% cobbles), and in the upper 2–6 m they are dominated by felsic clasts with relatively common Vicks Peak Tuff. Also present in the upper 2–6 m is a coarse feldspar-porphyry that is associated with Alamosa Creek. This felsic-dominated cap has a relatively sharp base and extends as far south as latitude 3°13’20” N. We hypothesize that it represents a rapid progradation or expansion of the Alamosa Creek alluvial fan.

Maar complexes

Maar complexes are formed when ascending magma, commonly basaltic in composition, encounters groundwater at relatively shallow depths and low confining pressure. The heat of the basalt causes the groundwater to flash into steam, creating a powerful explosion that ejects abundant quantities of preexisting country rock or sediment. Even after it solidifies, lava within the crater can be brecciated from subsequent, nearby groundwater-related explosions. Four maar complexes are present on the Elephant Butte quadrangle that are named the Elephant Butte, Rattlesnake Island, Rock Canyon, and Lonely Heart Butte maars; Fig. 23.

On this quadrangle, we map two clastic units at 1:24,000 scale, which are intruded by, or interbedded with, minor basalts (Figs. 24 and 25). The basalt (Qb) locally exhibits hyaloclastic features and may be massive or columnar (locally random orientations), or may exhibit pillow features.

The first clastic unit is a brownish conglomeratic sandstone, where basaltic lapilli and pumice-lapilli are scattered in sand and slightly silty to clayey sand (Qmb). Strata are commonly in well-defined, relatively thin, tabular to slightly wavy beds that are hard. At the base of the sequence are base surge sediments that grade upward from mostly flat-bedded coarse-grained sands to the aforementioned conglomeratic sands. This first unit represents fall-out deposits from explosions initiated by rising magma encountering shallow groundwater. This unit has a high proportion of detritus derived from the Palomas Formation (primarily the axial-fluvial facies) and McRae Group; detritus also includes a lesser component of Precambrian metamorphics and mantle-derived olivine xenoliths.

The second clastic unit is characterized by clast-supported, basalt breccia that is relatively massive or chaotic (Qmv). Basalt clasts are vesicular and the inter-clast matrix consists of a chilled, fine-grained magma that is locally flow-foliated. We interpret this second unit as a basalt that accumulated and solidified within a volcanic vent; this basalt was then autobrecciated by subsequent explosions related to magma-groundwater interaction.

The maar eruptions on the Elephant Butte quadrangle began with a pre-eruptive phase evidenced by base surge sediments that grade upward from tan-colored, mostly flat-bedded coarse-grained sands to light-brown to reddish-brown conglomeratic sands (Qmb). Chaotic bedding orientations, cinder-rich sediments, and bomb sags +/- ashfall tuff mark the transition to eruptive lithologies.

Multitude episodes of basaltic volcanism are evident at each maar. Basalt locally intrudes both the Qmb and Qmv breccia units. For example, basalt ring dikes occur at Elephant Butte and Rattlesnake Island and may represent the final phase of volcanism. However, at Elephant Butte and the Rock Canyon maars, the basalt was also emplaced early, probably within subsurface vents, accounting for the roughly cylindrical form of Elephant Butte and the dike-like form at Rock Canyon. At Elephant Butte maar, the vent facies (Qmv) were deposited in a vent that formed within the earlier basalt. Erosion has removed the upper edifice/cone at both locations.

Two apparent basalt intrusions were dated at Rattlesnake Island maar, represented by samples EB-23 and EB-20, respectively (Fig. 26; Table 2). These two samples returned 2.5 Ma $^{40}Ar/^{39}Ar$ ages. The isochron age for EB-23 (2.447 ± 0.057 Ma) was chosen over the plateau age because of indications of excess argon. In contrast, sample EB-20 did not have excess argon and had better precision, so we prefer that age for the maar complex: 2.468 ± 0.014 Ma. The weighted mean of both samples is: 2.466 ± 0.013 Ma, and we consider that to be the representative age for the Rattlesnake Island maar. Until further dating is completed, we infer a 2.3–2.6 Ma age range for the other maar complexes on the Elephant Butte quadrangle.

Post-Santa Fe Group

The Santa Fe Group aggraded until around 800 ka (Mack et al., 1993, 1998b, 2006; Mack and Leeder, 1999; Sion et al., 2020), and its culmination is represented by the Cuchillo geomorphic surface (McCraw and Love, 2012), which is described below. After about 800 ka, the Rio Grande progressively incised 90 m to its present grade. During this incision, there were several periods of aggradation or base-level stability, which created terrace landforms. These terraces are associated with the Rio Grande (Qtr), Cuchillo Negro Creek (Qtc), and scattered fan-terrace deposits along low-order drainages in the northwestern part of the quadrangle (Qtf). For Cuchillo Creek and the Rio Grande, we map five general terrace levels throughout the Elephant Butte quadrangle, with the older (highest) level designated by a 1 in the map unit label (e.g., Qtr1, Qtc1) and progressively higher numerals (2, 3, 4, 5) indicating successively lower (younger) levels so that the youngest (lowest) level is designated by a 5 (e.g., Qtr5, Qtrr5). Because of greater uncertainty in correlation, the fan-terrace deposits are divided into three geomorphic levels: Qtfl, Qtfm, and Qtfh.

Rio Grande terrace deposits

Terrace deposits associated with the Rio Grande are mainly composed of weakly to moderately stratified sandy gravel with subordinate gravelly sand. Gravel beds are mostly tabular to lenticular. Sandy strata are horizontal-planar laminated to thinly bedded. Locally, gravels and sands are cross-stratified, with tangential foresets or trough forms. Typically, there is a gravel or gravelly sand layer 1–4 m thick overlain by alluvial fan deposits or surficial sand (units Qs, Qes) up to a few meters thick (e.g., Fig. 27). In the lower gravel layer, gravel is clast-supported and moderately imbricated and consists of pebbles, minor cobbles, and 1–10% boulders. Gravel is subrounded to rounded and poorly to moderately sorted and has the following compositions (estimated from several exposures): intermediate volcanic rocks, subordinate felsic volcanic rocks, 3–10% quartzite, 1–7% sedimentary rocks (mainly sandstone that includes rocks similar to nearby Cretaceous and Permian outcrops), 5–10% chert, 1–3% granite, and trace metamorphic rocks. Sand is very pale brown to light gray to pale brown, medium- to very coarse-grained, subrounded, moderately to well sorted, and composed of quartz, minor sanidine and plagioclase feldspars, about 10% volcanic-rich lithics, and about 10–15% grouped potassium feldspar, orange quartz, and chert (most to least). General tread heights, relative to the Rio Grande floodplain, for the five main geomorphic levels are 19–21 m (Qtr5), 23–30 m (Qtr4), 42–48 m (Qtr3), 49–52 m (Qtr2), and 58–59 m (Qtr1). Note that in the fourth and third levels (Qtr4 and Qtr3), there are two or three subsets of terrace treads.

Cuchillo Negro Creek terrace deposits

Terrace deposits associated with Cuchillo Negro Creek are composed of sandy gravel and subordinate to subequal gravelly sand (Fig. 28). These unconsolidated to weakly consolidated strata are in very thin to medium, tabular to lenticular beds. Gravel is subrounded, mostly clast-supported, poorly to moderately sorted, and moderately to well imbricated and consists of pebbles, 10–40% cobbles, and 0–3% boulders. Estimated gravel composition is predominately intermediate volcanic rocks (including basaltic andesite), 15–35% felsic volcanic rocks, trace to 1% Kneeling Nun Tuff, 0–1% Paleozoic sedimentary rocks (including reddish siltstone–very fine-grained sandstone and limestones), and trace to 0.5% monzonite–diorite intrusions. Sand is mostly medium- to very coarse-grained, subrounded, and mostly composed of volcanic lithic grains (volcanic litharenite); medium-grained sand is composed of quartz, feldspar, and subordinate to subequal volcanic lithics. The higher terrace levels, particularly Qtc1 and Qtc2, have 1–15% clay in the sand matrix as clay chips and clast coatings, imparting a reddish-brown to light reddish-brown color. The higher three levels (Qtc1, Qtc2, and Qtc3) are 5–10 m thick, whereas the younger two levels (Qtc4 and Qtc5) are thinner. General tread heights, relative to the Cuchillo Negro valley floor and outside of the modern channel, for the five main geomorphic levels are 9–10 m (Qtr5), 12–14 m (Qtr4), 22–28 m (Qtc3), about 29–30 m (Qtc2), and 48–49 m (Qcr1). Note that in the third level (Qtr3) there are two subsets of terrace treads, separated by about 5–7 m (Fig. 26). The lowest terrace deposit (Qtc5) has a 1–2 m thick, upper layer of sandy sediment, including clayey–silty fine-grained sand, that is yellowish brown and very fine- to medium-grained and includes sparse beds of gravelly sand.

Fan-terrace deposits

North of Cuchillo Negro Creek, on the northwestern part of the quadrangle, there are various high-level, gravelly fan-terrace sediments deposited by low-order, tributary drainages. These deposits are typically only a few meters thick and are composed of sandy gravel and gravelly sand in very thin to medium, lenticular to tabular beds (Fig. 29). Gravel is mainly pebbles with minor cobbles that are subrounded and composed predominately of volcanic clasts eroded from the upper Palomas Formation (Qppuc, Qppu, and Qppt). Sand is brownish and mostly medium- to very coarse-grained.

There are four geomorphic levels that we informally refer to as "oldest, high, medium, and low" (Qtfh, Qtfm, and Qtfl, respectively). Along the western quadrangle border 3 km west of downtown Elephant Butte, Qtfh correlates to the first (uppermost) terrace level of Cuchillo Negro Creek (Qtc1). At that location, Qtfm correlates to the second terrace level of Cuchillo Negro Creek (Qtc2). The tread of Qtfm is about 12–13 m above the modern grade of an adjoining, low-order drainage. The lowest terrace level (Qtfl) is only mapped along the northern quadrangle boundary along lower Cedar Canyon. It is several meters thick, and its tread is 4–6 m above the modern grade. Qtfm and Qtfl consist of sandy pebbles, pebbly sand, and fine-grained sand to silty-clayey fine-grained sand with minor pebbles. Finer grained sediment may be pedogenically altered (Stage I carbonate morphology, weak to moderate peds with faint clay films). Locally, two geomorphic surfaces are present, separated by 1–2 m. We tentatively correlate Qtfm with the fourth terrace levels to the south (Qtc4, Qtr4) and Qtfl with the fifth terrace levels (Qtc5, Qtr5).

Valley-floor deposits

Younger alluvium (Qay) consisting of unconsolidated to weakly consolidated sand, gravelly sand, and sandy gravel underlies Cuchillo Negro Creek and tributaries to this drainage. Related stratigraphic units and surfaces are illustrated in Figure 30. Strata are mostly in very thin to thick, lenticular to tabular beds with <10% cross-stratification (Fig. 31a). Gravel is composed predominantly of volcanic clasts, and clast size is mainly pebbles with minor cobbles. Sand is brown and fine- to very coarse-grained. The Qay unit extends to the Santa Fe Group or to bedrock and ranges in thickness from a few meters to possibly 20 m (Fig. 30). The maximum aggradational surface of the Qay valley fill is 3–4 m above the modern grade (Fig. 31b). The soil on this surface has a 5–20 cm thick Stage I+ to II calcic horizon, locally overlain by a 10–20 cm thick A horizon. The surface also sports a weakly developed desert pavement, with a moderate clast armor and weak varnishing of surface clasts. An intermediate geomorphic surface, roughly 1–2 m above the modern grade, is developed on this alluvium above recent alluvium, which typically has a Stage I or I+ carbonate morphology (Fig. 31c). The lowest geomorphic surface is occupied by recent alluvium (Qar), featuring bar-and-swale topography, steep-walled channels, sparse vegetation, and a lack of topsoil development (Fig. 31d). The weakly developed soils and correlations to similar deposits to the south (Jochems and Koning, 2015) indicate that the bulk of the Qay deposit is likely Pleistocene to middle Holocene, with the inset terraces (Qayi) being middle to late Holocene.

Younger alluvium also underlies the Rio Grande valley, which we call Qarrg. These unconsolidated to weakly consolidated deposits are inferred to be of similar age to Qay (uppermost Pleistocene to Holocene). The Rio Grande alluvium is probably 10–20 m thick based on subsurface interpretations in Person et al. (2024). This alluvium is dominated by sand based on a well log just east of the quadrangle border, with likely subordinate deposits of clay to silt and sandy gravel to gravelly sand.

Eolian and sheetflood deposits

Wind-blown (eolian) sand is mapped on the lee side of topographic highs (Qe) and as sheet-like deposits on mesa tops (Qes). The slope-draping eolian sand (Qe) lacks soils and is loose to weakly consolidated. The sand is light brown to light yellowish brown, fine- to medium-grained, well sorted, subangular to rounded, and quartzo-feldspathic. Mesa-top sands (Qes) can locally be silty and older than Qe. Qes sand is fine- to medium-grained, relatively massive, and quartzo-feldspathic. Weakly developed, buried soils are present with weak to moderate ped development and Stage I calcium carbonate morphology. Locally, coppice dunes are found on the surface of Qes.

Sheetflood deposits (Qs) drape gently sloping surfaces and are less than about 5 m thick. This unit consists of massive sand with minor, scattered pebbles. Sand is very fine- to fine-grained with subordinate medium- to very coarse-grained sand. Pedogenesis is indicated by Stage I calcic horizons and weak to moderate, subangular blocky ped development that typically lacks clay illuviation. The sand contain a high proportion of quartzo-feldspathic sand inputted via eolian processes or reworking of the axial-fluvial lithofacies of the Palomas Formation (QNpa).

GEOMORPHIC SURFACES

Three noteworthy geomorphic surfaces are present on the Elephant Butte quadrangle. The first is the Cutter surface in the Cutter sag (Lozinsky, 1986). This is an erosional surface that has beveled Upper Cretaceous strata. It is commonly covered by younger deposits (QNj) consisting of pale-red to buff silt and sand with pebble and cobble interbeds, probably representing a mix of eolian, sheetflood (an older version of the Qs map unit), and alluvial deposits. In places, the younger deposits are overlain by the QNb basalt flows. The Cutter surface generally slopes to the west, consistent with the slope of the overlying QNb basalts. Because of post-800 ka incision of tributaries of the Rio Grande, the Cutter surface only occurs in remnants, particularly beneath the QNb basalt flows and in the southeastern corner of the quadrangle. At its lowest elevation, the surface is 150 m above the modern base level. It likely formed during a period of quiescence of activity along the Hot Springs fault (Lozinsky, 1986).

In contrast to the Cutter surface, the Cuchillo surface has been interpreted as a constructional (aggradational) surface marking the culmination of the Santa Fe Group (Lozinsky, 1986; McCraw and Love, 2012, and references therein). It slopes 1–2° to the southeast and projects to about 90 m above the modern floodplain of the Rio Grande (McCraw and Love, 2012). It is typically underlain by the upper-coarse unit of the upper Palomas Formation (Qppwc) and has relatively mature, thick (commonly >1.5 m) soils consisting of thick argillic (Bt) horizons overlying petrocalcic horizons of Stage III to IV carbonate morphology (McCraw and Love, 2012). The surface extends farther west and north to occupy much of the Palomas basin and western Engle basin (McCraw and Love, 2012). The Cuchillo surface is sufficiently distinctive that it can be mapped.

The last geomorphic surface, also shown on the geologic map, is the top of the Holocene-age valley fill. This is mapped on fans and terraces flanking low-order drainages west of the Rock Creek road. As mentioned above, the surface is associated with a topsoil exhibiting Stage I+ to II calcic horizon(s) and local A horizons.

STRUCTURE

Noteworthy structures on the Elephant Butte quadrangle include faults and folds (Fig. 31). The most prominent structure is the Hot Springs fault, which extends northeast across the entire quadrangle. Down-to-the-west motion along this fault has juxtaposed the Palomas Formation (to the west) against Upper Cretaceous strata to the east. Near the southern border of the quadrangle, lowest Palomas Formation strata (Nppes) are juxtaposed against upper Paleozoic strata to the east. West of the Hot Springs fault, only one fault has been mapped in the Santa Fe Group, a western splay of the Hot Springs fault about 750 m southwest of the earthen auxiliary dam.

Palomas Formation strata are mostly subhorizontal, but older units (especially units Nppe and Nppes) are tilted relatively steeply northwestward along the Hot Springs fault in a manner consistent with normal drag along that fault in the late Neogene (Fig. 27). Away from the fault, Santa Fe Group strata dip relatively gently and are interpreted to form a broad syncline trending parallel to the Hot Springs fault and plunging gently northeastward (Fig. 23). In lower Cuchillo Negro Creek, attitudes using Nppe strata indicate northwest dips of about 3°. The difference in elevation of the top of Nppe in the City of Elephant Butte's No. 2 and No. 3 wells indicates an apparent westward dip of about 1°. A three-point attitude calculation of the top of Nppe using the Getty West Elephant Butte No. 2 Federal Well, City of Elephant Butte No. 3 well, and well RG-68920 gives a 1° along and a dip direction of 348 °. But 2–2.5 km northwest of the City of Elephant Butte No. 3 well, surface attitudes indicate a very slight easterly dip of 1°. The plotted syncline axis on the northwestern part of the quadrangle is plotted with these constraints and assuming an approximately parallel trend to the Hot Springs fault. This north-northeast-plunging syncline can be viewed as a slightly folded structural ramp between the overlapping Hot Springs fault and Mud Springs fault (Fig. 1).

Faults mapped in Cretaceous strata east of the Hot Springs fault are primarily normal and can be categorized into two sets: (1) north-northeast-trending faults with traces generally longer than 1.5 km and (2) randomly trending faults with traces generally shorter than 1.5 km that have throws less than 30 m (Lozinsky, 1986). The first set has experienced primarily normal movement with only very minor strike-slip. However, there are exceptions to this generalization: the Hot Springs fault and a pair of faults located north of Kettle Top have experienced some strike-slip (Lozinsky, 1986). Fault-plane dips are 40° to nearly vertical, and most of these faults have experienced west-down normal displacement. Stratigraphic throw is mostly a few tens of meters, but can range from about 3 m to more than 300 m. Because of lateral juxtaposition of lithologic units having differing resistance to erosion, these faults can produce prominent topographic lineaments (Lozinsky, 1986).

The second fault type also shows primarily normal motion, but such faults generally only have less than 30 m of stratigraphic throw (Lozinsky, 1986). Their fault-planes dip 60–80°. Included in this fault set are northwest-striking faults slightly offsetting Cretaceous contacts in Mescal Canyon. However, one newly mapped fault immediately east of the mouth of Mescal Canyon has northeast-down stratigraphic displacement of at least 400 m, such that the Mancos, Tres Hermanos, and Gallup Formations are down-dropped into the subsurface north of it (stratigraphic displacement magnitude considers the thickness of those units per Fig. 3).

By far, the most prominent structure is the Hot Springs fault, which trends N20–30°E, dips about 70–80° to the west, and extends across the entire quadrangle. This fault separates Cretaceous and older bedrock from the Santa Fe Group. Although it exhibited normal, west-side-down displacement during rifting (at least 500 m per Cross-Section A-A'), fault plane kinematic features and stratigraphic relations in pre-Santa Fe Group rocks indicate a notable component of earlier right-lateral offset (Harrison and Cather, 2004 Lozinsky, 1986), probably during the Laramide orogeny (Harrison and Cather, 2004). Two east-plunging anticlines in Ash Canyon Formation strata in the immediate hanging wall of the fault, 0.4 km south of the earthen auxiliary dam, is also consistent with right-lateral slip. The magnitude of this right-lateral slip varies, with estimates ranging from 460 m (Lozinsky, 1986) to 26 km (Harrison and Cather, 2004).

This mapping does not provide new constraints on this slip magnitude, but we think the lower end of the range of right-lateral slip values is probably more appropriate. We do interpret that the Hot Springs fault probably was a right-oblique reverse fault. Near the auxiliary dam, Cretaceous strata clearly steep westward towards the fault (see Cross-section A–A'). Also, folding observed in the San Andres Formation-cored butte immediately south of the mouth of the bedrock gorge carved by the Rio Grande (2.5 km WSW of the cement dam) is consistent with a reverse component of throw (Lucas et al., 2025). Furthermore, our preferred interpretation of sub-Santa Fe Group stratigraphy, based on the cuttings of the Getty No. 2 West Elephant Butte well and illustrated in Cross-section A–A", indicates that the majority of Cretaceous strata was eroded prior to deposition of the Santa Fe Group. Assuming relatively gentle stratal dips (consistent with the parallel nature of the cross section line trend with the gravity contours of Gilmer et al. [1986]), the top of the Cretaceous on the west side of the Hot Springs fault near Elephant Butte consists of Gallup Sandstone and lowest strata of the overlying Fence Canyon Formation. On the east side of the fault, the entire Fence Canyon Formation is preserved as well as 100 m of the Ash Canyon Formation. These observations and stratigraphic-structural relations are consistent with erosion of uplifted bedrock terrain west of the Hot Springs fault during the Laramide orogeny.

Our research also gives a minimum age constraint for the Hot Springs fault. Clear drag folding is present in unit Nppe on the immediate hanging wall of the Hot Springs fault (Fig. 27), and this drag folding caused angular unconformities in the underlying Nrpe unit (Fig. 6). Therefore, the fault was experiencing normal motion in the late Miocene and early Pliocene. However, the Hot Springs fault did not offset the maar deposits of Rattlesnake Island (Fig. 26). Considering the age of two dikes intruding the maar deposits (Table 2), this means that the last notable displacement of the Hot Springs fault occurred prior to 2.5 Ma. It should be noted that the position of the Hot Springs fault is relatively well constrained on the south side of Rattlesnake Island, due to the fact that in low lake levels Hall Lake Formation strata can be observed juxtaposed against easily erodible, sandy axial-fluvial facies of the Palomas Formation (QNpa).

Larger folds mapped in Cretaceous strata in the Cutter sag are typically open, symmetrical, and upright (Lozinsky, 1986). These folds strike 285° to north to 055°. Fold limb dips seldom exceed 20°. Strikes of the larger folds are nearly parallel or normal to the major fault trends. Northwest-trending folds inferred for the Truth or Consequences area (Kelley and Silver, 1952; Seager and Mack, 2003) have locally produced overturned strata, such as those observed in the isolated exposure of lower Abo and upper Bar B Formation strata between the Rio Grande and the northern Caballo Mountains (UTM coordinates of 292655 m E, 3668810 m N; NAD83, zone 13). The northwest folds in the Cretaceous strata in the southeast part of the quadrangle are interpreted to be formed early in the Laramide due to northeast-directed vergence (Seager et al., 1997).

Smaller folds east of the Hot Springs fault seldom exceed 100 m in length, and most appear to be north- to northwest-trending (Lozinsky, 1986). These small folds are primarily open, symmetrical, and upright. A fold along Long Ridge has a curved axial trace, which may be due to right-lateral strike slip along the Hot Springs fault (Lozinsky, 1986).

The prominent andesite dikes on the quadrangle are important because they are not folded and appear only minimally offset by faults. Faults thus postdate folding and may possibly postdate the majority of offset associated with faulting. The amount of offset by faults ranges from 0 to 50 m, with 10–20 m being typical. However, the dikes exhibit local stepping behavior in the absence of faults, and in many cases it is difficult to know if the dike is stepping in response to hetereogeneity associated with a previous fault or if it has been faulted. More fieldwork is planned to investigate both the age of the dikes and their cross-cutting relations with faults.

We postulate that each maar-related eruptive center may be located in a fault zone or at intersections of prominent faults. For example, Rattlesnake Island lies directly on the trend of the Hot Springs fault, although the fault does not displace its deposits. Also, the Elephant Butte vent and ring dike are centered on a rhombic depression bounded by normal faults in the surrounding Cretaceous sediments; this geometry may define a dilational domain along the Hot Springs fault.

SUMMARY OF GEOLOGIC HISTORY

Paleozoic

In this section, we provide a synopsis of the geologic history of the Elephant Butte quadrangle. We emphasize Cenozoic history because of the detailed coverage of Cretaceous and upper Paleozoic strata by earlier workers (e.g., Kelley and Silver, 1952; Seager and Mack, 2003; Lucas et al., 2012b, 2012c, 2019). The reader is referred to these and cited work below for further details of past depositional environments, history of geologic structures and tectonic episodes, and age control.

During the Ordovician, deposition of carbonates of the Montoya Formation occurred within 30° of the equator on a gently sloping carbonate ramp on a mature passive margin (Pope, 2004). Interestingly, this was a time of inferred glacial paleoclimates (Frakes et al., 1992). Younger strata are Upper Pennsylvanian (Gray Mesa and Bar B Formations) and lower to middle Permian (Abo Formation, Yeso Group, San Andres Formation). These strata record a transition from dominantly marine deposits in the Late Pennsylvanian (i.e., Desmoinesian through Virgilian) into fluvial and eolian, sabkha, and intertidal deposits associated with a broad coastal plain and adjoining shoreline during the early Permian (Wolfcampian and early Leonardian; Seager and Mack, 2003; Kues and Giles, 2004). During the late Leonardian to early Guadalupian, a marine transgression deposited limestones of the San Andres Formation. In the upper San Andres Formation, the limestones intertongue with fine- to medium-grained sand inferred to be associated with nearshore or eolian deposits.

The Upper Pennsylvanian is noteworthy for its cyclical ice ages and associated sea level changes as well as Ancestral Rocky Mountain tectonism (Kues and Giles, 2004). Ancestral Rocky Mountain tectonic activity in the Missourian and Virgilian likely accounts for the abrupt lithofacies and thickness changes in the Bar B Formation between the Mud Springs Mountains and the northern Caballo Mountains (Lucas et al., 2012a, 2012c). Tectonism decreased in the Truth or Consequences area during the early Permian. By the Permian, earlier temperate climates of the Pennsylvanian were replaced by arid conditions (Kues and Giles, 2004), possibly related to the continental effects of assembling Pangea (Mack and Dinterman, 2002).

Cretaceous through Paleocene

A major unconformity separates middle Permian from Upper Cretaceous strata, attributed to non-deposition and erosion during tilt-related uplift on the north side of the Bisbee basin and related Chihuahua trough (Cather, 2012). The Cretaceous strata begin with fluvial and marginal marine strata of the Dakota Sandstone, which are conformably overlain by the marine Mancos Shale. The lower Mancos

Shale (95–92 Ma; Hook et al., 2012) records a transgression (T1) followed by a regression (R1) (note that T and R nomenclature follows Molenaar [1983]). The regression resulted in deposition of the regressive Atarque Sandstone Member of the Tres Hermanos Formation (barrier island paleoenvironment), followed by swamps, floodplains, and fluvial deposits of the Carthage Member (Mack et al., 2015). A renewed transgression produced a nearshore sandstone (Fite Ranch Member of the Tres Hermanos Formation), followed by deposition of the marine D-Cross Tongue of the Mancos Shale. A sea level turnaround occurred within the D-Cross Tongue. During the ensuing R2 transgression, sea level decline allowed predominately deltaic sandstones to accumulate in the form of the Gallup Sandstone (Seager and Mack, 2003).

Terrestrial paleoenvironments characterized by fluvial deposition, with minor swamp and pond deposits, occurred during the Late Cretaceous after about 89 Ma (Seager and Mack, 2003; Hook et al., 2012; Lucas et al., 2019). These deposits typify the Flying Eagle Canyon Formation, which conformably overlies the Gallup Sandstone, has subordinate fine- to medium-grained sandstone tongues, and locally has coals at its base. As the shoreline of the Western Interior Seaway moved progressively farther to the east-northeast, fluvial sediment experienced a gradual, overall coarsening so that the Ash Canyon Formation has subequal or a dominance of sandstones compared to fine-grained strata. Relatively humid climatic conditions were the norm for both of these terrestrial formations (Seager and Mack, 2003; Lucas et al., 2019).

After about 75 Ma, strata accumulated in the northwest-trending, intraforeland Love Ranch basin, where tectonic subsidence occurred adjacent to northwest-trending reverse faults bounding the Rio Grande uplift (Seager et al., 1997; Amato et al., 2017). Drab-colored siltstones, mudstones, and sandstones of the José Creek Formation contain volcaniclastic conglomeratic sandstones shed from intermediate volcanoes to the southwest. Subhumid conditions transformed into more arid conditions so that oxidized, reddish mudstones are common in the Hall Lake Formation (Buck, 1992; Buck and Mack, 1995). Both the José Creek and Hall Lake Formations have yielded dinosaur fossils that include ceratopsians, *Ankylosaurus*, sauropods, and *Tyrannosaurus rex* (Lozinsky et al., 1984). New age controls (Schantz et al., 2024) indicate that the Cretaceous-Paleogene boundary occurs within the upper Hall Lake Formation, and the overlying, grayish-tannish Double Canyon Formation represents fluvial deposition during the Paleocene.

Neogene–Quaternary

Following emplacement of long, andesitic dikes sometime in the Eocene or Oligocene, prolonged deposition of rift-related sediment occurred during the Neogene. The earliest Neogene deposits are assigned to the Rincon Valley Formation. The lowest strata of the Rincon Valley are sandstones and clayey fine sand encountered at 1,330–1,680 ft depths of the Getty West Elephant Butte No. 2 Federal Well (Table 2), possibly of middle Miocene age. Overlying deposits are reddish and relatively clayey. Both represent deposition in a subsiding Engle basin, where distal alluvial fans from the Mud Springs Mountains sloped northeastward toward a flat, clayey basin floor. By the late Miocene, a playa lake deposit expanded and deposited reddish-brown clay (616–1,330 ft in the Getty well). In addition to flanking the northeastern Mud Springs Mountains, pebbly alluvial fans extended along the eastern side of the Engle basin (unit Nrpe), and the playa lake deposits were relatively sandy at the toes of these eastern fans. The eastern alluvial fans contain abundant intermediate volcanic clasts (Fig. 7), indicating more extensive coverage of the José Creek Formation in the Cutter sag during the late Miocene. The Rio Grande extended into the Engle basin in the late Miocene, the timing of which will be discussed in a future paper, and deposited quartz-rich sand as fluvio-deltaic lobes into a playa lake (Nrpd). Outcrops of interbedded quartz sand and reddish-brown clay (Fig. 8) indicate that the playa lake at this time extended into Truth or Consequences. The fluvio-deltaic system progressively prograded south, completing the transformation of a formerly closed basin to an open basin with a south-flowing axial river.

The Palomas Formation, assigned to strata of the Engle and surrounding basins that were deposited when an axial-fluvial system was present, has three vertically stacked intervals (layers), indicating differing stages of the Plio-Pleistocene basin evolution (Fig. 11). The lower layer, inferred to be early Pliocene, exhibits notably coarse alluvial fans that flanked a narrow axial river. Drainages associated with these alluvial fans inputted relatively high quantities of locally derived gravel into the axial river, as noted in previous stratigraphic studies in the Truth or Consequences area (e.g., Tpao of Koning et al. [2018a] and Tpal1 and Tpal2 of Koning et al. [2016]). At times, there was sufficient discharge to transport cobbly gravel and also form 2- to 2.5-m-thick lateral accretion sets in these gravelly deposits (e.g., Fig. 6; Koning et al., 2016).

The middle interval, which contains 3.5–3.0 Ma fossil deposits (Morgan and Lucas; 2012; Koning et al., 2018b), is characterized by notably finer grained sediment in both the piedmont and the axial-river deposits. Note that “piedmont” includes both distinctive alluvial fans closer to the mountain front and coalesced alluvial fans near the basin interior. In addition, the valley floor (i.e., the area occupied by river channels, floodplains, and floodplain margins) expanded at the expense of the piedmont, which narrowed. Paleoflow data indicate that the Cuchillo Negro fan was relatively larger than the Alamosa alluvial fan so that drainages could flow off of the northern Cuchillo Negro fan and then wrap back around southward so that, on the northwestern quadrangle, there is south to southeastward paleoflow measured for channel fills containing Cuchillo Negro clasts.

The upper interval of the Palomas Formation (map units Qppw, Qppuc) generally encompasses the early Pleistocene (Mack et al., 1993, 1998b; Jochems and Koning, 2015; Koning et al., 2019). It is noted for eastward progradation of the western piedmont and an eastward shift of the axial-fluvial environment. In the distal piedmont, paleoflow ranged from east to south. Also during this time, if not earlier, the Cutter geomorphic surface formed, presumably in conjunction with low (or perhaps near-zero per Koning et al. [2019]l) slip rates on the Hot Springs fault (Lozinsky, 1986). The Cuchillo Negro fan continued to be relatively large, and paleoflow of associated drainages at the distal coalesced fan continued to be southward. However, during the last stages of deposition of the upper interval, the Alamosa fan appears to have expanded southward, depositing a few meters of felsic-dominated gravel (with much Vicks Peak Tuff) over gravel previously deposited by Cuchillo Negro Creek drainages.

The Santa Fe Group stopped aggrading around 800 ka (Mack et al., 1993, 1998b, 2006; Mack and Leeder, 1999); this was followed by incision of the Rio Grande and local drainages. This incision left the former valley floor (including piedmont slopes) elevated and inactive, creating the Cuchillo geomorphic surface. The Rio Grande and linked tributaries progressively incised throughout the middle to late Pleistocene. Climatically driven episodes of aggradation, along both the Rio Grande and tributary streams, formed fill terraces (Davie and Spiegel, 1967; Gile et al., 1981; McCraw and Williams, 2012; Koning et al., 2018b; Sion et al., 2020). The five general terrace levels mapped on the Elephant Butte quadrangle record these back-filling events or prolonged periods where the base level was relatively stable.

Post-Santa Fe Group incision eroded variable amounts of the four maar complexes. The most eroded is the Rock Canyon maar, where all but the roots of the maar volcano has been eroded. Cinder-rich strata at the top of the base surge sequence and isolated tongues of a basalt flow suggest a cinder cone may have once existed here.

MINERAL AND AGGREGATE DEPOSITS

Manganese mining occurred in the western Truth or Consequences area, west of Locust Avenue, in the Ellis mining district (Wells, 1918; Russell, 1947; Farnham, 1961; Lueth et al., 2012). Manganese precipitation also occurred along the Hot Springs fault on the southernmost part of this quadrangle. The Solomon and Diamond Ranch prospects were filed in the 1950s, but minimal production was recorded (https://thediggings.com/mines/3210).

Of greater economic value is aggregate mining from fill terraces and, locally, relatively non-cemented axial-fluvial sand of the Palomas Formation. The largest of these operations is Bartoo Sand and Gravel. This quarry operation is found on the west-central part of the quadrangle northwest of New Mexico State Road 181, where mining has occurred in the valley of Cuchillo Negro Creek and slopes to the north. A smaller gravel operation exploited terrace gravel and gravel and axial-fluvial sand 1.5 km to the northeast. Possibly more terrace deposits could be exploited, but this is hampered by urbanization and, to the east, the fact that eastern piedmont deposits (Nppe) underlie the terrace gravels. These Nppe deposits are cemented and somewhat clayey-silty and probably considered as waste, whereas to the west, the lesser-cemented and relatively clay-free axial-fluvial deposits are of economic value.

HYDROGEOLOGIC IMPLICATIONS

We interpret that the axial-fluvial lithofacies of the Palomas Formation (which includes units QNpa and Npal2) is of notable hydrogeologic importance to the town of Elephant Butte. This lithofacies consists of a relatively clean sand that likely has high permeability and storage capacity. Its importance is illustrated by the fact that more than 90% of the investigated wells in Elephant Butte are screened in this lithofacies (based on our investigation of SEO well records from the Office of the State Engineer (SEO)). The underlying unit is generally eastern piedmont facies (Nppe), is notably cemented, and contains silty-clayey sand and pebbly sand tongues. The axial-fluvial unit has a lower coarse-grained interval observed near downtown Truth or Consequences (map unit Npal2, correlating to Tpal2 of Koning et al. [2018b]), and this coarse-grained interval is also interpreted in the Getty West Elephant Butte No. 2 Federal Well. However, unit Npal2 appears to interfinger eastward with the lower-permeability eastern piedmont facies (Nppe), and its east-west extent is relatively narrow, around 1 km (see cross section A–A'). The two units combined have a total a total thickness of 150 m, but where unit QNpa overlies Nppe it is 100 m thick; the top of the potentiometric surface is roughly 30–40 m deep, so the saturated thickness is 60–70 m. Based on our structural interpretations, the axial-fluvial lithofacies is part of a gently north-northeast-plunging syncline, so this lithofacies is thickest near the syncline axial and would likely thicken somewhat to the north. There are sufficient wells to produce a structural contour map of the base of the axial lithofacies. Combined with a map of the potentiometric surface, such a structural contour map would help in characterizing the region's groundwater resources.

REFERENCES

Amato, J.M., Athens, C., McIntosh, W.C., and Peters, L., 2012, U-Pb zircon ages from crustal xenoliths in a Pliocene basalt flow from the southern Rio Grande rift: New Mexico Geological Society Guidebook, 63rd Field Conference, Warm Springs Region, p. 273–284.

Amato, J.M., Mack, G.H., Jonell, T.N., Seager, W.R., and Upchurch, G.R., 2017, Onset of the Laramide orogeny and associated magmatism in southern New Mexico based on U-Pb geochronology: Geological Society of America Bulletin, v. 129, no. 9–10, p. 1209–1226.

Bachman, G.O., and Mehnert, H.H., 1978, New K-Ar dates and the late Pliocene to Holocene geomorphic history of the central Rio Grande region, New Mexico: Geological Society of America Bulletin, v. 89, p. 283–292.

Bauer, R.D., 1989, Depositional environments, sediment dispersal, and provenance of the Dakota Sandstone, Caballo Mountains, south-central New Mexico [M.S. thesis]: Las Cruces, New Mexico State University, 64 p.

Bryan, K., 1938, Geology and groundwater conditions of the Rio Grande depression in Colorado and New Mexico: *in* Natural Resources Planning Board (U.S.), The Rio Grande joint investigations in the upper Rio Grande Basin: Washington, D.C., U.S. Government Printing Office, v. 1, pt 2, p. 197–225.

Buck, B.J., 1992, Deterioration of paleoclimate in the Late Cretaceous, indicated by paleosols in the McRae Formation, south-central New Mexico [M.S. thesis]: Las Cruces, New Mexico State University, 69 p.

Buck, B.J., and Mack, G.H., 1995, Latest Cretaceous (Maastrichtian) aridity indicated by paleosols in the McRae Formation, south-central New Mexico: Cretaceous Research, v. 16, issue 5, p 559–572.

Bushnell, H.P., 1953, Geology of the McRae Canyon area, Sierra County, New Mexico [M.S. thesis]: Albuquerque, University of New Mexico, 106 p.

Bushnell, H.P., 1955a, Mesozoic stratigraphy of south-central New Mexico: New Mexico Geological Society, Guidebook 6, p. 81–87.

Bushnell, H.P., 1955b, Stratigraphy of the McRae Formation, Sierra County, New Mexico: The Compass of Sigma Gamma Epsilon, v. 33, p. 9–17.

Cather, S.M., 2012, The sub-Cretaceous unconformity in New Mexico: New Mexico Geological Society Guidebook, 63rd Field Conference, p. 407–412.

Cikoski, C.T., Nelson, W.J., Koning, D.J., Elrick, S., and Lucas, S.G., 2017, Geologic map of the Black Bluffs 7.5-minute quadrangle, Sierra County: New Mexico Open-file Geologic Map 262, scale 1:24,000.

Climate-Data.org, 2025, Truth or Consequences climate: https://en.climate-data.org/north-america/united-states-of-america/new-mexico/truth-or-consequences-131324/

Darton, N.E., 1922, Geologic structure of parts of New Mexico: U.S. Geological Survey, Bulletin 726-E, p. 173-275.

Davie, W., Jr., and Spiegel, Z., 1967, Geology and water resources of Las Animas Creek and vicinity, Sierra County, New Mexico: New Mexico State Engineer Hydrographic Survey Report, 44 p.

Doyle, J.C., 1951, Geology of the northern Caballo Mountains, Sierra County, New Mexico [M.S. thesis]: Socorro, New Mexico Institute of Mining and Technology, 51 p.

Estrada-Ruiz, E., Upchurch, G.R., Jr, Wheeler, E.A., Mack, G.H., 2012a, Late Cretaceous angiosperm woods from the Crevasse Canyon and McRae Formations, south-central New Mexico, USA., International Journal of Plant Science, v. 173, p. 412–428.

Estrada-Ruiz, E., Parrott, J.M., Upchurch, G.R. Jr., Wheeler, E.A., Thompson, D.L., Mack, G.H., and Murray, M.M., 2012b, The wood flora from the upper Cretaceous Crevasse Canyon and McRae Formations, south-central New Mexico, USA: A progress report: New Mexico Geological Society, 63rd Field Conference, p. 502–518.

Estrada-Ruiz, E., Wheeler, E.A., Upchurch, G.R. Jr., Mack, G.H., 2018, Late Cretaceous angiosperm woods from the McRae Formation, south-central New Mexico, USA, Part 2International Journal of Plant Sciences, v. 179, no. 2, p. 136–150.

Farnham, L.L., 1961, Manganese deposits of New Mexico: U.S. Bureau of Mines Circular 8030, 176 p.

Fitzsimmons, J.P., ed., 1955, South-central New Mexico: New Mexico Geological Society, 6th Field Conference, 193 p.

Foster, R., 2009, Basin-fill architecture of the Pliocene-Lower Pleistocene Palomas Formation adjacent to the intrabasinal Mud Springs Mountains, southern Rio Grande rift [unpublished M.S. thesis]: Las Cruces, New Mexico State University, 81 p.

Frakes, L.A., Francis, J.E., and Syktus, J.I., 1992, Climate modes of the Phanerozoic: Cambridge, Cambridge University Press, 274 p.

Gile, L.H., Hawley, J.W., and Grossman, R.B., 1981, Soils and geomorphology in the Basin and Range area of southern New Mexico—Guidebook to the Desert Project: New Mexico Bureau of Geology and Mineral Resources, Memoir 39, 222 p.

Gillette, D.D., Wolberg, D.L., and Hunt, A.P., 1986, *Tyrannosaurus rex* from the McRae Formation (Lancian, Upper Cretaceous), *in* Clemons, R.E., King, W.E., Mack, G.H., and Zidek, J., eds., Truth or Consequences Region: New Mexico Geological Society, Guidebook 37, p. 235–238.

Gilmer, A.L., Mauldin, R.A., and Keller, G.R., 1986, A gravity study of the Jornada del Muerto and Palomas Basins: New Mexico Geological Society, 37th Annual Fall Field Conference Guidebook, p. 131–134.

Gordon, C.H., 1910, Sierra and central Socorro Counties, in Lindgren, W., Graton, L.C., and Gordon, C.H.. eds., The Ore Deposits of New Mexico: U.S. Geological Survey Professional Paper 68, p. 213–285.

Gordon, C.H., and Graton, L.C., 1907, Lower Paleozoic formations in New Mexico: Journal of Geology, v. 15, p. 91–92.

Harbour, R.L., 1970, The Hondo Sandstone Member of the San Andres Limestone of south-central New Mexico: U.S. Geological Survey, Professional Paper 700-C, p. C175–C182.

Harley, G.T., 1934, The geology and ore deposits of Sierra County, New Mexico: New Mexico Bureau of Mines and Mineral Resources, Bulletin 10, 220 p.

Harrison, R., and Cather, S., 2004, The Hot Springs fault system of south-central New Mexico—evidence for northward translation of the Colorado Plateau during the Laramide orogeny, *in* Cather, S.M., McIntosh, W.C., and Kelley, S.A., eds., Tectonics, geochronology, and volcanism in the southern Rocky Mountains and Rio Grande rift: New Mexico Bureau of Geology and Mineral Resources, Bulletin 160, p. 161-180.

Hawley, J.W., and Kottlowski, F.E., 1969, Quaternary geology of the south-central New Mexico border region: New MexicoBureau of Mines and Mineral Resources, Circular 104, p. 89–115.

Hawley, J.W., Bachman, Hook, S.C., and Cobban, W.A., 2015, The type section of the Upper Cretaceous Tokay Tongue of the Mancos Shale (new name), Carthage coal field, Socorro County, New Mexico: New Mexico Geology, v. 37, p. 27–46.

Hook, S.C., Mack, G.H., and Cobban, W.A., 2012, Upper Cretaceous stratigraphy and biostratigraphy of south-central New Mexico: New Mexico Geological Society Guidebook, 63rd Field Conference, Warm Springs Region, p. 413-430.

Hook, S.C., and Cobban, W.A., 2015, The type section of the Upper Cretaceous Tokay Tongue of the Mancos Shale (new name), Carthage coal field, Socorro County, New Mexico: New Mexico Geology, v. 37, p. 27–46. https://doi.org/10.58799/NMG-v37n2.27

Hunter, J.C., 1986, Laramide synorogenic sedimentation in south-central New Mexico: petrologic evolution of the McRae basin [M.S. thesis]: Golden, Colorado School of Mines, 75 p.

Jochems, A.P., 2015, revised 2019, Geologic map of the Williamsburg NW 7.5-minute quadrangle, Sierra County, New Mexico: New Mexico Open-file Geologic Map 251, scale 1:24,000.

Jochems, A.P., and Koning, D.J., 2014, revised May-2023, Geologic map of the Williamsburg 7.5-minute quadrangle, Sierra County, New Mexico: New Mexico Open-file Geologic Map 250, scale 1:24,000.

Jochems, A.P., and Koning, D.J., 2015, Holocene stratigraphy and a preliminary geomorphic history for the Palomas Basin, south-central New Mexico: New Mexico Geology, v. 37, no. 4, p. 77–88.

Kelley, V.C., 1971, Geology of the Pecos country, southeastern New Mexico: New Mexico Bureau of Mines and Mineral Resources, Memoir 24, 78 p.

Kelley, V.C., and Silver, C., 1952, Geology of the Caballo Mountains, with special reference to regional stratigraphy and structure and mineral resources, including oil and gas: University of New Mexico, Publications in Geology, no. 4, 286 p.

Koning, D.J., Jochems, A.P., and Cikoski, C., 2015, Geologic Map of the Skute Stone Arroyo 7.5-Minute Quadrangle, Sierra County, New Mexico: New Mexico Bureau of Geology and Mineral Resources, Open-file Geologic Map 252, scale 1:24,000.

Koning, D.J., Jochems, A.P., Morgan, G.S., Lueth, V., and Peters, L., 2016, Stratigraphy, gravel provenance, and age of early Rio Grande deposits exposed 1-2 km northwest of downtown Truth or Consequences, New Mexico, *in* Frey, B.A., Karlstrom, K.E., Lucas, S.G., Williams, S., Ziegler, K., McLemore, V., and Ulmer-Scholle, D., eds., The Geology of the Belen area: New Mexico Geological Society, 67th Annual Field Conference, Guidebook, p. 459–478.

Koning, D.J., Jochems, A.P., and Heizler, M.T., 2018a, Early Pliocene paleovalley incision during early Rio Grande evolution in southern New Mexico, *in* Mack, G.H., Hampton, B.A., Ramos, F.C., Witcher, J.C., and Ulmer-Scholle, D.S., eds., Las Cruces Country III: New Mexico Geological Society, 69th Field Conference Guidebook, p. 93–108.

Koning, D.J., Jochems, A.P., Foster, R., Cox, B., Lucas, S., Mack, G.H., and Zeigler, K.E., 2018b, Geologic map of the Cuchillo 7.5-minute quadrangle, Sierra County, New Mexico: New Mexico Bureau of Geology and Mineral Resources, Open-file Geologic Map 271, scale 1:24,000.

Koning, D.J., Jochems, A.P., Zimmerer, M.J., Kelley, S.A., and Gavel, M.M., 2019, Neogene-Quaternary evolution and decreases in throw rates on major faults in the northern Palomas Basin and its structural boundary with the Engle Basin, southern Rio Grande rift, N.M.: Geological Society of America *Abstracts with Programs*, vol. 51, no. 5, Paper No. 51-5.

Kottlowski, F.E., Flower, R.H., Thompson, M.L., and Foster, R.W., 1956, Stratigraphic studies of the San Andres Mountains, New Mexico: New Mexico Bureau of Mines and Mineral Resources, Memoir 1, 132 p.

Krainer, K., Lucas, S.G., and Brose, R., 2012, Principal reference section of the Permian San Andres Formation: New Mexico Geological Society, 63rd Field Conference Guidebook, Warm Springs Region, p. 395–406.

Kues, B.S., and Giles, K.A., 2004, The late Paleozoic Ancestral Rocky Mountains system in New Mexico, in Mack, G.H., and Giles, K.A., eds., The Geology of New Mexico, A Geologic History: New Mexico Geological Society, Special Publication 11, p. 95–136.

Lawton, T.F., Giles, K.A., Mack, G.H., Singleton, D.S., and Thompson, A.D., 2002, Lower Wolfcampian conglomerate in the southern Caballo Mountains, Sierra County New Mexico—stratigraphy, correlation, and implications for late Pennsylvanian–Early Permian tectonics: New Mexico Geological Society, 53rd Fall Field Conference Guidebook, Geology of White Sands, p. 257–265.

Lee, W.T., 1905, The Engle coal field, New Mexico: U.S. Geological Survey, Bulletin 285, p. 240.

Lee, W.T., 1907a, Water resources of the Rio Grande valley in New Mexico and their development: U.S. Geological Survey, Water Supply Paper 188, 59 p.

Lee, W.T., 1907b, Notes on red beds of the Rio Grande region in central New Mexico: Journal of Geology, v. 15, p. 52–58.

Levron, R.Z., 1995, Morphology and geochemistry of paleosols of the José Creek Member of the McRae Formation (Cretaceous: Maastrichtian), south-central New Mexico [M.S. thesis]: Las Cruces, New Mexico State University, 104 p.

Lozinsky, R.P., 1986, Geology and late Cenozoic history of the Elephant Butte area, Sierra County, New Mexico: New Mexico Bureau of Geology and Mineral Resources, Circular 187, Memoir 49, 40 p. and 2 plates.

Lozinsky, R.P., 1987, Cross section across the Jornada del Muerto, Engle, and northern Palomas Basins, south-central New Mexico: New Mexico Geology, v. 9, no. 3, p. 55–57, 63.

Lozinsky, R.P., and Hawley, J.W., 1986, The Palomas Formation of south-central New Mexico—A formal definition: New Mexico Geology, v. 8, no. 4, p. 73–78, 82.

Lozinsky, R.P., Hunt, A.P., Wolberg, D.L., and Lucas, S.G., 1984, Late Cretaceous (Lancian) dinosaurs from the McRae Formation, Sierra County, New Mexico: New Mexico Geology, v. 6, no. 4, p. 72–77.

Lucas, S.G., and Krainer, K., 2012, The lower Permian Yeso Group in the Fra Cristobal and Caballo Mountains, Sierra County, New Mexico: New Mexico Geological Society Guidebook, 63rd Field Conference, Warm Springs Region, p. 377–394.

Lucas, S.G., and Oakes, W., 1986, Pliocene (Blancan) vertebrates from the Palomas Formation, south-central New Mexico: New Mexico Geological Society, 37th Field Conference Guidebook, p. 277–283.

Lucas, S.G., and Zeigler, K.E., 2004, Permian stratigraphy in the Lucero uplift, central New Mexico: New Mexico Museum of Natural History and Science Bulletin 25, p. 71–82.

Lucas, S.G., Krainer, K., and Colpitts, R.M., Jr., 2005, Abo-Yeso (Lower Permian) stratigraphy in central New Mexico: New Mexico Museum of Natural History and science, Bulletin 31, p. 101–117.

Lucas, S.G., Krainer, K., and Spielmann, J.A., 2012a, Pennsylvanian stratigraphy in the Fra Cristobal and Caballo Mountains, Sierra County, New Mexico: New Mexico Geological Society Guidebook, 63rd Field Conference, Warm Springs Region, p. 327–344.

Lucas, S.G., Krainer, K., Chaney, D.S., DiMichele, W.A., Voigt, S., Berman, D.S., and Henrici, A.C., 2012b, The lower Permian Abo Formation in the Fra Cristobal and Caballo Mountains, Sierra County, New Mexico: New Mexico Geological Society Guidebook, 63rd Field Conference, Warm Springs Region, p. 345–376.

Lucas, S.G., Krainer, K., McLemore, V.T., Spielmann, J.A., and Lueth, V.W., 2012c, Mud Springs Mountains, Third-day road log from Truth or Consequences to Mud Mountain and Whiskey Canyon: New Mexico Geological Society Guidebook, 63rd Field Conference, Warm Springs Region, p. 97–121.

Lucas, S.G., Nelson, W.J., Krainer, K., and Elrick, S., 2019, The Cretaceous system in central Sierra County, New Mexico: New Mexico Geology, v. 41, no. 1, p. 3–39 + appendices.

Lucas, S.G., Nelson, W.J., Krainer, K., Barrick, J.E., Amato, J.M., Elrick, S.D., and Vachard, D., 2025, Geology of the Fra Cristobal Range, Sierra County, New Mexico: New Mexico Museum of Natural History, Bulletin 98, 163 p.

Lueth, V.W., The Ellis Manganese deposits at Truth or Consequences, New Mexico: A link between hot springs and ore deposits: New Mexico Geological Society, 63rd Fall Field Conference Guidebook, p. 126–128.

Mack, G.H., and Dinterman, P.A., 2002, Depositional environments and paleogeography of the Lower Permian (Leonardian) Yeso and correlative formations in New Mexico: The Mountain Geologist, v. 39, p. 75–88.

Mack, G.H., and Leeder, M.R., 1999, Climatic and tectonic controls on alluvial-fan and axial-fluvial sedimentation in the Plio-Pleistocene Palomas half graben, southern Rio Grande Rift: Journal of Sedimentary Research, v. 69, no. 3.

Mack, G., and Seager, W.R., 1993, Geologic map of the Engle quadrangle, Sierra County, New Mexico: New Mexico Bureau of Geology and Mineral Resources, Open-file Geologic Map 207, scale 1:24,000.

Mack, G.H., and Seager, W.R., 1995, Transfer zones in the southern Rio Grande rift: Journal of the Geological Society, v. 152, no. 3, p. 551–560.

Mack, G.H., and Suguio, K., 1991, Depositional environments of the Yeso Formation (Lower Permian), southern Caballo Mountains, New Mexico: New Mexico Geology, v. 13, p. 45–49, 59.

Mack, G.H., Salyards, S.L., and James, W.C., 1993, Magnetostratigraphy of the Plio-Pleistocene Camp Rice and Palomas Formations in the Rio Grande rift of southern New Mexico: American Journal of Science, v. 293, p. 49–77.

Mack, G.H., Lawton, T.F., and Giles, K.A., 1998a, First-day road log from Las Cruces to Derry Hills and Mescal Canyon in the Caballo Mountains: New Mexico Geological Society, Field Conference 49 Guidebook, p. 1–21.

Mack, G.H., Salyards, S.L., McIntosh, W.C., and Leeder, M.R., 1998b, Reversal magnetostratigraphy and radioisotopic geochronology of the Plio-Pleistocene Camp Rice and Palomas Formations, southern Rio Grande rift, in Mack, G.H., Austin, G.S., and Barker, J.M.. eds., Las Cruces country II: New Mexico Geological Society Guidebook 49, p. 229–236.

Mack, G.H., Cole, D.R., and Treviño, L., 2000, The distribution and discrimination of shallow, authigenic carbonate in the Pliocene-Pleistocene Palomas Basin, southern Rio Grande rift: Geological Society of America Bulletin, v. 112, no. 5, p. 643–656.

Mack, G.H., Seager, W.R., Leeder, M.R., Perez-Arlucea, M., and Salyards, S.L., 2006, Pliocene and Quaternary history of the Rio Grande, the axial river of the southern Rio Grande rift, New Mexico, USA: Earth-Science Reviews, v. 77, p. 141–162.

Mack, G.H., Dunbar, N., and Foster, R., 2009, New sites of 3.1-Ma Pumice beds in axial-fluvial strata of the Camp Rice and Palomas Formations, southern Rio Grande rift: New Mexico Geology, v. 31, p. 31–37.

Mack, G.H., Foster, R., and Tabor, N.J., 2012, Basin architecture of Pliocene-lower Pleistocene alluvial-fan and axial-fluvial strata adjacent to the Mud Springs and Caballo Mountains, Palomas half graben, southern Rio Grande rift, *in* Lucas, S.G., McLemore, V.T., Lueth, V.W., Spielmann, J.A., and Krainer, K., eds., Geology of the Warm Springs Region: New Mexico Geological Society, 63rd Annual Field Conference, Guidebook, p. 431–445.

Mack, G.H., Hook, S., Giles, K.A., and Cobban, W.A., 2015, Sequence stratigraphy of the Mancos Shale, lower Tres Hermanos Formation, and coeval middle Cenomanian to middle Turonian strata, southern New Mexico, USAL Sedimentology, v. 63, issue 4, p. 781–808.

Mason, J.T., 1976, Geology of the Caballo Peak quadrangle, Sierra County, New Mexico [M.S. thesis]: Albuquerque, University of New Mexico, 131 p.

McCraw, D.J., and Love, D.W., 2012, An overview and delineation of the Cuchillo geomorphic surface, Engle and Palomas Basins, New Mexico: New Mexico Geological Society, 63rd Field Conference Guidebook, Warm Springs Region, p. 491–498.

McCraw, D.J., and Williams, S.F., 2012, Terrace stratigraphy and soil chronosequence of Canada Alamosa, Sierra and Socorro Counties, New Mexico: New Mexico Geological Society Guidebook, 63rd Field Conference, Warm Springs Region, p. 475–490.

Melvin, J.W., 1963, Cretaceous stratigraphy in the Jornada del Muerto region, including the geology of the Mescal Creek area, Sierra County, New Mexico [M.S. thesis]: Albuquerque, University of New Mexico, 121 p.

Molenaar, C.M., 1983, Major depositional cycles and regional correlations of Upper Cretaceous rocks, southern Colorado Plateau and adjacent areas, *in* Reynolds, M.W., and Dolly, E.D., eds., Mesozoic paleogeography of the west-central United States, Rocky Mountain Paleogeography Symposium 2: Society of Economic Paleontologists and Mineralogists, Rocky Mountain Section, Denver, Colorado, p. 201–224.

Morgan, G.S., and Lucas, S.G., 2012, Cenozoic vertebrates from Sierra County, southwestern New Mexico: New Mexico Geological Society Guidebook, 63rd Field Conference, Warm Springs Region, p. 525–540.

Nelson, W.J., Lucas, S.G., Krainer, K., McLemore, V.T., and Elrick, S., 2012, Geology of the Fra Cristobal Mountains, New Mexico: New Mexico Geological Society, 63rd Field Conference Guidebook, Warm Springs Region, p. 195–210.

Pope, M.C., 2004, Upper Ordovician and lower to middle Silurian miogeoclinal rocks

Russell, P.L., 1947, Ellis Manganese deposit, Sierra County, New Mexico: U.S. Bureau of Mines, Report of Investigations 3997, 4 p.

Schantz, E., Amato, J., and Lawton, T., 2024, Dating dinosaurs in the Laramide foreland: U-Pb geochronologic constraints on a stratigraphic section containing Alamosaurus and the postulated *Tyrannosaurus mcraeensis* in the Love Ranch Basin, New Mexico [abstract]: GSA Connects 2024 Meeting in Anaheim, California, 13-29 September 20024, v. 58, id 405342, doi 10.1130/abs/2024AM-405342

Seager, W.R., 2015, Geology of the Palomas Gap 7.50-Minute Quadrangle, Sierra County, New Mexico: New Mexico Bureau of Geology and Mineral Resources, Open-file Geologic Map 260, scale 1:24,000.

Seager, W.R., and Mack, G.H., 2003, Geology of the Caballo Mountains, New Mexico: New Mexico Bureau of Geology and Mineral Resources, Memoir 49, 136 p.

Seager, W.R., Mack, G.H., and Lawton, T.F., 1997, Structural kinematics and depositional history of a Laramide uplift-basin pair in southern New Mexico: implications for development of intraforeland basins: Geological Society of America Bulletin, v. 109, p. 1389–1401.

Singleton, D., 1990, Depositional environments and tectonic significance of the Bar B Formation (Virgilian), Sierra County, New Mexico [M.S. thesis]: Las Cruces, New Mexico State University, 132 p.

Sion, B.D., Phillips, F.M., Axen, G.J., Harrison, J.B.J., Love, D.W., and Zimmerer, M.J., 2020, Chronology of terraces in the Rio Grande rift, Socorro basin, New Mexico: Implications for terrace formation: Geosphere, v. 16, https:doi.org/10.1130/GES02220.1.

Soil Survey Staff, 1992, Keys to soil taxonomy: U.S. Department of Agriculture, 541 p.

Spiegel, Z., and Baldwin, B., 1963, Geology and water resources of the Santa Fe Area, New Mexico: U.S. Geological Society Water-Supply Paper 1525, 258 p.

Thompson, S., III, 1961, Geology of the southern part of the Fra Cristobal Range, Sierra County, New Mexico: New Mexico Bureau of Mines and Mineral Resources, thesis file (revision of Thompson, 1955), 89 p.

Upchurch, G.R., Jr., and Mack, G.H., 1998, Latest Cretaceous leaf megafloras from the Jose Creek Member, McRae Formation of New Mexico: New Mexico Geological Society, Annual Field Conference Guidebook 49, p. 209–222.

U.S. Census Bureau, 2022, 2020 Census: https://www.census.gov/programs-surveys/decennial-census/decade/2020/2020-census-main.html

Verville, V.G., Sanderson, G.A., and Madsen, M.E., 1986, Pennsylvanian fusulinids from the Fra Cristobal Range, Sierra County, New Mexico: New Mexico Geological Society, 37th Fall Field Conference Guidebook, p. 215–223.

Wallin, E.T., 1983, Stratigraphy and paleoenvironments of the Engle coal field, Sierra County, New Mexico [M.S. thesis]: Socorro, New Mexico Institute of Mining and Technology, 127 p.

Wells, E.H., 1918, Manganese deposits of New Mexico: New Mexico School of Mines Bulletin 2, p. 62–63.

Wells, S.G., and Granzow, H., 1980, Hydrogeology of the thermal aquifers near Truth or Consequences, New Mexico: New Mexico Energy Institute/Department of Energy Subcontract, final report, part II, no. 314-150178-00493-D, 40 p.

Figure Captions, Elephant Butte 7.5-minute quadrangle

Note: Figures are in the pages following the figure captions

Figure 1. Geographic setting and topography of the region around the Elephant Butte 7.5-minute quadrangle. The quadrangle boundary is depicted by the red rectangle. Thick, black lines are major faults, with the ball on the downthrown side. The inset map (lower right) shows the location of the quadrangle within the state.

Figure 2. Geographic setting and topography of the region around the Elephant Butte 7.5-minute quadrangle. Landmarks referred to in this report are labeled in black and roads in yellow. The inset map (lower right) shows the location of the quadrangle within the state.

Figure 3. Stratigraphic section illustrating thicknesses and relative proportion of lithologies of the Paleozoic and Mesozoic strata found on the Elephant Butte 7.5-minute quadrangle.

Figure 4. Gray shales and interbedded siltstones of the Tokay Tongue of the Mancos Shale.

Figure 5. Illustration of Bridge Creek Limestone beds on the eastern slopes of lower Mescal Canyon. The thick line near the top of the exposure is an inferred fault that is down-to-the-northeast. View is to the north-northeast.

Figure 6. Tabular to broadly lenticular, relatively thick-bedded conglomeratic sandstone of unit Nrpe at the base of the Santa Fe Group, at a location about 700 m south of the earthen auxiliary dam. Note the local angular unconformity between units B and C, which indicates movement along the Hot Springs fault system during Nrpe deposition in the late Miocene. The clast composition of these sandstones has abundant volcanic rocks, indicating that the José Creek Formation was more extensive in the upstream drainage during the late Miocene than today.

Figure 7. Matrix-supported debris flow deposit in unit Nrpe. Sharpie pen for scale. The greenish clasts are Cretaceous sandstones, but the light-gray clasts are intermediate-volcanic clasts. The high proportion of these volcanic clasts is a notable difference between this unit and the younger unit Nppe.

Figure 8. Stratigraphic section along the southern quadrangle boundary illustrating clay and siltstone of a playa lake deposit and intertonguing, fine-grained quartzo-feldspathic sands (Nrpd) similar in composition to axial-fluvial sands of unit QNpa. These sands are intricately cross-laminated, including ripple marks, and are interpreted to represent an axial-fluvial, deltaic lobe that prograded into a playa lake. Rose diagrams illustrate imbrication-paleoflow data from conglomeratic deposits at the base of the section. These conglomeratic strata are interpreted as distal alluvial fan deposits that predate the playa-lake, an interpretation consistent with the west–southwest paleoflow in the basal conglomerate.

Figure 9. Closeup of a fine-grained, quartzo-feldspathic sand body of unit Nrpd. It shows distinct cross-laminations. Note the light-colored, wedge-shaped channel fill immediately above the scraper.

Figure 10. Reddish-brown, sandy playa lake deposit near the Hot Springs fault. The playa-lake deposits appears to become sandier eastwards (closer to the Caballo Mountains). Note the calcium carbonate nodules, suggesting periodic drying of the sediment.

Figure 11. Stratigraphic column illustrating the thicknesses and relations of Santa Fe Group map units. Note the scale change.

Figure 12. Relatively tabular-bedded, conglomeratic, and well-cemented strata of unit Nppe. This conglomerate is readily mappable due to its slightly greenish color and its relative resistance to erosion.

Figure 13. Reddish, well-cemented, conglomeratic strata of unit Nppes, as observed near the trailhead for the Tortuga Peak trail. The reddish-brown color is probably due to alluvial-fan deposition of clastic material eroded from the Abo Formation in the nearby mountain front.

Figure 14. Reddish fanglomerates of the Palomas Formation (Nppes) sharply overlying finer-grained Rincon Valley Formation strata (Nrpd).

Figure 15. Trough cross-stratification and minor pebbly sandstone beds in the lower part of the axial-fluvial facies. Scraper (20 cm long) for scale. Photograph taken with permission from Bartoo Sand and Gravel quarry just east of New Mexico State Road 181.

Figure 16. Horizonal-planar lamination and tangential foresets of the axial-fluvial facies. Scraper (20 cm long) for scale. The lack of clay and moderately to well-sorted nature of the sand make it a productive aquifer. Wells in the town of Elephant Butte are screened in this lithologic unit.

Figure 17. Unit QNpf, with backpack for scale. The axial-fluvial facies (QNpa) interfingers laterally with QNpf and is also gradationally overlain by it. Unit QNpf is composed of silt, very fine- to fine-grained sand, silt, and clay and has less than 5% gravels.

Figure 18. Tabular-bedded nature of unit QNpf. The outcrop is about 5–6 m tall. Near the top of the exposure, note the reddish-brown, illuviated clay horizon with calcium carbonate precipitation (Btk horizon). Below is about 1 m of whitened, fine-grained sediment that represents a stage II calcic paleosol. In the lower 1 m of the exposure lie 1- to 1.5-m-thick, very thin- to medium-bedded, grayish, sandy pebbles.

Figure 19. Fine-grained nature and tan color of unit QNpf. Note the paucity of gravel beds.

Figure 20. Gravel beds of unit Qpt, and a minor amount of reddish-brown beds, overlying the tanner, middle, fine-grained unit (QNpf). Unit Qpt represents a gravelly transition between the middle and upper Palomas Formation and ranges from 3 to about 10 m thick.

Figure 21. Two photographs illustrating the piedmont facies of the upper Palomas Formation (unit Qppw). Note the general reddish-brown (5YR) color, tabular-bedded and non-gravelly sediment, and the relatively tabular intervals of grayish gravel. The non-gravelly sediment generally consists of very fine- to fine-grained sand and clayey-silty fine sand, with sparse to common overprinting by weak pedogenesis characterized by ped development, weak reddening, and local calcium carbonate precipitation. Gravel bodies are typically 10–30% of the Qppw unit.

Figure 22. An assemblage of photographs illustrating features of the piedmont lithofacies of the upper Palomas Formation. A and B: Note the grayish, tabular bodies of clast-supported gravel that have sharp tops. Gravelly intervals can commonly be traced laterally tens to hundreds of meters. These attributes suggest deposition as broad sheets, probably at the terminus of a piedmont channel, and abandonment of lobes by avulsion processes. C: The silty-clayey fine sand and very fine- to fine-grained sand in unit Qppw commonly has minor, scattered, outsized grains of medium to very coarse sand and sparser pebbles, as seen in this photograph a few cm to the right of the pen tip. D and E: Paleosols in unit Qppw, commonly characterized by reddish-brown colors, illuviated clay, and calcium carbonate precipitation; the latter can be diffuse or as calcium carbonate nodules (seen here). Note how the calcium carbonate nodules extend below the reddish-brown, illuviated clay horizons.

Figure 23. Map showing faults, folds, and location of maars on the Elephant Butte 7.5-minute quadrangle. These features are taken directly from GIS data of the geologic map.

Figure 24. The Lonely Heart Butte maar. A: View looking east from of the Lonely Heart Butte maar. A basalt dike intrudes base surge sediments (Qmb) in the middle of the frame. B: View north from the west flank of the maar. Lava pillows are enclosed by upper base surge sediments (Qmb). At the top of the frame is basalt hyaloclastite.

Figure 25. Schematic stratigraphic section illustrating the common units and stratigraphic relations found in the four maars mapped on the quadrangle. Unit labels in the middle of the diagram is for detailed mapping and can be translated to the map's units as follows: vm is mapped as Qmv; h and b are mapped as Qb; and vt, Vc3, vc2, and vc1 are mapped as Qmb.

Figure 26. View of the south side of Rattlesnake Island maar (looking north). The top photograph shows the approximate location of basalt samples (likely from dikes). The Hot Springs fault is constrained by Cretaceous outcrops and does not offset the maar-related breccia deposits. Below are analytical plots for the $^{40}Ar/^{39}Ar$ analyses, with the spectrum plot of EB-20 at the top and the isochron plot of EB-23 at the bottom. The fact that 2.5 Ma strata are not offset by the Hot Springs fault means that this section of the Hot Springs fault has been inactive since 2.5 Ma.

Figure 27. Rio Grande terrace deposit Qtr4 overlain by eastern alluvial fan deposits (Qftme). Note the angular unconformity, below which lies unit Nppe. Steep northwest-directed dips in Nppe immediately adjacent to the Hot Springs fault are highly suggestive of normal drag and post-Nppe displacement along that fault. Steepened tilts in this unit is observed along the entire fault.

Figure 28. Thin to medium-bedded, sandy gravel and gravelly sand of terrace deposit Qtc2. Beneath the scoured contact of the gravel lies sand of unit QNpa.

Figure 29. A: Qtfh terrace deposit. B: Well-developed desert pavement on its surface. This deposit is the most extensive of the high-level fan-terraces on the northwestern quadrangle. It represents a period of alluvial fan deposition by low-order tributaries of the Rio Grande. Relative base level stability allowed the associated sediment to be relatively widespread. Typically, it is a few meters thick and consists of sandy gravel and gravelly sand. Its tread is about 12–13 m above the modern grade. The desert pavement has less than 5% space between clasts (strong clast armor) and moderate varnishing. Contrast the varnished clasts to the light-gray gravel color on younger surfaces (e.g., Figs. 31c and 31d).

Figure 30. Schematic illustration of valley floor alluvial stratigraphy.

Figure 31. Younger valley floor alluvium and associated landforms. A: Sandy alluvium with about 5% pebbles, the latter being scattered or in very thin to thin, tabular to lenticular beds. The topsoil has an A horizon and an underlying stage I+ horizon; beneath lie buried soils (Bk = calcic horizon, buried soil; A = organic-enriched, darkened horizon; refer to Soil Survey Staff [1992]). B: Gravelly Qay sediment in an alluvial fan at the mouth of a low-order drainage; note the very thin to thin, tabular to lenticular beds characteristic of deposition by unconfined flow on alluvial fans. C: Intermediate terrace of unit Qay. These terraces have smooth surfaces but weak desert pavement. They are likely associated with thin, underlying allostratigraphic deposits dated elsewhere as late Holocene (Fig. 29; Jochems and Koning, 2015). D: Recent alluvium (Qar) underlying a valley floor. Note the bar-and-swale topography and sparse vegetation.

Figure 1

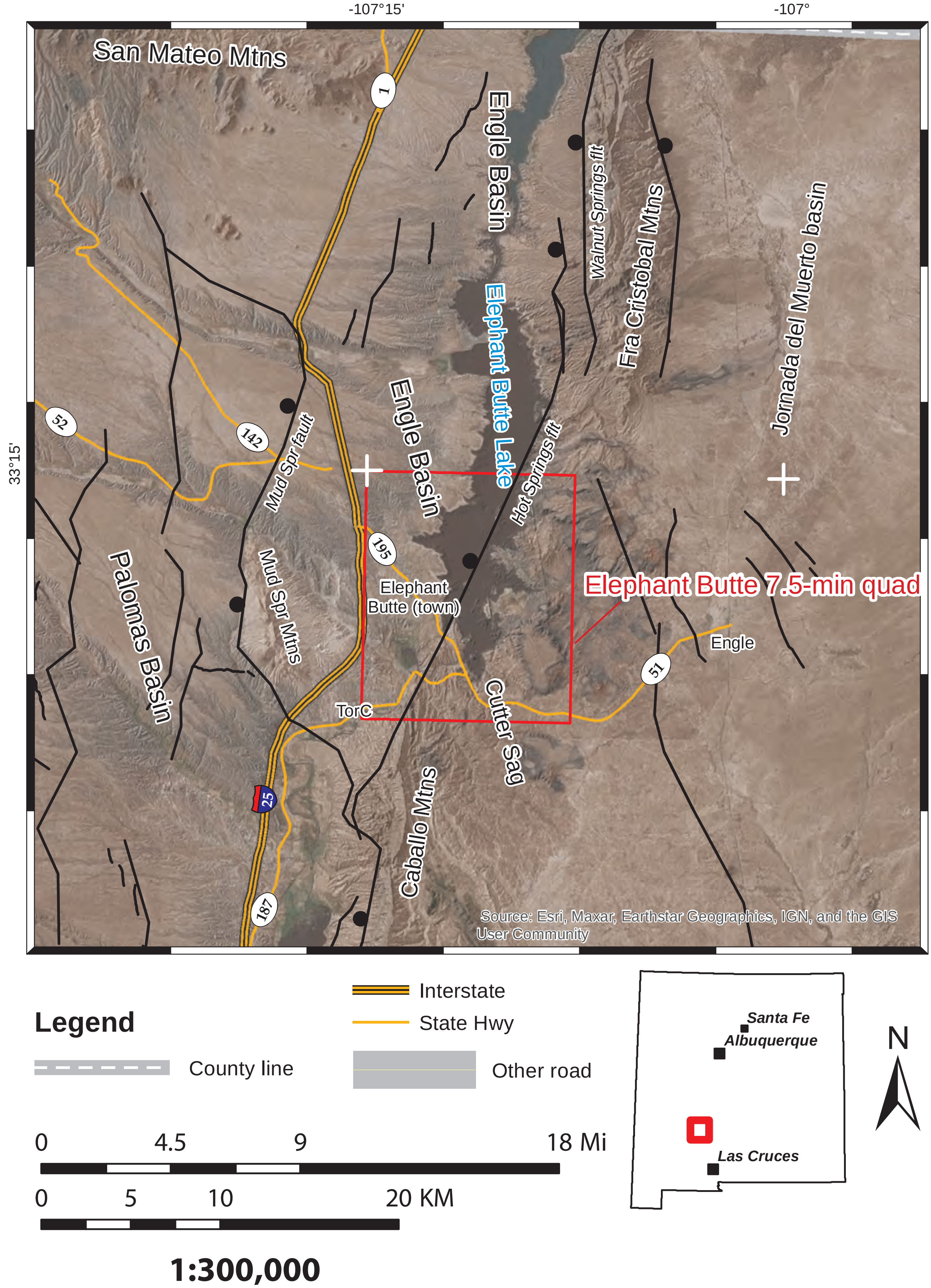

-107°15'
-107°
33°15'
San Mateo Mtns
Engle Basin
Walnut Springs flt
Fra Cristobal Mtns
Jornada del Muerto basin
Elephant Butte Lake
Hot Springs flt
Mud Spr fault
Mud Spr Mtns
Palomas Basin
Elephant Butte (town)
Elephant Butte 7.5-min quad
Engle
TorC
Cutter Sag
Caballo Mtns
1
52
142
195
51
25
187
Source: Esri, Maxar, Earthstar Geographics, IGN, and the GIS User Community
Legend
Interstate
State Hwy
County line
Other road
0
4.5
9
18 Mi
0
5
10
20 KM
1:300,000
Santa Fe
Albuquerque
Las Cruces
N

Figure 2

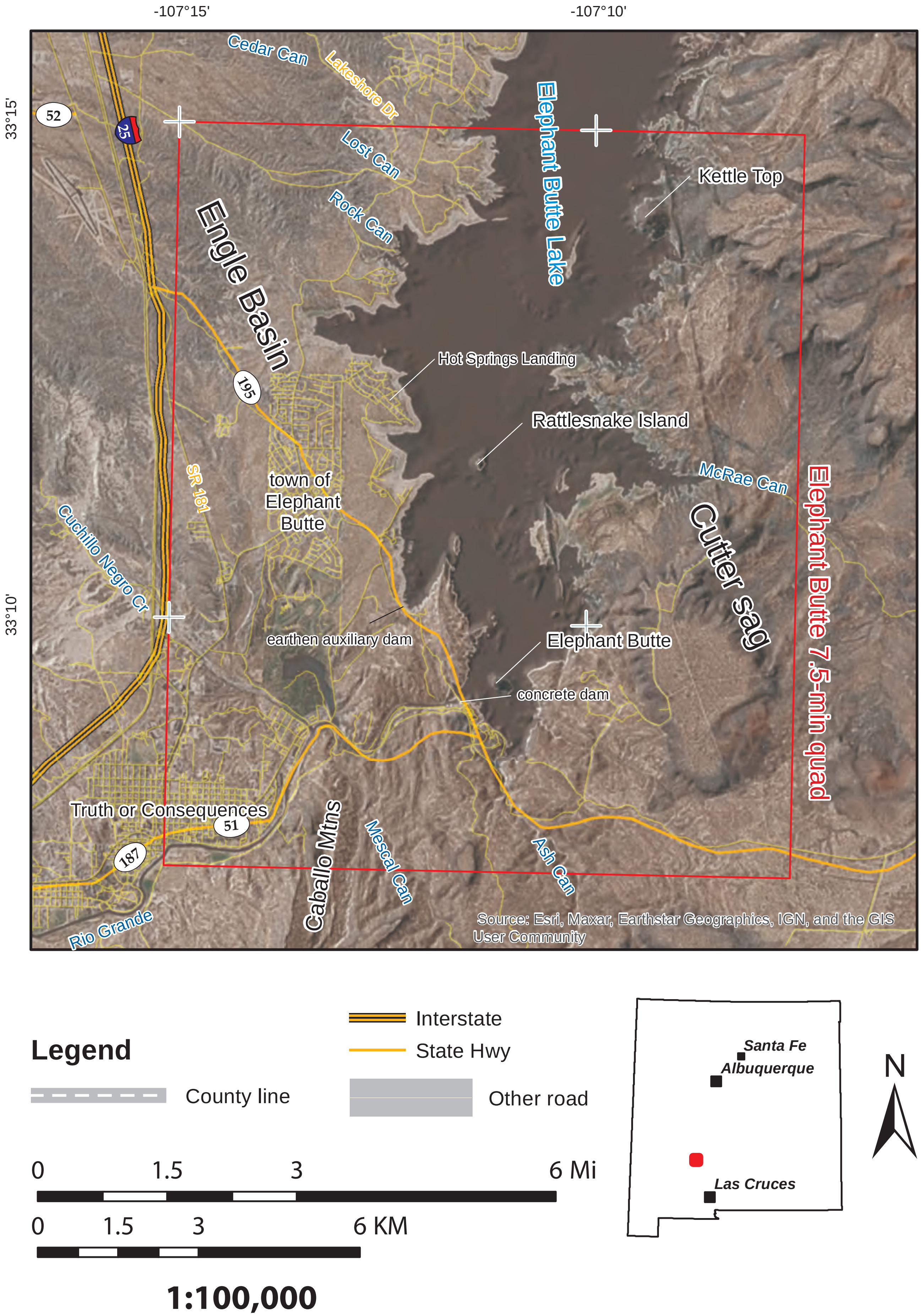

-107°15'
-107°10'
33°15'
33°10'
Cedar Can
Lakeshore Dr
Lost Can
Rock Can
Elephant Butte Lake
Kettle Top
Engle Basin
52
25
195
Hot Springs Landing
Rattlesnake Island
McRae Can
Cutter sag
Elephant Butte 7.5-min quad
SR 181
town of Elephant Butte
Cuchillo Negro Cr
earthen auxiliary dam
Elephant Butte
concrete dam
Truth or Consequences
51
187
Caballo Mtns
Mescal Can
Ash Can
Rio Grande
Source: Esri, Maxar, Earthstar Geographics, IGN, and the GIS User Community
Legend
Interstate
State Hwy
County line
Other road
0
1.5
3
6 Mi
0
1.5
3
6 KM
1:100,000
Santa Fe
Albuquerque
Las Cruces
N

Figure 3

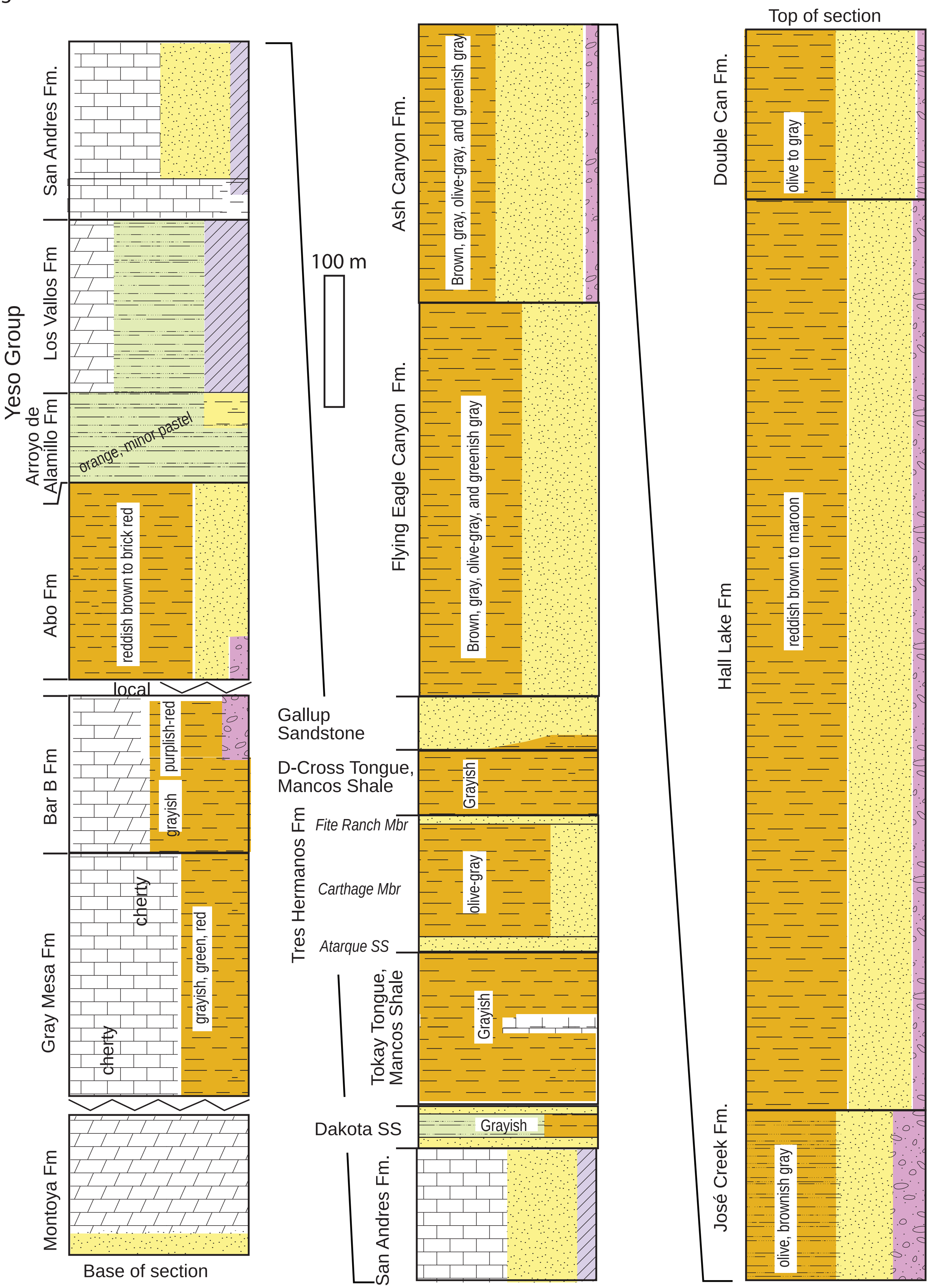

San Andres Fm.
Los Vallos Fm
Yeso Group
Arroyo de Alamillo Fm
orange, minor pastel
Abo Fm
reddish brown to brick red
local
Bar B Fm
purplish-red
grayish
Gray Mesa Fm
cherty
grayish, green, red
cherty
Montoya Fm
Base of section
100 m
Gallup Sandstone
D-Cross Tongue, Mancos Shale
Grayish
Tres Hermanos Fm
Fite Ranch Mbr
Carthage Mbr
olive-gray
Atarque SS
Tokay Tongue, Mancos Shale
Grayish
Dakota SS
Grayish
San Andres Fm.
Ash Canyon Fm.
Brown, gray, olive-gray, and greenish gray
Flying Eagle Canyon Fm.
Brown, gray, olive-gray, and greenish gray
Top of section
Double Can Fm.
olive to gray
Hall Lake Fm
reddish brown to maroon
José Creek Fm.
olive, brownish gray

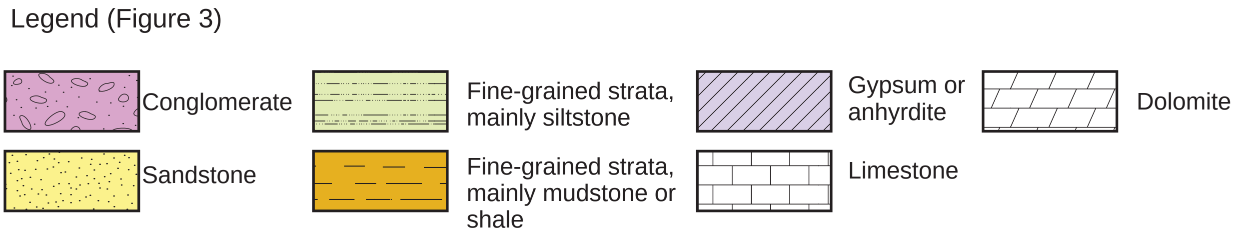
Legend (Figure 3)
Conglomerate
Fine-grained strata, mainly siltstone
Gypsum or anhyrdite
Dolomite
Sandstone
Fine-grained strata, mainly mudstone or shale
Limestone

Figure 4

Figure 5

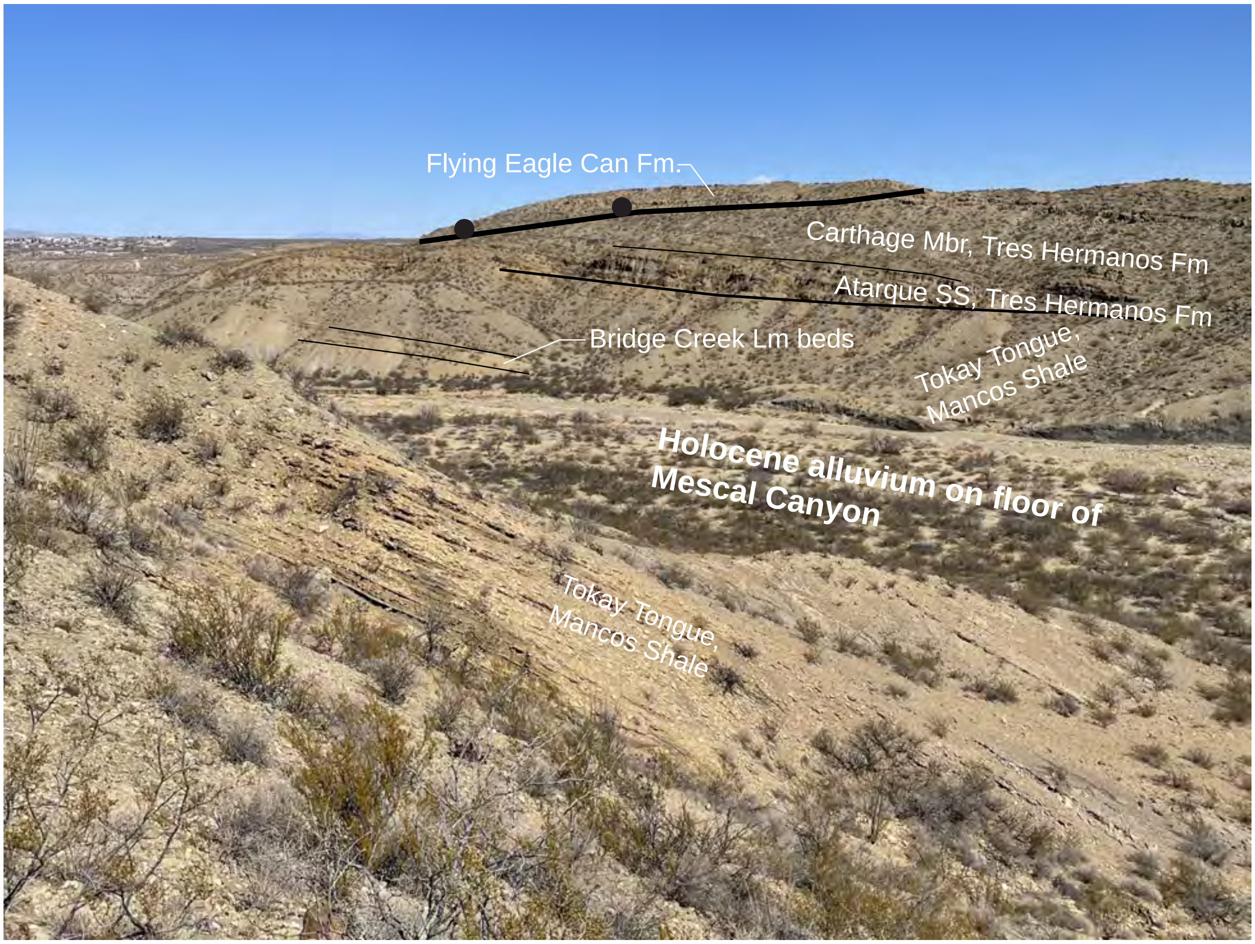

Flying Eagle Can Fm.
Carthage Mbr, Tres Hermanos Fm
Atarque SS, Tres Hermanos Fm
Bridge Creek Lm beds
Tokay Tongue,
Mancos Shale
Holocene alluvium on floor of
Mescal Canyon
Tokay Tongue,
Mancos Shale

Figure 6


View to south
Lower Santa Fe Group, Unit C
Unit B

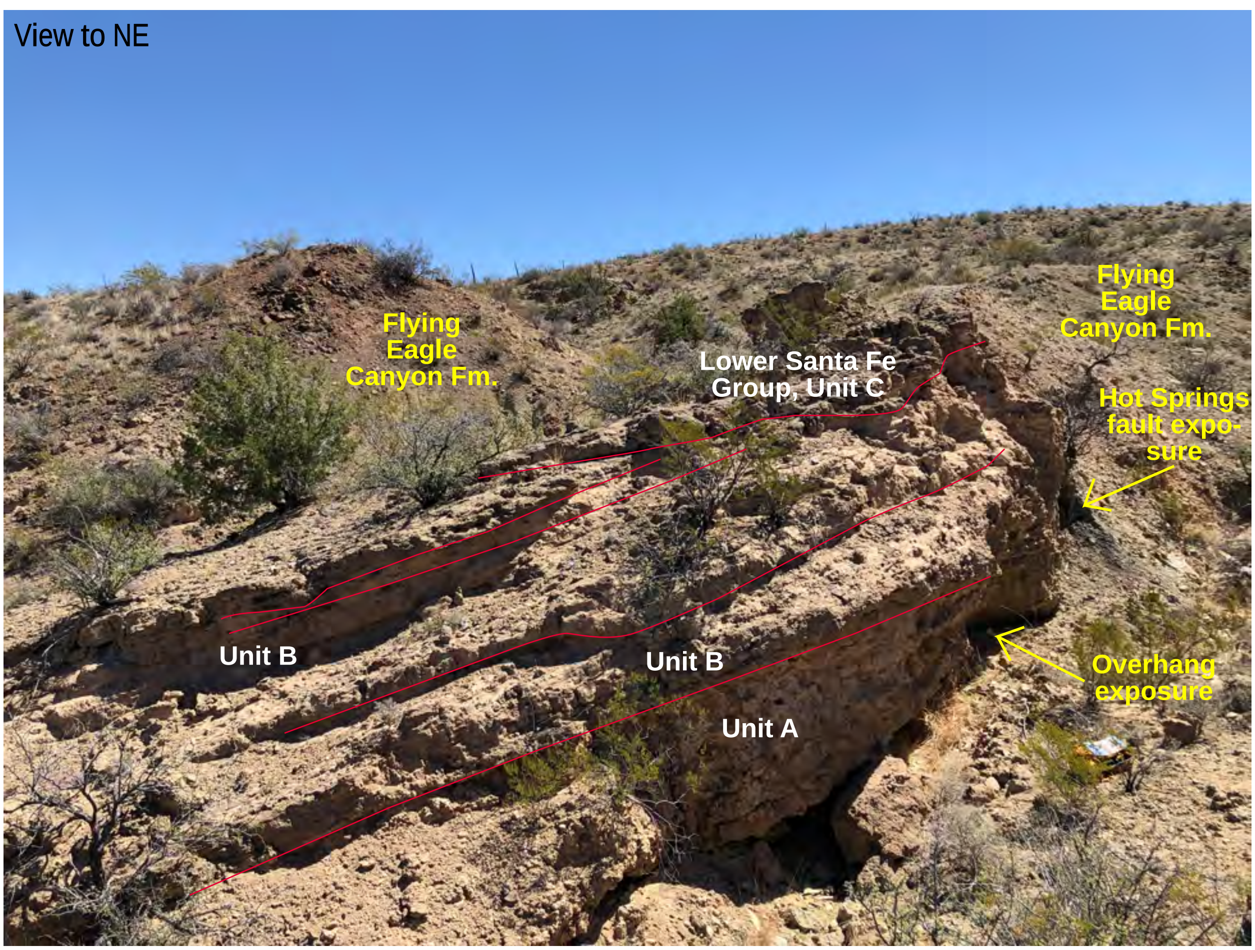
View to NE
Flying Eagle Canyon Fm.
Lower Santa Fe Group, Unit C
Flying Eagle Canyon Fm.
Hot Springs fault expo-sure
Unit B
Unit B
Overhang exposure
Unit A

Figure 7

Figure 8

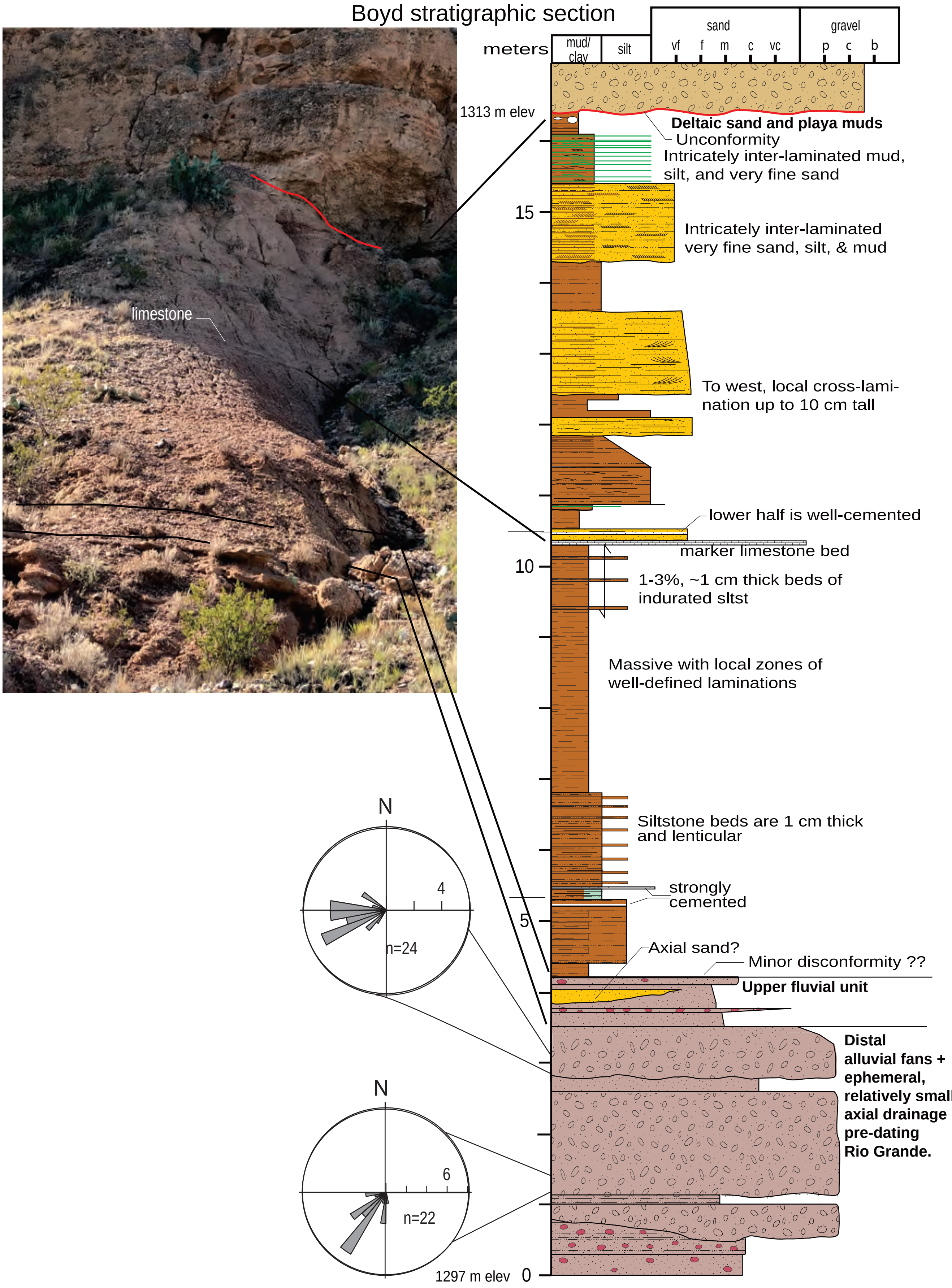

Boyd stratigraphic section
meters
mud/ clay
silt
sand
vf
f
m
c
vc
gravel
p
c
b
1313 m elev
Deltaic sand and playa muds
Unconformity
Intricately inter-laminated mud, silt, and very fine sand
15
Intricately inter-laminated very fine sand, silt, & mud
To west, local cross-lamination up to 10 cm tall
lower half is well-cemented
marker limestone bed
10
1-3%, ~1 cm thick beds of indurated sltst
Massive with local zones of well-defined laminations
Siltstone beds are 1 cm thick and lenticular
strongly cemented
5
Axial sand?
Minor disconformity ??
Upper fluvial unit
Distal alluvial fans + ephemeral, relatively small axial drainage pre-dating Rio Grande.
1297 m elev
0
limestone
N
4
n=24
N
6
n=22

Figure 9

Figure 10

Figure 11

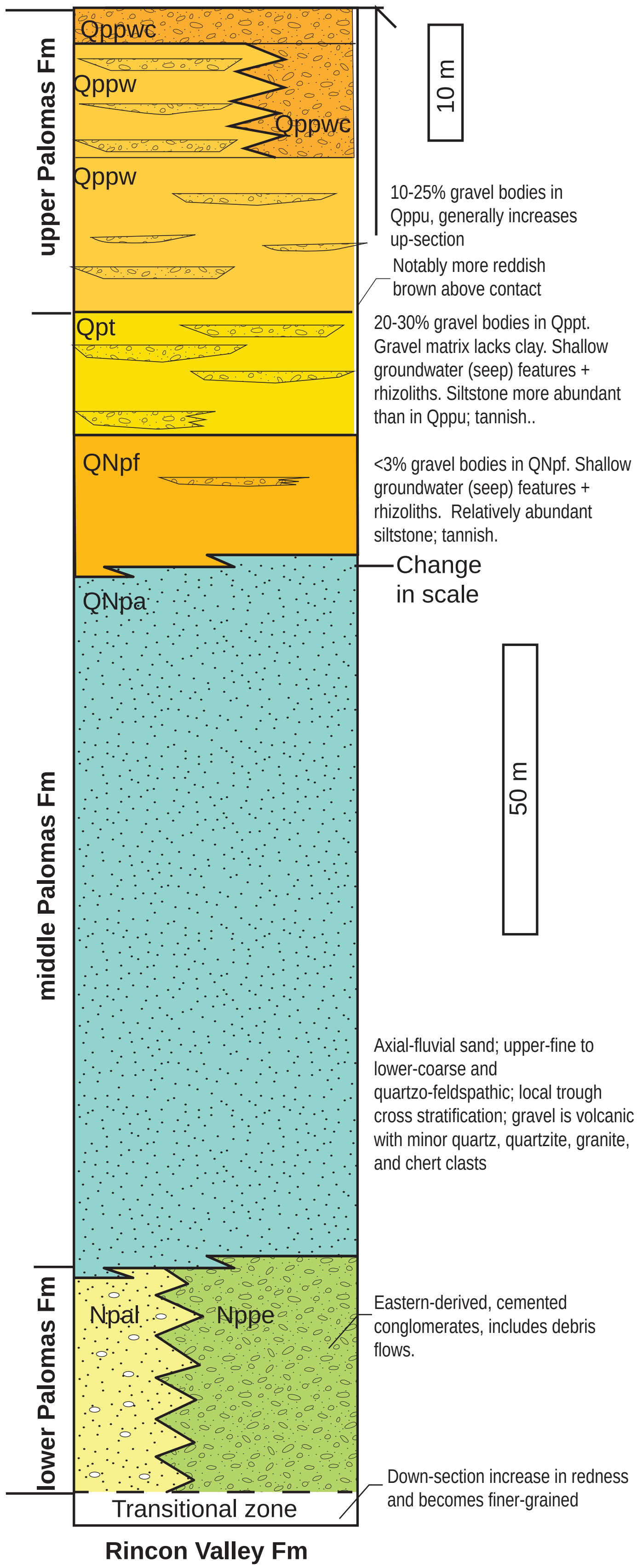

upper Palomas Fm
middle Palomas Fm
lower Palomas Fm
Qppwc
Qppw
Qppwc
Qppw
Qpt
QNpf
QNpa
Npal
Nppe
Transitional zone
Rincon Valley Fm
10 m
50 m
10-25% gravel bodies in Qppu, generally increases up-section
Notably more reddish brown above contact
20-30% gravel bodies in Qppt. Gravel matrix lacks clay. Shallow groundwater (seep) features + rhizoliths. Siltstone more abundant than in Qppu; tannish..
<3% gravel bodies in QNpf. Shallow groundwater (seep) features + rhizoliths. Relatively abundant siltstone; tannish.
Change in scale
Axial-fluvial sand; upper-fine to lower-coarse and quartzo-feldspathic; local trough cross stratification; gravel is volcanic with minor quartz, quartzite, granite, and chert clasts
Eastern-derived, cemented conglomerates, includes debris flows.
Down-section increase in redness and becomes finer-grained

Figure 12

Figure 13

Figure 14

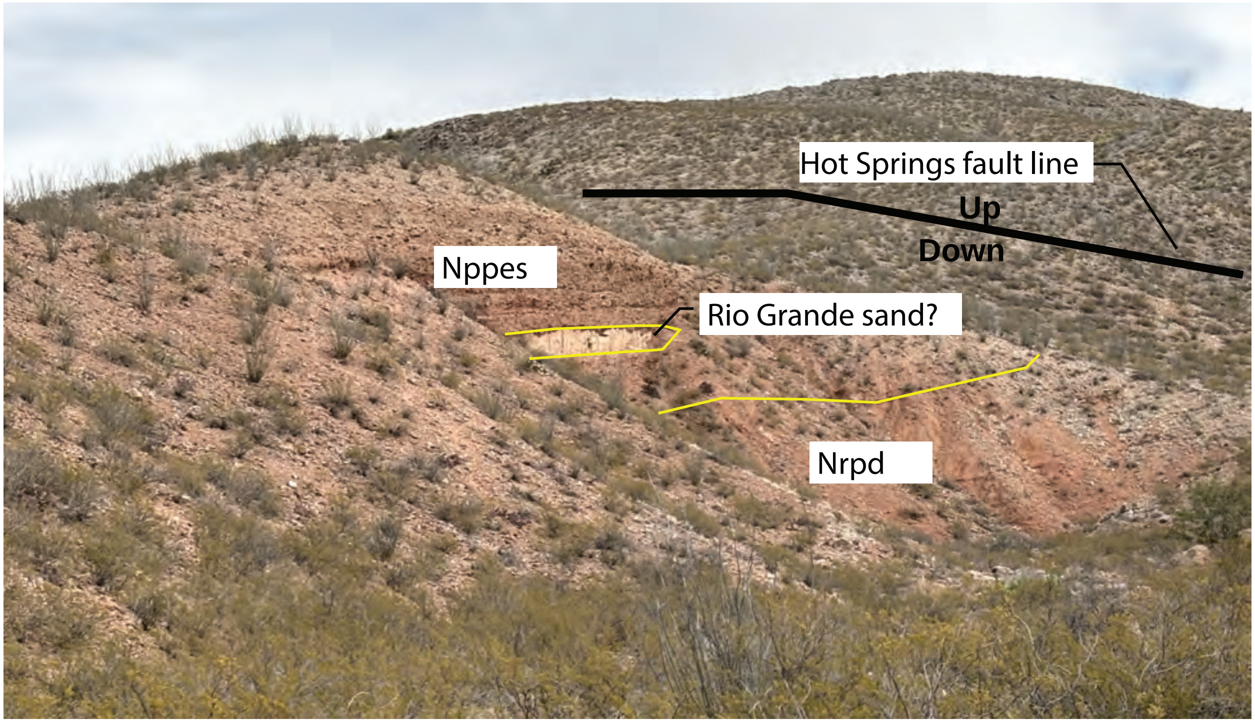

Figure 15

Figure 16

Figure 17

Figure 18

Figure 19

Figure 20

Figure 21

Figure 22

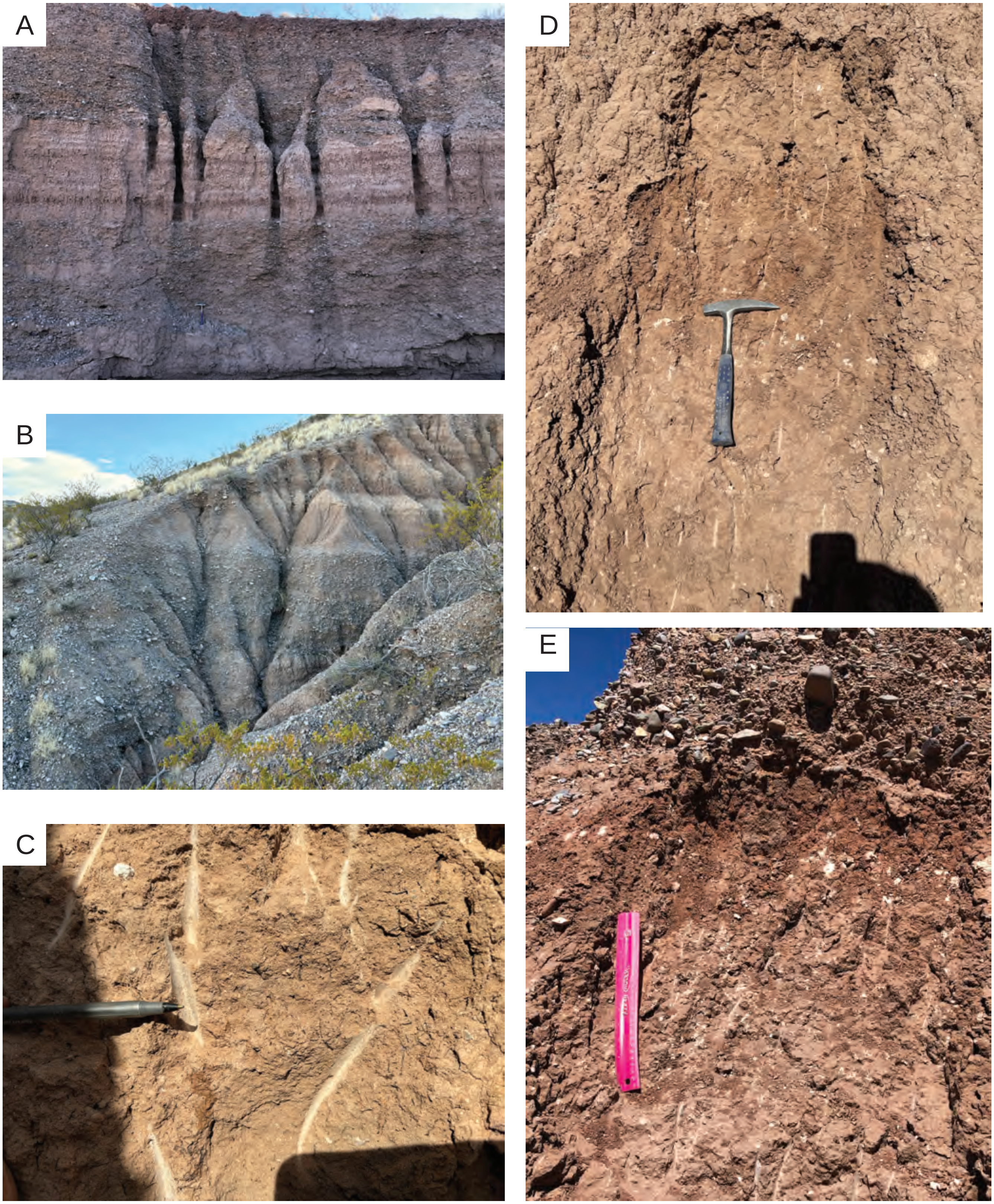

Figure 23

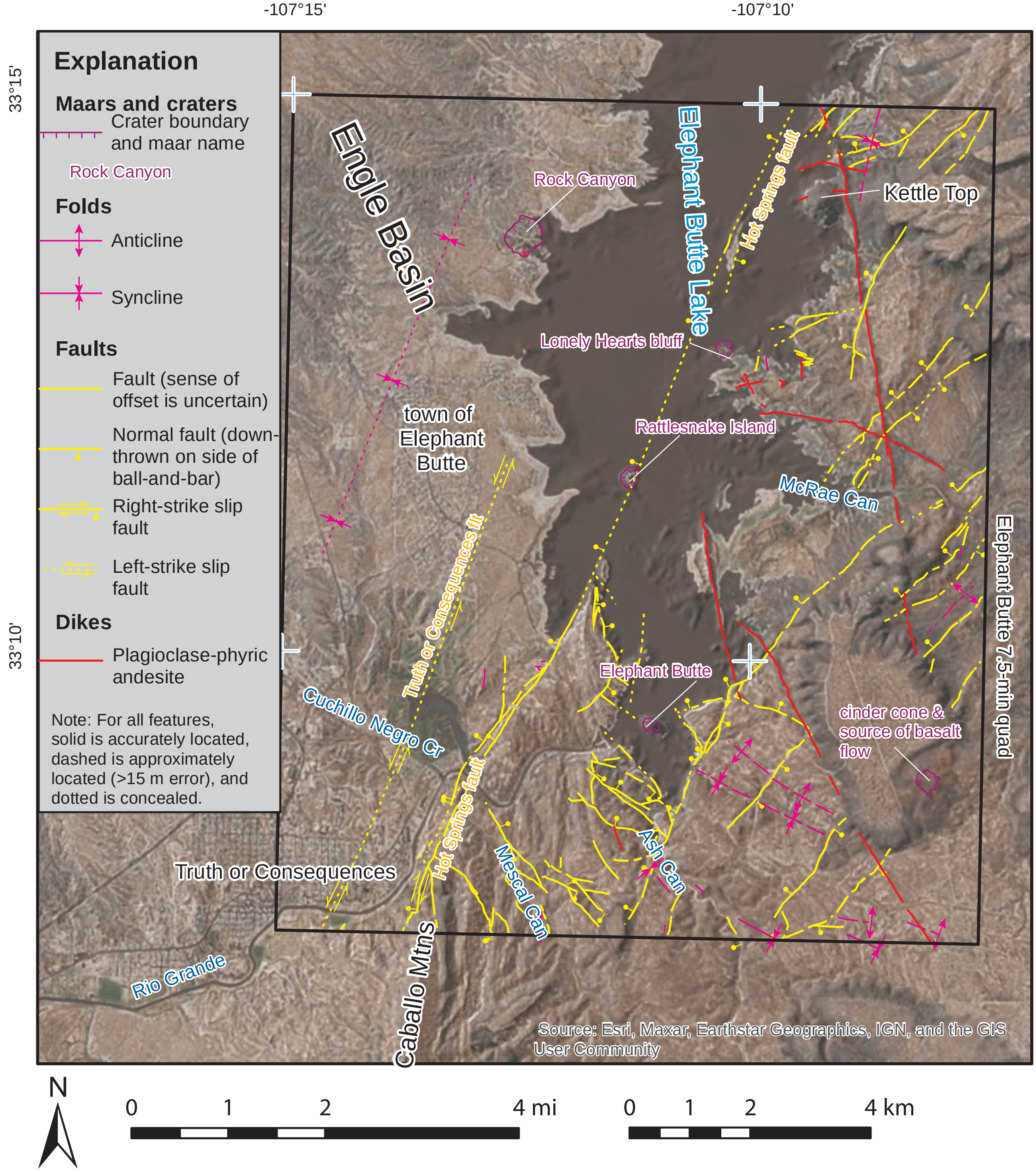

-107°15'
-107°10'
33°15'
33°10'
Explanation
Maars and craters
Crater boundary and maar name
Rock Canyon
Folds
Anticline
Syncline
Faults
Fault (sense of offset is uncertain)
Normal fault (down-thrown on side of ball-and-bar)
Right-strike slip fault
Left-strike slip fault
Dikes
Plagioclase-phyric andesite
Note: For all features, solid is accurately located, dashed is approximately located (>15 m error), and dotted is concealed.
Engle Basin
Rock Canyon
Elephant Butte Lake
Hot Springs fault
Kettle Top
Lonely Hearts bluff
town of Elephant Butte
Rattlesnake Island
McRae Can
Elephant Butte 7.5-min quad
Truth or Consequences flt
Cuchillo Negro Cr
Elephant Butte
cinder cone & source of basalt flow
Hot Springs fault
Truth or Consequences
Mescal Can
Ash Can
Rio Grande
Caballo Mtns
Source: Esri, Maxar, Earthstar Geographics, IGN, and the GIS User Community
N
0 1 2 4 mi
0 1 2 4 km

Figure 24

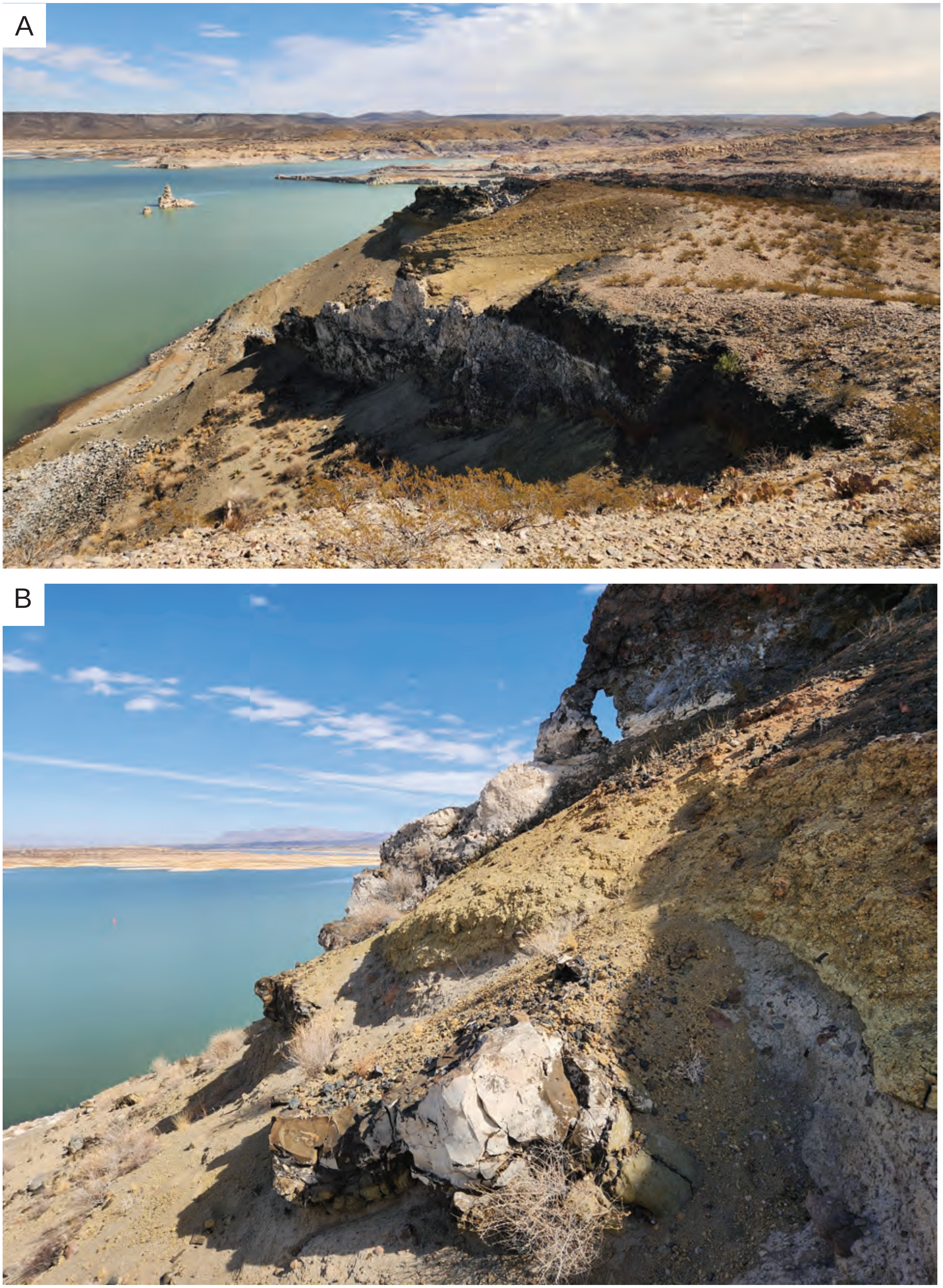

Figure 25

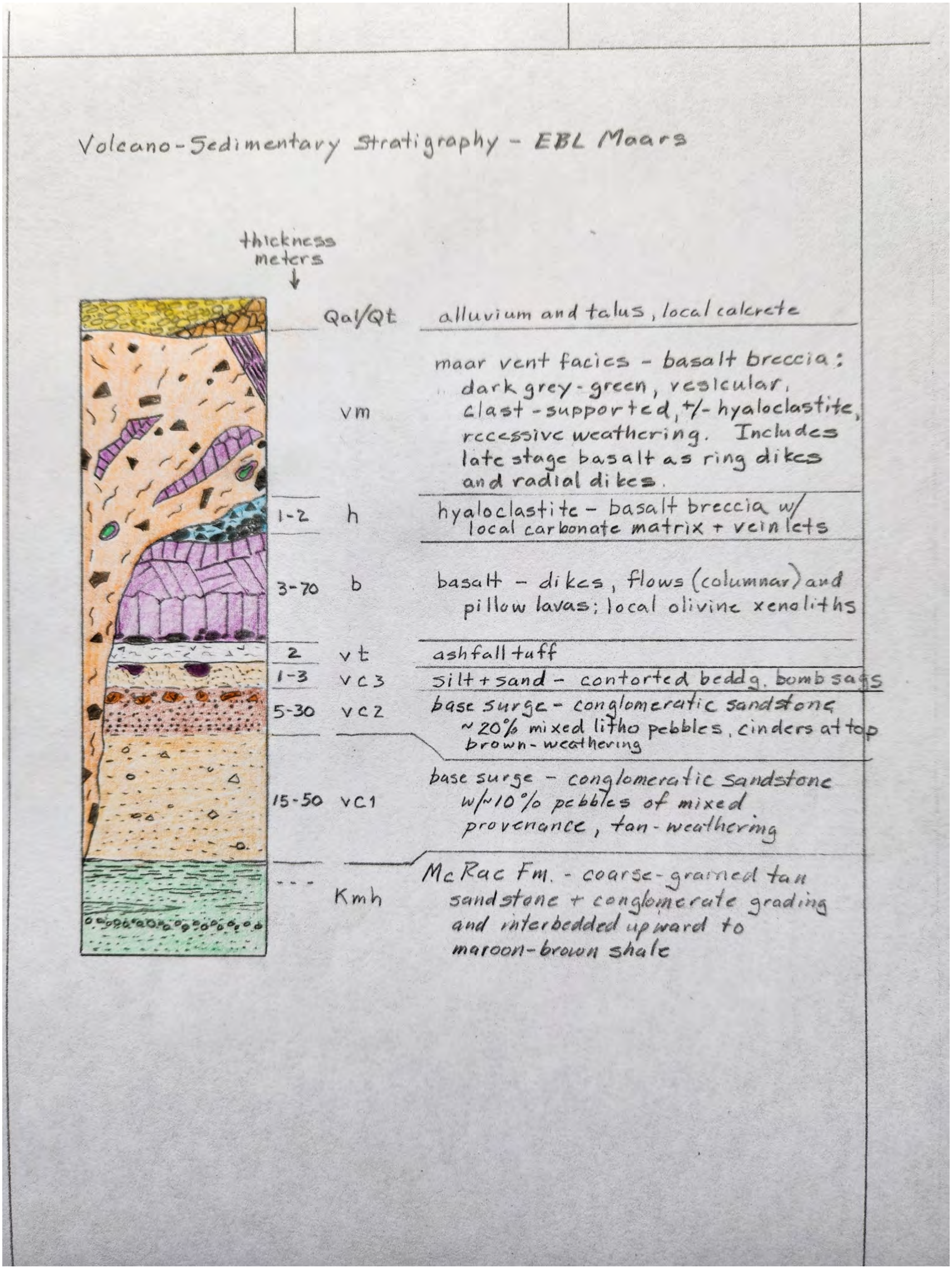

Volcano-Sedimentary Stratigraphy - EBL Maars
thickness meters
Qal/Qt
alluvium and talus, local calcrete
vm
maar vent facies - basalt breccia: dark grey-green, vesicular, clast-supported, +/- hyaloclastite, recessive weathering. Includes late stage basalt as ring dikes and radial dikes.
1-2
h
hyaloclastite - basalt breccia w/ local carbonate matrix + veinlets
3-70
b
basalt - dikes, flows (columnar) and pillow lavas; local olivine xenoliths
2
vt
ashfall tuff
1-3
vc3
silt + sand - contorted beddg. bomb sags
5-30
vc2
base surge - conglomeratic sandstone ~20% mixed litho pebbles, cinders at top brown-weathering
15-50
vc1
base surge - conglomeratic sandstone w/~10% pebbles of mixed provenance, tan-weathering
Kmh
McRae Fm. - coarse-grained tan sandstone + conglomerate grading and interbedded upward to maroon-brown shale

Figure 26

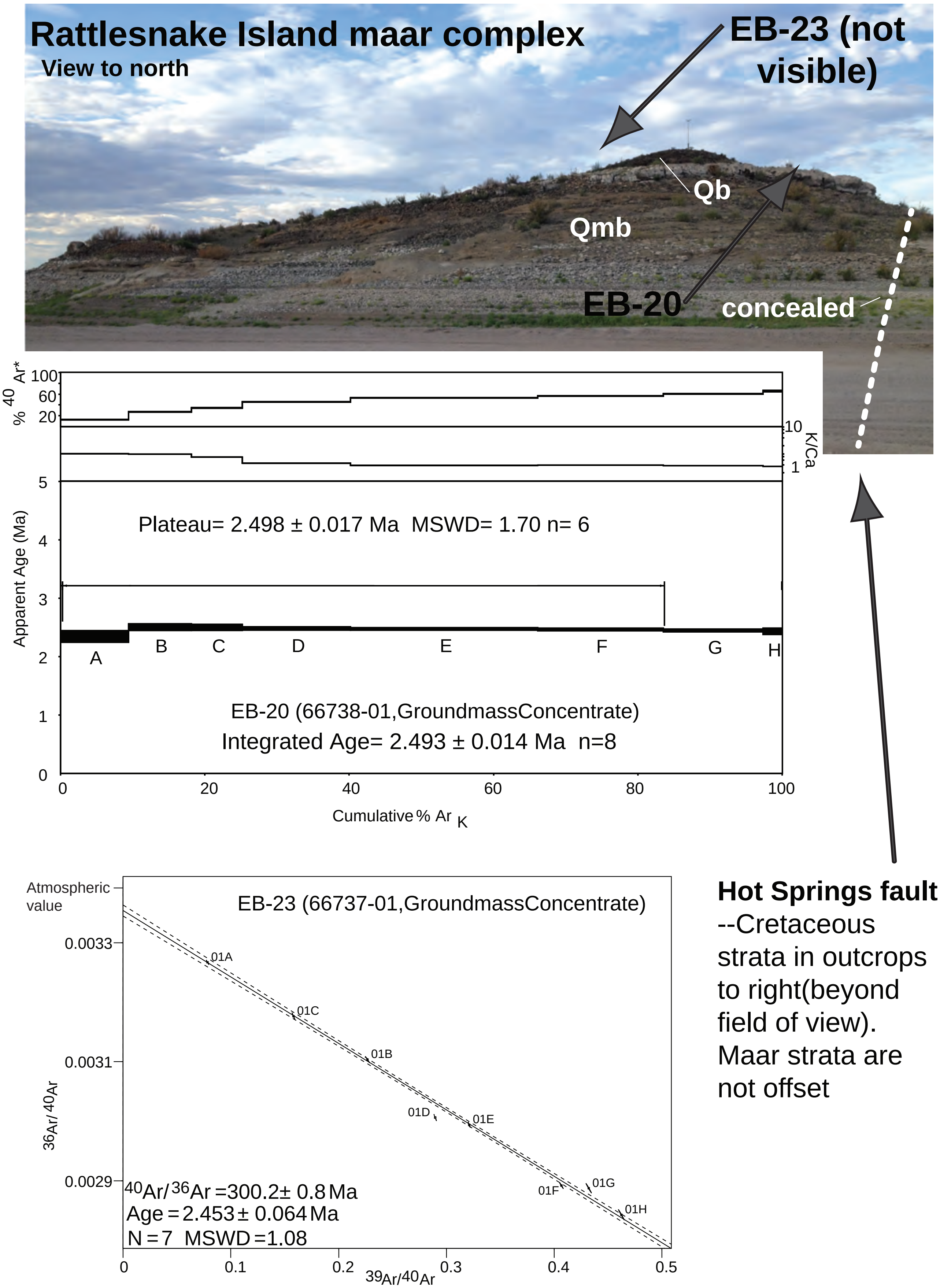

Rattlesnake Island maar complex
View to north
EB-23 (not visible)
Qb
Qmb
EB-20
concealed
% 40Ar*
100
60
20
10
1
K/Ca
5
4
3
2
1
0
Apparent Age (Ma)
Plateau= 2.498 ± 0.017 Ma MSWD= 1.70 n= 6
A
B
C
D
E
F
G
H
EB-20 (66738-01,GroundmassConcentrate)
Integrated Age= 2.493 ± 0.014 Ma n=8
0
20
40
60
80
100
Cumulative % Ar K
Hot Springs fault
--Cretaceous strata in outcrops to right(beyond field of view). Maar strata are not offset
Atmospheric value
0.0033
0.0031
0.0029
36Ar/40Ar
EB-23 (66737-01,GroundmassConcentrate)
01A
01C
01B
01D
01E
01F
01G
01H
40Ar/36Ar =300.2± 0.8 Ma
Age = 2.453 ± 0.064 Ma
N = 7 MSWD = 1.08
0
0.1
0.2
0.3
0.4
0.5
39Ar/40Ar

Figure 27

Figure 28

Figure 29

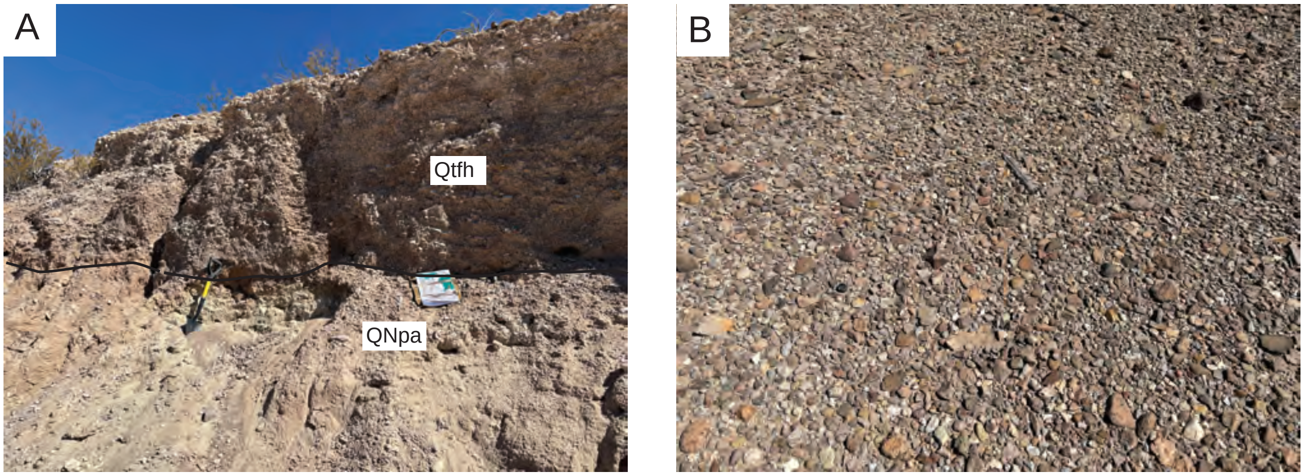

Figure 30

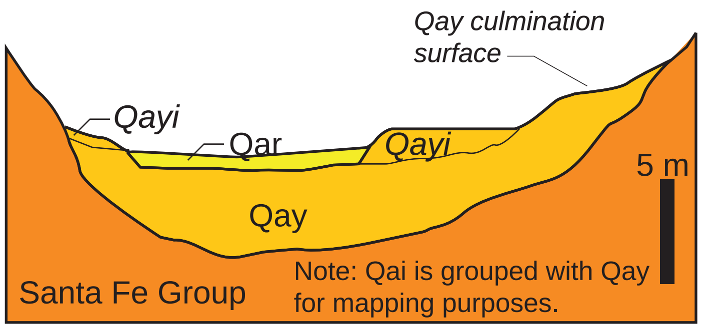

Qay culmination surface
Qayi
Qar
Qayi
5 m
Qay
Santa Fe Group
Note: Qai is grouped with Qay for mapping purposes.

Figure 31

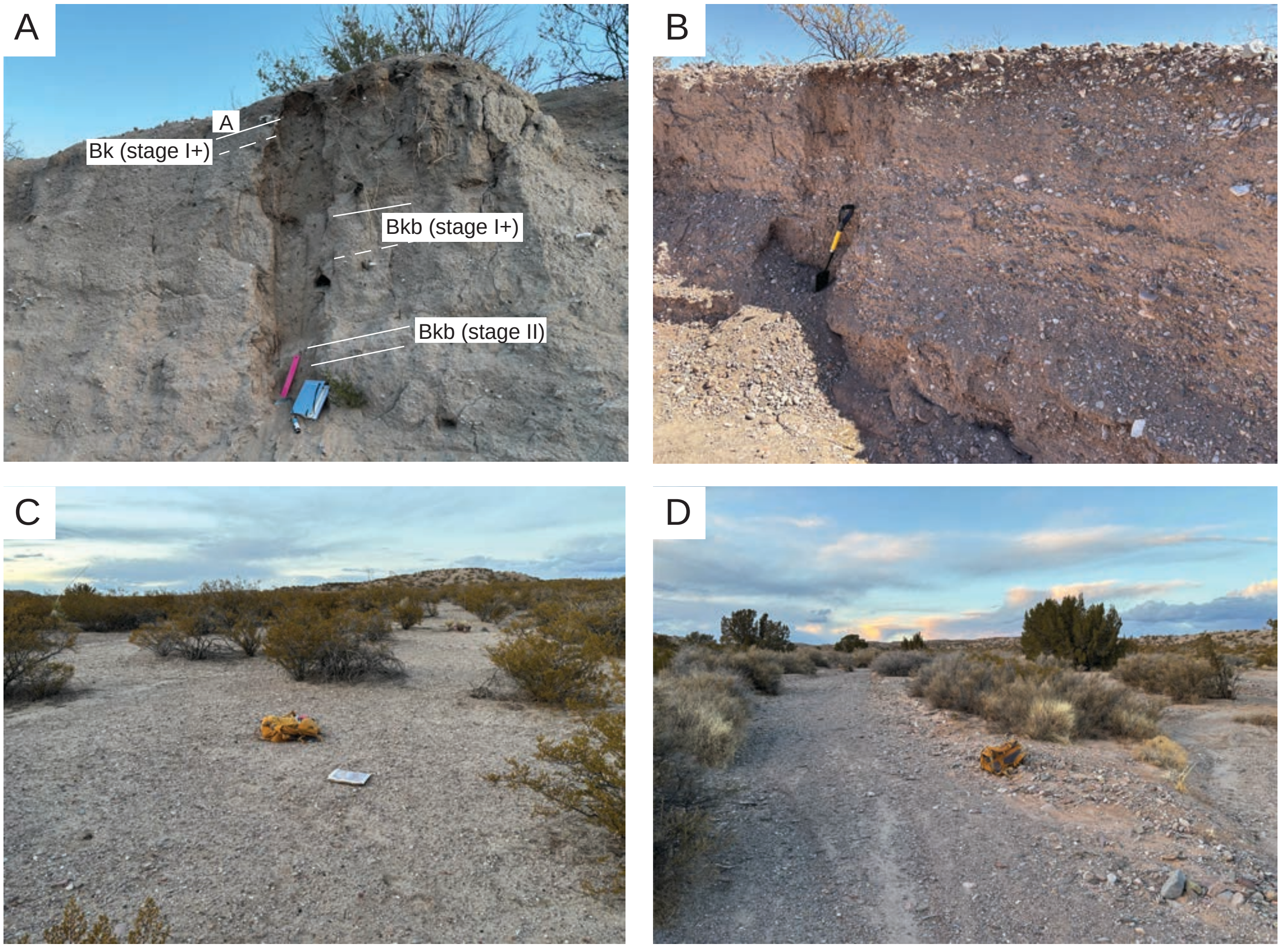

APPENDIX 1. DESCRIPTIONS OF MAP UNITS

Methods

The units described below were mapped using aerial photography coupled with field checks or by examining well cuttings and comparing them to existing lithologic descriptions in the case of subsurface units. Stereo photogrammetry software (Stereo Analyst 16.6, a Hexagon Geospatial extension for ArcMap 10.8.2) allowed for accurate placement of geologic contacts. Grain sizes follow the Udden-Wentworth scale for clastic sediments (Udden, 1914; Wentworth, 1922) and are based on field estimates. The term "clast(s)" refers to the grain size fraction greater than 2 mm in diameter. Descriptions of bedding thickness follow Ingram (1954). Colors of sediment are based on visual comparison of dry samples to Munsell Soil Color Charts (Munsell Color, 2009). Soil horizon designations and descriptive terms follow those of Birkeland et al. (1991), Soil Survey Staff (1992), and Birkeland (1999). Stages of pedogenic calcium carbonate morphology follow those of Gile et al. (1966) and Birkeland (1999). Descriptions of sedimentary, igneous, and metamorphic rocks were based on inspection using a hand lens.

Surface characteristics and relative landscape position were used in mapping middle Pleistocene to Holocene units. Surface processes dependent on age (e.g., desert pavement development, clast varnish, calcium carbonate accumulation, and eradication of original bar-and-swale topography) were used to differentiate stream terrace, alluvial fan, and valley floor deposits. Younger deposits are generally inset below older deposits (e.g., terrace deposit suites), or they occur as a thin sheet on older deposits.

POST-SANTA FE GROUP DEPOSITS

Water

water (modern)—Liquid water occupying Elephant Butte Lake. Annual surface-elevation changes are as much as 15 m. Maximum depth during investigation is ≈170 ft (≈50 m). Representative shoreline elevation shown on map is 4380 ft. A highstand of 4441 ft occurred in June 1942 and the lake was near this level (≈full capacity) from the mid-1980s through 2000, allowing development of notable shoreline deposits (**Qsl**).

Artificial Fill

af **Artificial fill (0–100 years old)**—Thick accumulations of sand with minor gravel and silt–clay from construction activities related to terracing, roads, levees or dams. The fill is 1–10 m thick.

Eolian Units

Qe **Eolian sand (recent to middle Holocene)**—

Short—

Windblown sand on the leeward side of topographic highs. Sand is light-brown to light-yellowish-brown (7.5–10YR 6/3–4), mostly massive, well-sorted, fine- to medium-grained, and quartzo-feldspathic. Commonly vegetated, with little or no soil development. The sediment is deflated from the Rio Grande floodplain or Palomas Formation (i.e., **QNpa**). The deposit is weakly consolidated and 1–5 m thick.

Long—

Windblown sand on the leeward (east or northeast) side of topographic highs and ridges. The sand is light-brown to light-yellowish-brown (7.5–10YR 6/3–4), well-sorted, subangular to rounded, fine- to medium-grained, and quartzo-feldspathic. The deposit is mainly massive but locally has laminae or very thin beds semi-parallel to the slope. Commonly vegetated, with little or no soil development. Most of the sediment is probably derived from the floodplain of the Rio Grande and deflated Palomas Formation (i.e., **QNpa**) deposits. Locally, the deposit is mapped as an eolian mantle on older units (see **Qes**). The deposit is unconsolidated to weakly consolidated and 1–5 m thick.

Qes Eolian sand sheets (Holocene to late Pleistocene(?))—

Short—

Sand and silty sand forming a sheetlike deposit. The sand is pale-brown to light-yellowish-brown (10YR 6/3–4), massive, well-sorted, fine- to medium-grained, and quartzo-feldspathic. Weakly developed soils with weak to moderate ped development and $CaCO_3$ precipitation. Some coppice dunes are present on the surface. Sands are loose to weakly consolidated. The unit is generally less than 4 m thick.

Long—

Sand and silty sand forming a sheetlike deposit, commonly on mesas. The sand is pale-brown to light-yellowish-brown (10YR 6/3–4), massive, well-sorted, subangular to rounded, fine (lower) to medium (lower)-grained, and quartzo-feldspathic. Weakly developed buried soils are characterized by weak to moderate ped development and calcium carbonate ($CaCO_3$) precipitation. Some coppice dunes are present on the surface. Sands are loose to weakly consolidated. The deposit is generally less than 4 m thick.

Surficial Deposits on Slopes

Qs Sheetflood deposits (recent to middle Holocene)—

Short—

Sheetflood deposits with a high proportion of quartzo-feldspathic sand input via eolian processes or reworking of **QNpa**. The sediment is massive and variably overprinted by weakly developed, calcic soils (Stage I carbonate morphology). The sand is very fine- to fine-grained, with minor medium- to very coarse-grained sand and scattered pebbles. The deposits are weakly consolidated and 1–5 m thick.

Long—

Sheetflood deposits with a high proportion of quartzo-feldspathic sand input via eolian processes or reworking of unit **QNpa**. The sediment is massive and variably overprinted by weakly developed, calcic soils. The sand is very fine- to fine-grained, with subordinate medium- to very coarse-grained sand and minor scattered pebbles. Pedogenesis is indicated by Stage I calcic horizons and weak to moderate, subangular, blocky ped development that typically lacks clay illuviation. The deposit is weakly consolidated and 1–5 m thick.

Qtal Talus deposits (Holocene to late Pleistocene)—Accumulation on steep hillslopes of angular to subangular blocks of basalt, primarily boulder-size, that weather from columnar basalt flanking the central vent breccia of maars. The proportion of sandy matrix is variable. It is mapped only on Elephant Butte. The deposit thickness is greater than 3 m.

Valley-Floor Units

Qa Alluvium, undivided (Holocene to late Pleistocene)—Sand, gravelly sand, and sandy gravel occupying valley-floor positions. Includes units **Qar** and **Qay** (described below), but these could not be differentiated due to anthropogenic disturbance. The deposit is 1–10 m thick.

Qarg Alluvium of the Rio Grande (recent to late Pleistocene)—

Short—

Alluvium underlying the Rio Grande floodplain and in the active channel. Floodplain deposits consist of sand, silt, and clay. The active channel has sandy pebbles and cobbles that are subrounded to rounded and composed of diverse lithologies (including quartzite, sandstone, chert, and volcanic rocks). The sand is fine- to coarse-grained and quartzo-feldspathic. The deposit thickness is 10–20 m.

Long—

Alluvium underlying the Rio Grande floodplain and in the active channel. Floodplain deposits consist of sand, silt, and clay. The active alluvium includes sand, pebbles, and cobbles in the axial channel of the Rio Grande, commonly in longitudinal or transverse bars. Clasts consist of poorly to moderately sorted, subrounded to rounded pebbles and cobbles. Boulders may be present, having been transported from local tributaries to the active channel during larger flood events. Clast lithologies are diverse and include quartzite, sandstone, chert, and a variety of volcanic rocks. The gravel matrix consists of moderately to very well-sorted, subangular to rounded, fine- to coarse-grained, quartzo-feldspathic sand. The inferred deposit thickness is 10–20 m (from fig. 3B of Person et al., 2024, assuming Qs of that figure is correlative to unit **Qarg**).

Qar Recent alluvium of ephemeral drainages (modern to historic)—

Short—

Loose sand and gravel (pebbles, minor cobbles) that form bars and underlie channels in ephemeral drainages. The sand is light-gray to brown to grayish-brown and mostly medium- to very coarse-grained. Bar-and-swale topography, steep-walled channels, sparse vegetation, and lack of topsoil development characterize the surface. The deposit overlies and inset into **Qay**. The deposit is ≈0.1–2 m thick.

Long—

Gravelly sand and sandy gravel that form bars and underlie channels in ephemeral drainages; excludes Rio Grande channel and floodplain (unit **Qarg**). The gravel is mainly very fine to very coarse pebbles with minor cobbles; clasts are subrounded, poorly sorted, and composed of volcanic clasts (primarily intermediate to felsic types), with minor sedimentary rocks. The sand is brown (10YR 5/3–4) and light-gray to grayish-brown (10YR 5–7/2), fine- to very coarse-grained (mostly medium- to very coarse-grained), subangular to subrounded, and poorly to moderately sorted. Sand grains are composed of quartz and subordinate clear feldspar (sanidine and plagioclase) and volcanic lithics; coarse to very coarse grains are composed wholly of volcanic lithic grains. Ephemeral drainage bottom exhibits bar-and-swale (gully) topography with ≈10 to ≈100 cm of relief. Vegetated highs (≈1 m tall) may be topped by very fine- to medium-grained sand deposited by floodwaters whose flow velocities are locally slowed down by shrubs. Sparse vegetation and no topsoil development characterize the surface. The deposit disconformably overlies and is inset into **Qay**. Estimated unit thickness is 0.1 to ≈2 m.

Qay Younger alluvium (late Holocene to latest Pleistocene)—

Short—

Interbedded pebbly sand, sand, and sandy gravel that underlies a smooth geomorphic surface (no bar-and-swale topography) typically 1–3 m above the modern grade. The sand is brown, fine- to very coarse-grained, and weakly consolidated. The topsoil on maximum aggradation surface (mapped separately) has Stage I to II calcium carbonate morphology. The deposit extends under **Qar** and is 1–30(?) m thick.

Long—

Interbedded pebbly sand, sand, sandy gravel, and silty to clayey sand. The sediment underlies a smooth geomorphic surface (no bar-and-swale topography) typically 1–3 m above the modern grade; this surface and underlying deposit underlies terraces parallel to the main-stem drainage and includes small tributary alluvial fans. The sandy gravel is clast- to sand-supported and in very thin to medium, lenticular to tabular beds exhibiting <10% cross-stratification with very thin, planar foresets. Pebbly sand, sand, and silty to clayey sand are in thin to thick, broadly lenticular to tabular beds; pebbles are commonly scattered in massive to horizontal-planar laminated sand. Gravel is typically volcanic-dominated pebbles and minor cobbles that are subrounded and poorly to moderately sorted in a bed. Sand typically has <10% clay-silt and commonly has minor scattered pebbles. The sand is typically brownish (10YR 5/3–4), fine- to very coarse-grained (<20% very fine- to fine-grained), subangular to subrounded, moderately sorted, and composed of volcanic grains with variable plagioclase, sanidine, and quartz (depending on source lithologies). Topsoil development is minimal, with calcic horizon development up to a Stage I+ carbonate morphology (weak to no HCl effervescence); rarely, the topsoil exhibits Stage II carbonate morphology. A geomorphic surface approximating maximum aggradation is mapped separately and consists of a relatively high surface 3–4 m above the modern grade. The surface soil on this mapped surface commonly contains a 5–20 cm thick Stage I to II calcic horizon, locally overlain by a 10–20 cm thick A horizon. Sparse buried calcic horizons are observed within the deposit (10–50 cm thick), exhibiting Stage I to II carbonate morphologies. The surface has a weakly developed desert pavement and weak varnishing of surface clasts. The unit extends beneath **Qar** down to the strath of valley-bottom alluvium. The deposit is 1 to possibly tens of meters thick.

Qayr Younger alluvium and subordinate recent alluvium, undivided (recent to latest Pleistocene)— Unit that combines younger alluvium underlying low-level terraces and small tributary alluvial fans (**Qay**) with subordinate recent alluvium (**Qar)**, the latter occurring primarily in incised drainages. See detailed descriptions of units **Qay** and **Qar**. This deposit is <30 m thick.

Qary Recent alluvium and subordinate younger alluvium undivided (present to latest Pleistocene)— Recent deposits (**Qar**) underlying recently reworked drainage floors flanked by slightly older sediment (**Qay**) underlying low-level terraces and small tributary alluvial fans. See detailed descriptions of units **Qar** and **Qay**. This deposit is <30 m thick.

Qai Intermediate alluvium (late Pleistocene)—

Short—

Sandy gravel and pebbly sand; the topsoil exhibits a weak cambic horizon (20–30 cm thick) and a Stage II calcic horizon (>15 cm thick). Sand is fine- to very coarse-grained and pebbles are subrounded, poorly sorted, and volcanic. Tread height is ≈2 m above adjoining valley floor. **Qai** is differentiated from **Qay** primarily based on its slightly more developed topsoil. The deposit is 1–3 m thick.

Long—

Sandy gravel and pebbly sand with a topsoil exhibiting a weak cambic horizon (20–30 cm thick and a Stage II calcic horizon (>15 cm thick). Poorly exposed. Shallow excavations show a fine- to very coarse-grained sand that is subangular to subrounded and poorly sorted. Pebbles are very fine to very coarse, clast-supported, subrounded, poorly sorted, and volcanic. There is <5% clay-silt. The tread height is about 2 m above adjoining valley floor. The surface exhibits a weak desert pavement with 30–80% clast density and weak Av ped development. The unit may correlate with sediment underlying the oldest surfaces of **Qay**, but differentiated here based on higher degree of soil development. The deposit is 1–3 m thick.

Modern Lake Deposits

Qsl Shoreline deposits along the margin of Elephant Butte Lake (recent)—Loose sand, gravelly sand, and gravel along the margin of Elephant Butte Lake. Sediment is principally reworked from underlying deposits (Cretaceous strata, Santa Fe Group, and post-Santa Fe Group). There are common small benches (generally less than a few meters wide) created by wave erosion and nearshore currents. The unit is <30 years old (postdates high lake levels of the mid-1990s).

Alluvial Fan Units

Qfr Recent fan alluvium (0 to 100 years old)—Small alluvial fans at the mouth of low-order drainages on the southern border of the Rio Grande floodplain near Truth or Consequences. Bar-and-swale topography, steep-walled channels, sparse vegetation, and lack of topsoil development characterize the surface. Probably less than 2 m thick and overlies **Qfy**.

Qfy Younger fan alluvium (Holocene to latest Pleistocene)—
Short—
Gravelly sediment underlying small alluvial fans. It is composed mainly of sandy gravel and gravelly sand in very thin to medium, tabular to broadly lenticular beds. The sand is brownish and medium- to very coarse-grained. The thin topsoil (tens of centimeters) has a Stage I to I+ carbonate morphology. The deposit has a smooth geomorphic surface with weak desert pavement and is 2–5(?) m thick.
Long—
Gravelly sediment similar to unit **Qay** but underlying small alluvial fans at the mouths of low-order drainages. It is composed mainly of sandy gravel and gravelly sand in very thin to medium, tabular to broadly lenticular beds. The sand is brownish, medium- to very coarse-grained, subangular to subrounded, poorly to moderately sorted, and a volcanic litharenite. The relatively thin topsoil (tens of centimeters) has a Stage I to I+ carbonate morphology. The deposit has a smooth geomorphic surface with a weak desert pavement and is 2–5(?) m thick.

Qfyr Younger fan alluvium and subordinate recent alluvium (recent to latest Pleistocene)—Gravelly sediment underlying small alluvial fans at the mouths of low-order drainages. Consists mainly of **Qfy** with subordinate **Qar,** the latter being inset below smooth, slightly elevated geomorphic surfaces associated with **Qfy** (exhibiting weak desert pavement development). See descriptions of **Qfy** and **Qar**. This deposit is 2–5(?) m thick.

Qfry Recent alluvium and subordinate younger fan alluvium (recent to latest Pleistocene)—Gravelly sediment underlying small alluvial fans at the mouths of small, low-order drainages. Consists mainly of unit **Qar** with subordinate **Qfy** deposits. **Qar** deposits are inset below smooth, slightly elevated geomorphic surfaces associated with **Qfy** (exhibiting weak desert pavement development). See descriptions of **Qar** and **Qfy**. This deposit is 2–5(?) m thick.

High-level piedmont deposits west of the Rio Grande
Qftl Lower unit of high-level fan-terraces (late Pleistocene)—
Short—
Sandy pebbles, pebbly sand, and fine-grained sand to silty-clayey fine-grained sand with minor pebbles. Finer grained sediment may be pedogenically altered (Stage I carbonate morphology, weak to moderate peds with faint clay films). The geomorphic surface is 4–6 m above the modern grade, its topsoil has Stage I+ to II calcic horizons, and it exhibits weak to moderate clast varnishing. The deposit is several meters thick.
Long—
Interbedded sandy pebbles, pebbly sand, and fine-grained sand to silty-clayey fine-grained sand with minor pebbles. Sandy pebbles and pebbly sand are grayish to brownish-gray; clasts are subrounded, and there are minor cobbles; the sandy matrix of these gravelly deposits is relatively coarse and dominated by volcanic grains. Also present are relatively fine-grained sand (very fine- to fine-grained sand is more abundant than medium to very coarse-grained sand) and silty-clayey fine-grained sand that has scattered, minor pebbles. This finer grained sediment may be overprinted by pedogenesis characterized by Stage I carbonate morphology and weak to moderate, subangular blocky peds with faint clay films. The geomorphic surface is 4–6 m above the modern grade. Locally, there are two geomorphic surfaces separated by 1–2 m of relative height, but it is not known if separate allostratigraphic units underlie the two treads. The surface is smooth and shows weak to moderate clast varnishing, and its calcic topsoil

exhibits a Stage I+ to II carbonate morphology. The deposit is weakly consolidated and several meters thick.

Qftm Middle unit of high-level fan terraces (middle Pleistocene)—
Short—
Sandy gravel and gravelly sand in very thin to medium, lenticular to tabular beds. The sediment underlies a tread 12–13 m above the modern grade and is at same geomorphic level as **Qtc2**. Gravel is composed of volcanic-dominated pebbles with minor cobbles. Sand is brownish and mainly medium- to very coarse-grained. The topsoil has Stage II to III+ carbonate morphology. The deposit is <5 m thick.
Long—
Sandy gravel and gravelly sand in very thin to medium, lenticular to tabular beds. The deposit is derived from the erosion of the Santa Fe Group. Gravel is composed of volcanic-dominated pebbles with minor cobbles that are subrounded and poorly to moderately sorted. Sand is brownish and mostly medium- to very coarse-grained. The topsoil is characterized by Stage II to III+ carbonate morphologies. The desert pavement on the deposit's surface has a dense (95–99%) clast armor, moderate degrees of varnishing, and moderate Av ped development. The deposit underlies geomorphic surfaces 12–13 m above the modern grade. It lies at the same general geomorphic level as terrace deposit **Qtc2**. The deposit is <5 m thick, and commonly 2–3 m thick.

Qfth Higher unit of high-level fan terraces (middle Pleistocene)—Gravelly sediment similar to **Qftm** (as described above) underlying terrace deposits a few meters above the surface of adjoining **Qftm**. The deposit lies at the same geomorphic level as the **Qtc1** terrace deposit and is a few meters thick.

High-level piedmont deposits east of Rio Grande
Qfcm High-level fan deposit flanking western Caballo Mountains (late to middle Pleistocene)—Sandy gravel, gravelly sand, and sand in fans at the mouths of ephemeral streams draining the western Caballo Mountains. Typically overlies **Qtr4** terrace deposit. Gravel is angular to subangular, poorly sorted, and composed of sandstone, limestone, and siltstone. Clast composition varies depending on the bedrock exposed in a given drainage. The deposit is 2–15 m thick.

Qftme High-level fan and terrace deposits associated with Mescal Canyon (late to middle Pleistocene)—
Short—
Sandy gravel, gravelly sand, and sand in medium to thick, broadly lenticular to tabular beds. This sediment underlies high-level terraces of Mescal Canyon and its alluvial fan at the north end of the Caballo Mountains; tread heights are 25–32 m above the modern grade. The well-graded pebbles through boulders are composed of sandstone, siltstone, and limestone clasts. The deposit is 2–11 m thick.
Long—
Sandy gravel, gravelly sand, and sand in medium to thick, broadly lenticular beds; sand is commonly horizontal-planar laminated. This sediment underlies terraces and fan-terraces associated with Mescal Canyon whose treads are 25–32 m above the modern grade and mostly project to the geomorphic level of **Qtr4**. The gravel includes relatively well-graded pebbles through boulders that are subangular to subrounded, poorly sorted, mostly clast-supported, and composed of greenish sandstone and siltstone with subordinate limestone sourced from Permian and Cretaceous strata. Sand is mostly medium- to very coarse-grained, subrounded, and composed mainly of sedimentary lithic grains. Near the Rio Grande, there are ≤1 m-thick tongues of very fine- to medium-grained sand and silty, very fine- to fine-grained sand that is massive or planar bedded (up to 10 cm thick). The sand in these finger tongues is light-brown (7.5YR 6/4) to brown (10YR 5/4), subrounded to subangular, well sorted, and composed of quartz, minor

feldspar, and minor (commonly 10–15%) sedimentary-lithic grains; locally there are 1% scattered coarse to very coarse sand grains. The deposit is 2–11 m thick.

Qaoc Older alluvium in Cutler sag (late to middle Pleistocene)—Deposits east of Rio Grande underlying fan-terraces and minor stream terraces that are >3 m above the modern grade. Sediment consists of sand, clayey–silty sand, and gravel. The gravel is subangular and composed of sandstone and siltstone eroded from local Cretaceous units. Sand include quartz, feldspar, and sedimentary and volcanic lithic grains. The deposit is 1–5(?) m thick.

QNj Surficial deposits in the Jornada del Muerto (Pleistocene)—Pale-red to buff silt and sand with pebble and cobble interbeds. Clasts are angular to rounded and poorly sorted and include sandstone, quartzite, granite, limestone, and a variety of volcanic types. Capped by weak to strong calcic soils. The unit is generally <6 m thick.

Cuchillo Negro Creek Terrace Deposits
Weakly to moderately stratified and weakly consolidated sand and gravel. Terraces occur at five main levels above the present base level, with one (1) denoting the oldest (highest) level and progressively higher numbers indicating progressively younger (lower) deposits. Similar numbers in Cuchillo Negro Creek vs. Rio Grande terrace labels indicate the same geomorphic level. Weakly consolidated. The older two deposits are thicker than the younger deposits.

Qtc5 Lower terrace deposit (late Pleistocene)—Gravelly terrace deposit whose tread lies 9–14 m above younger valley fill alluvium. The deposit includes two subunits (**Qtc5b** and **Qtc5a**) whose treads are separated by ≈2 m. Inferred to represent two stratigraphic units, but the associated buttress unconformity has not been confirmed. The deposit is 2–4 m thick.

Qtc5b Lower subunit of lower terrace deposit (late Pleistocene)—
Short—
Sandy pebbles and cobbles underlying 1–2 m of finer sediment. Lower gravel consists of pebbles through coarse cobbles and 10% fine boulders, and composed mainly of dark intermediate volcanic rocks (minor felsics). Upper 1–2 m is mostly very fine- to medium-grained sand. The tread lies 9–11 m above the modern grade. Topsoil carbonate morphology is less than Stage III. The deposit is 3–4 m thick.
Long—
Approximately 2 m thick sandy pebbles and cobbles underlying 1–2 m of sandy sediment. Gravel consists of well-graded pebbles through coarse cobbles and 10% fine boulders. Clasts are subrounded and composed mostly of dark, intermediate volcanic rocks (20% porphyritic and 60% fine-grained); a subordinate portion (15–20%) of gravel is felsic volcanic (mostly fine-grained). Sparse clasts include 1–2% monzonite-diorite intrusives and 0.5% reddish siltstone to very fine-grained sandstone (eroded from Permian strata). The upper part of the deposit consists of yellowish-brown (10YR 5/4) to light-brown (7.5YR 6/3–4), very fine- to medium-grained sand (mostly very fine- to fine-grained) and clayey-silty fine-grained sand; a few beds contain minor fine to very coarse pebble beds and 10% cobbles. The upper part of the deposit coarsens slightly up-section. The terrace tread lies 9–11 m above younger alluvium of Cuchillo Negro Creek. The terrace deposit correlates with Qtc2a of Koning et al. (2018). Topsoil has a carbonate morphology that is less developed than Stage III. The unit is 3–4 m thick.

Qtc5a Upper subunit of lower terrace deposit (late Pleistocene)—Sandy pebbles through cobbles and 1–10% fine boulders; similar to gravelly sediment in unit **Qtc5**. The terrace tread lies 12–14 m above younger alluvium in Cuchillo Negro Creek and ≈2 m above the tread of **Qtc5**. The terrace deposit correlates with Qtc3a of Koning et al. (2018). The unit is 2–3 m thick.

Qtc4 Lower-middle terrace deposit (early-late Pleistocene)—
Short—
The deposit is approximately similar to that of **Qtc3**. Gravel consists of subrounded pebbles with 10–15% cobbles. The tread is ≈22 m above the unincised valley floor of Cuchillo Negro Creek. Both tread and strath lie 4–5 m below the respective tread and strath of **Qtc3**, and so **Qtc4** appears to be a separate cut-and-fill event that postdates **Qtc3**. The deposit is ≈5 m thick.
Long—
The deposit is approximately similar to that of **Qtc3**. Gravel consists of pebbles with 10–15% cobbles. Gravel is subrounded and composed of 10% porphyritic intermediate volcanics; 40–50% fine-grained, dark, intermediate volcanics; trace granite; trace monzonite-diorite intrusions; 5–10% porphyritic felsic volcanics; 1–2% Kneeling Nun Tuff; and 25–30% fine-grained felsic volcanics. The tread is ≈22 m above the unincised valley floor of Cuchillo Negro Creek. Both tread and strath lie 4–5 m below the respective tread and strath of **Qtc3**, and so **Qtc4** appears to be a separate cut-and-fill event that postdates **Qtc3**. May correlate to Qtc3b or Qtc3c of Koning et al. (2018). The deposit is weakly consolidated and ≈5 m thick.

Qtc3 Upper-middle terrace deposit (middle Pleistocene)—
Short—
Sandy gravel and subequal gravelly sand in very thin to medium, lenticular to tabular beds. Gravel is clast-supported, subrounded, and a volcanic-dominated suite of pebbles, 10–20% cobbles, and 1–2% boulders. Sand is mostly coarse- to very coarse-grained and reddish-brown. The terrace tread is 27–28 m above the modern grade and has a moderately varnished desert pavement. The deposit is ≈5 m thick.
Long—
Sandy gravel and subequal gravelly sand in very thin to medium, lenticular to tabular beds. Sandy gravel is clast-supported and composed of very fine to very coarse-grained pebbles with 10–20% fine to coarse cobbles and 1–2% boulders. Clasts are well-imbricated. Gravel is subrounded, poorly sorted, and composed of 20–25% porphyritic intermediate volcanics, 40–50% fine-grained intermediate volcanics, 20% fine-grained felsic volcanics, 5% porphyritic felsic volcanics, 1% porphyry with block potassium-feldspar phenocrysts (similar to that seen along Alamosa Creek), trace to 1% Kneeling Nun Tuff, trace to 0.5% monzonite-diorite intrusives, trace to 0.5% Paleozoic limestone, and 0.5% reddish siltstone to very fine-grained sandstone clasts (eroded from Permian strata). The gravel matrix is reddish-brown to light-reddish-brown (5YR 5–6/3), fine- to very coarse-grained sand (mostly very coarse) that is subrounded to rounded, moderately sorted, and a volcanic litharenite with 1% clay films. The pebbly sand is clast- to sand-supported, and pebbles are very fine to very coarse. The associated sand is brown to reddish-brown to reddish-yellow (5-7.5YR 5/4–6/6), has trace to 0.5% clay, and is medium to very coarse-grained (mostly coarse- to very coarse-grained). Sand is poorly to moderately sorted. The medium-grained sand is composed of quartz, feldspar, and 10–20% volcanic lithics, whereas coarser grained sand is composed of volcanic lithics. The base of the deposit has up to 1 m of scour relief. The terrace tread is 27–28 m above the modern grade and has a moderately developed desert pavement, dense clast armor (10% spacing between clasts), minor Av ped development, and weak to moderate clast varnish. Topsoil has a calcic horizon with Stage II to III+ carbonate morphology. The unit correlates to Qtc3d of Koning et al. (2018). The unit is weakly consolidated and ≈6 m thick.

Qtc2 Lower-upper terrace deposit (middle Pleistocene)—
Short—

Sandy gravel and subordinate gravelly sand in lenticular to tabular beds. Gravel is subrounded, mostly composed of intermediate-composition volcanic rocks, and consists of pebbles, 20–40% cobbles, and 1–2% boulders. The tread lies ≈29–30 m above **Qay** in Cuchillo Negro Creek. The unit correlates with **Qftm** of this work and Qtc4 of Koning et al. (2018). The unit is weakly consolidated and 5–10 m thick.
Long—
Sandy gravel and subordinate gravelly sand in very thin to medium, lenticular to tabular beds. Gravel is subrounded and poorly sorted and consists of very fine to very coarse pebbles, subordinate (20–40%) cobbles, and 1–2% boulders. Gravel is clast- to sand-supported and composed of dark, fine-grained, intermediate-composition volcanic rocks, 15–20% porphyritic volcanic rocks, ≈20% fine-grained felsic volcanic rocks, 0.5% reddish siltstones to very fine-grained sandstones (eroded from Permian strata), and 0.5% Kneeling Nun Tuff. Sand is medium- to very coarse-grained, subrounded, moderately sorted, and a volcanic litharenite with 1–6% clay as films on clasts and grains. The geomorphic surface locally has moderately varnished clasts, and the tread lies ≈29–30 m above **Qay** in Cuchillo Negro Creek. The unit correlates with **Qftm** of this work and Qtc4 of Koning et al. (2018). The deposit is weakly consolidated and 5–10 m thick.

Qtc1 Upper terrace deposit (middle Pleistocene)—
Short—
Sandy gravel in very thin to medium, tabular to lenticular beds. Gravel is mostly composed of intermediate-volcanic rocks and consists of pebbles, 10–40% cobbles, and 0–1% boulders. Sand is reddish-brown and mostly medium- to very coarse-grained. The tread lies ≈9 m above the **Qtc2** tread, 48–49 m above Cuchillo Negro Creek. The deposit correlates to **Qfth** and is 9–10 m thick, tapering northward.
Long—
Sandy gravel and subordinate gravelly sand in very thin to medium (minor thick), tabular to lenticular beds. Gravel is clast-supported, subrounded to rounded, poorly to moderately sorted, moderately imbricated, and composed of very fine to very coarse pebbles with 10–40% cobbles and 0–1% boulders. The estimated gravel composition is 20–35% porphyritic intermediate volcanics, 30–50% fine-grained intermediate volcanics (including basaltic andesite), 15–35% felsic volcanic rocks, trace to 1% Kneeling Nun Tuff, 0–1% Paleozoic sedimentary rocks, and trace monzonite intrusions. Sand is reddish-brown (5YR 5/3–4/4), fine- to very coarse-grained (mostly medium- to very coarse-grained), subrounded to subangular, poorly to moderately sorted, and mostly composed of volcanic lithic grains. There is 1–15% clay in the sand matrix as clay chips and clast coatings. The deposit is weakly cemented by clays and moderately consolidated. The deposit thins (wedge-out) laterally away from Cuchillo Negro Creek. The tread lies about 9 m above the tread of **Qtc2**, 48–49 m above the unincised valley floor of Cuchillo Negro Creek. The unit correlates to **Qfth** of this work and Qtch1 of Koning et al. (2018). The deposit is 9–10 m thick.

Qtco Uppermost terrace deposit (middle Pleistocene)—
Short—
Sandy gravel that is clast-supported and in poorly defined, tabular to lenticular, very thin to medium beds. The unit caps buttes whose tops are ≈55 m above Cuchillo Negro Creek. Gravel is clast-supported, subrounded and consists of pebbles (mostly very coarse) with 25–30% cobbles. A calcic topsoil with Stage III carbonate morphology is preserved locally. The deposit is 2–3 m thick.
Long—
Sandy gravel that is clast-supported and in poorly defined, tabular to lenticular, very thin to medium beds. The deposit caps buttes whose tops are ≈55 m above Cuchillo Negro Creek. Gravel is clast-supported, subrounded, and consist of pebbles (mostly very coarse) with 25–30% cobbles. Gravel is composed of dark, fine-grained intermediate volcanic rocks, 25–30% porphyritic intermediate volcanic rocks, 20% fine-

grained rhyolites, 1% Paleozoic limestone, and trace reddish siltstone and very fine-grained sandstones (eroded from Permian strata). A calcic topsoil with Stage III carbonate morphology is preserved locally. The unit is weakly to moderately consolidated and 2–3 m thick.

Rio Grande Terrace Deposits

Weakly to moderately stratified sand and gravel with sparse silt lenses. Gravel clasts are up to 30 cm, subrounded to rounded, poorly to moderately sorted, and composed of volcanic rocks, quartz, granite, sandstone, and metamorphic clasts. Terraces occur at five main levels above the present base level, with one (1) denoting the oldest (highest) deposit and increasing numbers progressively indicating progressively younger (lower) deposits. The deposits are weakly consolidated.

Qtr5 Lowest terrace deposit (late Pleistocene)—

Short—

Poorly bedded, imbricated sandy gravel consisting of ≈60% pebbles and ≈40% cobbles. Clasts are composed of intermediate volcanic rocks, subordinate felsic volcanic rocks, 5–10% quartzite and quartz, and 5–10% granite. Pale-brown to light-gray sandy matrix. Stage I+ carbonate morphology in topsoil. The tread height is 8–14 m above the modern grade, increasing upstream. The deposit is 1.5–3 m thick.

Long—

Imbricated, cobbly gravel in vague, medium, lenticular beds. Gravel is subrounded to rounded, poorly sorted, and consist of ≈60% pebbles, 35–40% cobbles, and 5% fine boulders. The gravel is composed of intermediate volcanic rocks, subordinate felsic volcanic rocks, 5–10% quartzite, 5–10% granite, 1–3% quartz, and trace to 0.5% reddish siltstone and very fine-grained sandstone. Gravel matrix is pale-brown to light-gray (10YR 6/3–7/2) sand that is fine- (upper) to medium- (upper) grained, subangular to subrounded, poorly sorted, and composed of quartz, minor clear feldspars (sanidine, plagioclase), and minor volcanic-rich lithic grains. Stage I+ carbonate morphology in the upper 80 cm is indicated by carbonate coats and/or rinds on up to 90% of clasts and common carbonate cement. The tread height is 8–14 m above the modern grade, increasing upstream. The unit correlates to Qtr3 of Jochems and Koning (2014). The deposit is 1.5–3 m thick.

Qtri Intermediate Terrace deposit between Qtr4 and Qtr5 (late Pleistocene)—Medium- to thick-bedded and well-imbricated. Contains up to 15% boulders. Light-yellowish-brown (10YR 6/4) sandy matrix. Sandy pebble lenses are common and ≤25 cm thick. The topsoil has a 35 cm thick Stage II+ calcic horizon. The tread height is 19–21 m above the modern grade. The unit may correlate to Qtr4 of Jochems and Koning (2014), whose description is used here. The deposit is ≈3 m thick.

Qtr4 Upper-lower terrace deposit, undivided (early-late Pleistocene)—

Short—

Clast-supported, sandy gravel in tabular to lenticular beds and subordinate gravelly sand. Stage II+ to III carbonate morphology in the upper 0.5–1 m. The tread height is 23–26 m and the strath has several meters of relief. The deposit correlates to Qtr5 of Jochems and Koning (2014) and is generally several meters (up to 25 m) thick. It is locally subdivided into two subunits (**Qtr4a** and **Qtr4b**).

Long—

Clast-supported, sandy gravel in tabular to lenticular beds. Subordinate gravelly sand that is horizontal-planar laminated or cross-stratified. Gravel is variably imbricated, subrounded to rounded, and poorly sorted. It consists of pebbles, 10–40% cobbles and trace to 10% boulders. Clast composition is dominated by intermediate and felsic volcanic rocks with 3–7% quartzite, 1–3% quartz, 3–5% granite, trace to 3% limestone, trace to 3% reddish siltstone and very fine-grained sandstone, trace to 3% greenish sandstone, trace to 1% tannish sandstone, and 1–5% chert. Sandy matrix is pale-brown to light-yellowish-brown

(10YR 6/3–4) or grayish (10YR 6–7/2), medium- to very coarse-grained, subrounded, moderately to poorly sorted, and composed of quartz, clear feldspar (sanidine, plagioclase), 5–10% lithic grains, and 5–10% orange grains (potassium feldspar, chert, orange-stained quartz). Stage II+ to III carbonate morphology in the upper 0.5–1 m. The surface may be mantled by 0.5–2 m of **Qes**. The tread height is 23–26 m above the modern grade, and the strath has several meters of relief. The deposit correlates to Qtr5 of Jochems and Koning (2014) and is generally several meters (up to 25 m) thick. It is locally subdivided into two subunits (**Qtr4a** and **Qtr4b**).

Qtr4b Lower subunit of the upper-lower terrace deposit, undivided (early-late Pleistocene)— The tread height is 23–26 m above the modern grade of the Rio Grande.

Qtr4a Upper subunit of the upper-lower terrace deposit, undivided (early-late Pleistocene)— The tread height is 25–30 m above the modern grade of the Rio Grande.

Qtr3 Middle terrace deposit (middle Pleistocene)—Poorly exposed sandy gravel, mainly coarse to very coarse pebbles and fine cobbles. Gravel is rounded to subrounded and composed of volcanic rocks, sedimentary clasts, quartzite, chert, and granite. The tread height is 42–48 m above the modern grade of the Rio Grande. **Qtr3** is not mapped stricto sensu but divided into three subunits based on the tread height.

Qtr3c Lower subunit of the middle terrace deposit (middle Pleistocene)—The tread height is 42–43 m above the modern grade of the Rio Grande. The deposit is a few meters thick.

Qtr3b Middle subunit of the middle terrace deposit (middle Pleistocene)—The tread height is ≈44 m above the modern grade of the Rio Grande. The deposit is a few meters thick.

Qtr3a Upper subunit of the middle terrace deposit (middle Pleistocene)—The tread height is 46–48 m above the modern grade of the Rio Grande. The deposit is a few meters thick.

Qtr2 Lower-upper terrace deposit (middle Pleistocene)—The deposit is approximately similar to that of **Qtr1**. The tread height is 49–52 m above the modern grade of the Rio Grande. The deposit is a 1–4 m thick.

Qtr1 Uppermost terrace deposit (middle Pleistocene)—Poorly exposed, mesa-capping, sandy gravel. Clasts are mainly rounded to subrounded (minor subangular) and poorly sorted. The gravel consists of pebbles, 5–15% cobbles, and 1–3% fine boulders. The clasts are composed of felsic to intermediate volcanic rocks with 10–20% quartzite, 10–15% chert, and 3% granite. The tread is 58–59 m above the modern grade of the Rio Grande. The deposit is 3–4 m thick.

SANTA FE GROUP

Pyroclastic Deposits and Lava Flows

Qmb Maar-related, bedded breccia deposits (earliest Pleistocene)—

Short—

Brownish sandstone and slightly silty to clayey sandstone with proportionally variable, scattered basaltic and pumiceous lapilli. Sand has a high proportion of detritus from the Palomas Formation (**QNpa**) and McRae Group. The strata are in well-defined, relatively thin, tabular to slightly wavy beds and conformably underlain by flat-bedded, base surge sediments. The deposit is greater than tens of meters thick.

Long—

Brownish sandstone and slightly silty to clayey sandstone with variable (in terms of abundance) basaltic lapilli and pumice lapilli. Sand has a high proportion of detritus from the Palomas Formation (**QNpa**) and McRae Group. The strata are commonly in well-defined, relatively thin, tabular to slightly wavy beds that are hard. At the base of the sequence are base surge sediments that grade upward from mostly flat-bedded coarse sands to the aforementioned lapilli-bearing sandstone. The deposit is greater than tens of meters thick.

Qmv Maar-related vent facies (earliest Pleistocene)—Clast-supported, basalt breccia that accumulated inside of volcanic vents. It is an autobreccia probably formed from interaction with groundwater. Basalt clasts are vesicular and matrix between clasts is a chilled, fine-grained magma that is locally flow-foliated. This unit occurs as vertical bodies that likely extend downwards at least several meters.

Qb Maar-related, basaltic lavas (earliest Pleistocene)—Very dark-gray to black, basaltic rocks extruded from structurally controlled vents into the ancestral Rio Grande valley. Columnar basalt, pillows, and hyaloclastite are common at each volcanic center. Xenoliths include Cretaceous sediments, Precambrian metamorphics, and mantle-derived olivine xenoliths. Basalt ring dikes occur at Elephant Butte and Rattlesnake Island.

QNcc Cinder cone deposits (earliest Pleistocene to latest Pliocene)—Slightly reddish basaltic lapilli and scoria, inferred to have steeply inclined bedding. Spatter and agglutinate is abundant near the crater rim and within the crater. Deposit thickness of ≈30 m.

QNb Basalt flows (earliest Pleistocene to latest Pliocene)—Mesa-capping, basaltic lavas. This extrusive rock contains very dark-gray to black, aphanitic groundmass with sparse phenocrysts up to 2 mm long composed of olivine and plagioclase. Mostly ‘a‘ā lava with minor pāhoehoe. Columnar and platy jointing is well expressed. The flows are 3–23 m thick.

Sedimentary basin fill
Palomas Formation of Santa Fe Group
Upper Palomas Formation
Qppwc Western piedmont deposits, upper coarse unit (early Pleistocene)—
Short—
Sandy gravel in thin to medium, lenticular to tabular beds. Gravel is mainly clast-supported and pebbles with 10–20% cobbles, and is composed of felsic to intermediate volcanics. To the north, the upper 2–6 m of deposit has abundant Vicks Peak Tuff clasts. Sand is medium- to very coarse-grained and contains 1–10% clay chips and coatings. The unit is typically 2–6 m thick, and up to 15 m thick.
Long—
Sandy gravel in vague, thin to medium (minor thick), lenticular to tabular beds. Gravel is mainly clast-supported, subrounded (lesser rounded), poorly sorted, and volcanic and consists of very fine to very coarse pebbles with 10–20% fine to coarse cobbles and 1% boulders. In the upper 2–6 m, gravel is typically dominated by felsic compositions containing abundant Vicks Peak Tuff, with subordinate amounts of intermediate volcanic clasts. If the deposit is greater than 7 m thick, then the lower part (below 6–7 m) is composed of intermediate volcanic rocks with 20–50% light-colored, mostly fine-grained felsic rocks. The estimated clast composition of gravel below 7 m of the surface is 10–15% porphyritic intermediate volcanic rocks, 40% fine-grained intermediate volcanic rocks, 20–35% fine-grained felsic volcanic rocks, and 5–10% porphyritic felsic volcanic rocks, trace to 1% of a coarse feldspar porphyry associated with Alamosa Creek, trace Kneeling Nun Tuff, and trace reddish siltstones and very fine-grained sandstones

(eroded from Permian strata). The gravel matrix consists of reddish-gray to reddish-brown (5YR 5/2–4), medium- to very coarse-grained sand (<20% fine-grained sand) that is subrounded (minor rounded), poorly to moderately sorted, and a volcanic litharenite with 1–10% clay as chips or clast coatings (films). There are minor fine-grained beds similar to those in unit **Qppw**. Buried calcic paleosols (Stage I, locally Stage II, carbonate morphology) are sparse to common. The unit is weakly to moderately consolidated and weakly cemented by clay and variable calcium carbonate. It is typically 2–6 m thick and caps underlying, finer-grained western piedmont deposits. Capping soil commonly has a Stage III carbonate. Locally, the unit is as thick as 15 m, in which case the lower parts of the unit intertongue with the upper part of **Qppw**.

Qppw **Western piedmont deposits (early Pleistocene)—**

Short—

Fine-grained strata (very fine- to fine-grained sand, clayey-silty fine-grained sand, silt, and clay) intertonguing with 15–30% gravelly bodies. Fine strata are in 0.1–2.0 m thick, tabular beds and internally massive to vaguely horizontally laminated; slightly redder (commonly 5YR) compared to **Qpt**. Gravels are subrounded and composed of felsic to intermediate volcanic rocks. The deposit is ≈20 m thick.

Long—

Fine-grained strata consisting of very fine- to fine-grained sand, clayey-silty fine-grained sand, silt, and clay intertonguing with 15–30% gravelly bodies that generally increase in abundance upsection (so that the upper third to half of the unit has up to 50% gravelly bodies and the lower half to two-thirds has 10–20% gravelly bodies). Fine-grained sediment is light-reddish-brown to reddish-brown (5YR 4–6/3–4), light-brown to brown (7.5YR 4–6/3–4), or pinkish-gray (5–7.5YR 6–7/2); clay-rich and silty strata are commonly characterized by 5YR and 7.5YR hues, respectively. Fine-grained strata are in medium to thick (up to ≈2 m), tabular beds that are internally massive to vaguely horizontal-planar laminated and moderately sorted. Bedding contacts are planar and gradational (minor sharp) over 1–20 cm. Sand in the fine-grained interval is very fine- to fine-grained, with lesser medium-grained, and commonly contains trace to 10% (mostly 1–5%) grains of coarse and very coarse-grained sand that is scattered or in vague, laminated to very thin beds, along with trace to 5%, scattered very fine to medium pebbles. Commonly overprinted by weak pedogenesis characterized by 1–5 cm long, subangular to angular blocky (minor coarse to very coarse and prismatic), slightly hard to very hard ped development, and up to 10% root pores (<2 mm wide). In addition to ped development, paleosols may have illuviated clay and calcic horizons. In illuviated clay horizons, there are faint (locally distinct) clay films on ped faces or root pores; illuviated clay horizons are reddish-brown to yellowish-red (5YR 4/4–6) and 10–30 cm thick and commonly exhibit weak calcium carbonate accumulation (Btk horizons). Calcic horizons manifest weak (Stage I) calcium carbonate precipitation in 5–30 cm thick intervals; the carbonate is disseminated or precipitated as nodules (1–5% in area, mostly 0.5–1 cm wide but up to 4 cm wide). One to 10% of beds consist of 7.5YR 6/3 silt and very fine-grained sand that is well-sorted. There are sparse (≈1%) sand beds that are fine- to medium-grained and lack silt and clay. Gravelly strata, consisting of clast-supported sandy gravel and lesser gravelly sand, are commonly in tabular to broadly lenticular, one-story intervals 1–4 m thick (commonly 1–2 m thick) with relatively sharp to abrupt (i.e., gradation occurs over <3 cm), planar to slightly wavy tops and scoured bases. These gravelly bodies exhibit thin to thick (mostly medium), tabular to broadly lenticular beds (lesser lenticular); there is minor (<5%) cross-stratification characterized by planar foresets up to 1 m tall. Gravelly strata also occur as narrower, single-story, broadly U-shaped or wedge-shaped paleochannels 0.1–1.5 m thick; these are composed of thin- to medium-bedded sandy gravel, where sand is medium- to very coarse-grained. Gravel clasts are very fine to very coarse pebbles with <10% cobbles. Clasts are subrounded (minor rounded), poorly to moderately sorted, and composed predominantly of volcanic rocks. These volcanic rocks consist of intermediate compositions with 30–70% felsic volcanics. Intermediate volcanic rocks are mostly fine-grained and contain lesser (≈10–30% relative to total gravel) porphyritic types. Felsic volcanic clasts are also mostly fine-grained, but 5–20% (relative to total gravel) consists of porphyritic felsic clasts. Gravels also have trace to 0.5% reddish siltstone to very fine-grained sandstone clasts (eroded from Permian strata) and trace to 0.5% coarse-grained Kneeling Nun Tuff, along with ≈1% monzonite-diroite, phaneritic clasts. Gravel contains no to very sparse feldspar-porphyry derived from Alamosa Creek.. The gravel matrix is a brown (7.5YR 4–5/3–4) to reddish-brown (5YR 4–5/3–4) to light-reddish-brown (5YR 6/3) sand that is mainly medium- to very coarse-grained (minor fine-grained), subrounded (minor subangular, minor rounded), and poorly to moderately sorted. Coarse- to very coarse-grained sand is composed of volcanic lithics; medium-grained sand is composed of subordinate to subequal volcanic lithics, with the remainder being feldspar and quartz. Interstitial clay occurs in the coarse-grained bodies (estimated to be 1–5% locally up to 15% of volume), typically as films on clasts and grains. The deposit is well consolidated and weakly cemented by clay and variable, relatively weak accumulation of calcium carbonate (with weak to moderate HCl effervescence). The unit is ≈20 m thick.

Middle Palomas Formation

Qpt Upper transitional zone (early Pleistocene)—

Short—

Brownish (7.5YR) transition between **Qppw** and **QNpf**. Strata are mainly composed of very fine- to fine-grained sand, silt, and clay in medium to thick, tabular beds with 1–5% authigenic carbonates. Contains 10–35% gravelly bodies that are relatively tabular and mostly 0.5–2 m thick. Gravel is pebble-rich and volcanic; the matrix is a clay-free, fine- to very coarse-grained sand. Deposit is ≈3–10 m thick.

Long—

The unit represents a brownish (7.5YR) transitional zone between the upper Palomas Formation (**Qppw**) and the finer-grained, middle Palomas Formation (**QNpf**). The unit is relatively similar to the lower part of the upper unit, but is lighter in color (7.5YR hues), contains slightly more gravel bodies (10–35%) compared to the lower part of **Qppw**, and has local authigenic shallow-groundwater calcium carbonates. Strata are mainly fine-grained and composed of very fine- to fine-grained sand, silty fine-grained sand, silt, and clay exhibiting colors of brown to light brown (7.5YR 4/4 to 5–6/3–4) and pinkish gray (7.5YR 6/2); there is minor reddish-brown (5YR 4–5/3) colors seen mostly commonly in clayey strata. Fine-grained strata are in medium to thick, tabular beds. There are 0.5% strongly cemented beds of very fine- to fine-grained sandstone. Minor (3–10%), variably distributed, 3–30 cm thick intervals with abundant pebble-sized nodules of calcium carbonate (mostly 0.5–2 cm in diameter). Weak paleosols are present, characterized by medium to coarse, angular blocky peds and no to weak clay films. Authigenic carbonates (1–5%), associated with shallow groundwater, exhibit sharp basal and upper contacts. Local burrow forms are strongly cemented by calcium carbonate.

Gravel bodies are relatively tabular and 0.5–3 m thick (mostly 0.5–2 m thick); their lateral continuity results in concordant gravel-capped ridges extending several hundred meters. Also observed are U-shaped paleochannels <1 m deep. Within these gravelly bodies are beds that are 1–30 cm thick, tabular (minor cross-stratified), and composed of clast- to sand-supported gravel or volcanic-lithic arenite sand (horizontal-planar laminated to cross-laminated). Gravel consists of very fine to very coarse pebbles with 1–7% cobbles that are mainly clast-supported, subrounded (minor rounded), moderately sorted, and composed of very fine to very coarse pebbles with 1–5% fine cobbles. Gravels are composed of felsic and intermediate volcanic clasts (each ranging from 20–80%); felsic volcanics are mostly fine-grained with ≈15% porphyritic types; intermediate types are mostly fine-grained with 5–15% porphyritic varieties (percentage is relative to total gravel). The gravel also contains trace to 0.5% reddish siltstone and very fine-grained sandstones (eroded from Permian strata) and trace to 0.5% Kneeling Nun Tuff. The gravel matrix consists of clay-free sand that is gray (10YR 5/1) to brownish (10–7.5YR 5–6/2–3; minor 4/2), fine-to very coarse-grained, subrounded (minor rounded), moderately sorted, and a lithic arenite. Vertically or laterally adjacent to gravelly bodies are 1–2 m thick sand and silty-clayey, fine- to medium-grained sand intervals whose upper and lower contacts are planar and gradational to sharp. The deposit is moderately consolidated and non- to weakly cemented (outside of authigenic carbonate beds). The upper contact is placed at the topmost gravel of the gravel-rich zone, above which reddish-brown colors are common. The deposit is ≈3–10 m thick.

QNpf Fine-grained strata of middle Palomas Formation (early Pleistocene to late Pliocene)—
Short—
Fine-grained, light-brown (7.5YR), tabular-bedded strata with <5% gravelly bodies. Beds are medium to thick and internally massive. Sediment is silt, very fine- to fine-grained sand, silt-clay, and subordinate clay to clayey fine-grained sand. Paleosols (1–10%) exhibit Bt over Bk horizons. Local shallow-groundwater authigenic carbonates, including nodules and tabular bodies. The deposit is 10–90 m thick.
Long—
Fine-grained, tabular-bedded strata with <5% gravelly bodies. Fine sediment is light-brown to light-reddish-brown (7.5YR 6/3–4), brown (7.5YR 5/3–4), or pinkish-gray (5–7.5YR 6/2). Beds are medium to thick and internally massive. Sediment is silt, very fine- to fine-grained sand, silt-clay, and subordinate clay to clayey fine-grained sand; clayey strata tend to be light-reddish-brown to reddish-brown (5YR 5–6/3–4) and may have 1–3% scattered, medium to coarse sand grains and up to 1% scattered, very fine to coarse volcanic pebbles up to 2 cm long. The fine-grained strata have minor (1–3%), 10–30 cm thick intervals with abundant, 1–3 cm long, in-situ calcium carbonate nodules inferred to be related to shallow groundwater carbonate. Very fine- to fine-grained sandstone beds (0.5–5%) are strongly cemented by authigenic groundwater carbonates (Seager and Mack, 2003). Paleosols (1–10%) exhibit illuviated clay horizons overlying calcic horizons; ped development is moderate, coarse, and subangular blocky.

The sparse gravelly bodies are narrower than in overlying strata and up to 2 m thick, locally occupying U-shaped paleochannel fills. The sediment in these coarser bodies consists of pebbly sand and sand that is in thin to medium, tabular to broadly lenticular beds; the sand is pinkish-gray to light-brown (7.5YR 6/2–3) or grayish-brown to light-brownish-gray (10YR 5–6/2) or gray to light-gray (10YR 6–7/1), fine- to very coarse-grained (mostly medium-grained), subrounded (mostly) to subangular, and poorly to well-sorted. Medium- (upper) to very coarse- (upper) grained sand is composed of volcanic lithic grains; fine- to medium-grained sand is composed mostly of feldspar with minor dark lithic (volcanic) grains and 5–20% quartz. This sandy matrix lacks clay. Pebbles are commonly scattered in the sand (1–10%) or form clast-supported beds containing up to 5% fine to coarse cobbles; these gravel clasts are very fine to very coarse, subrounded, moderately sorted, and composed of felsic volcanic rocks (containing much Vicks Peak Tuff) with minor (10–20%) intermediate types, 1–2% Kneeling Nun Tuff, and 0–0.5% reddish siltstones and very fine-grained sandstones (eroded from Permian strata). These gravelly bodies are observed to interfinger laterally with bodies of interstratified coarser sediment (fine- to medium-grained sand) and finer sediment (silt to fine-grained sand) in 2–20 cm thick, tabular to lenticular beds. There are very sparse channel fills occupied by fine-grained, quartzo-feldspathic sandstone associated with the axial-fluvial system (indicating a back-filled floodplain channel). However, the majority of pebbly sandstones and sandstone channel-fills are associated with western sources (Black Range or Cuchillo Mountains). Moderate to strong HCl effervescence. The deposit is well consolidated and 10–90 m thick.

QNpa Sandy axial-fluvial deposits of middle Palomas Formation (early Pleistocene to early)—
Short—
Light-colored sand and 1–15% pebbly sand. Pebble composition is mostly felsic volcanic rocks and intra-formational clasts with 5–20% granite, 3–30% greenish sandstone, 1–5% chert, 1–2% reddish Permian

clasts, and 1–20% intermediate volcanic rocks; pebbles in uppermost strata have 15–20% chert and 1–5% quartzite. Sand is medium- to coarse-grained and quartzo-feldspathic. The deposit is ≈100 m thick.

Long—

Light-colored sand and minor (1–15%) pebbly sand in tabular to broadly lenticular, 0.5–3 m thick beds. Within these beds, sand is horizontally laminated with variable, but typically minor, cross-stratification <1 m thick; foresets consist of tangential laminae that commonly dip toward the south (ranging from southwest to southeast). U-shaped and narrow paleochannel forms are sparse and <1 m deep. Sand is white to light gray to pale brown (2.5Y 7–8/1–2, 10YR 6–7/2). Gravels are in very thin to medium, lenticular beds, rounded to subangular, and poorly to moderately sorted. Clasts mostly consist of very fine to medium pebbles, but include lesser coarse to very coarse pebbles and locally include 1–3% fine cobbles. Gravel composition is dominated by felsic volcanic rocks and intraformational clasts (mainly calcium carbonate nodules plus cemented sandstone and siltstone) and includes the following accessory lithologic types: 5–20% granite, 0–3% gneiss, 3–30% greenish sandstone resembling those in the Flying Eagle Canyon Formation (**Kfe**), trace to 5% limestone, 1–5% chert, 1–2% reddish Permian clasts, and 1–20% intermediate volcanic rocks. In the uppermost part of the unit, there are 15–20% brown and black cherts, trace petrified wood, and 1–5% quartzite. Sand is mostly medium- (lower) to coarse-grained (lower) but ranges from fine- to very coarse-grained, subrounded to subangular, and moderately to well-sorted and is composed of quartz with subordinate sanidine and plagioclase, 5–15% orangish grains (potassium feldspar, stained quartz, minor chert), ≈10–15% yellow-stained quartz, 7–20% dark lithic grains dominated by volcanic rocks (may include very minor dark chert), and 1–5% mafic grains. The unit is weakly to moderately consolidated; mostly non-cemented, with local strong cementation occurring in tabular to somewhat irregular horizontal bodies less than 1 m thick; these cement bodies typically develop in coarser, gravel-bearing strata and have sharp bases and tops. The top of the unit transitions into overlying the **Qpt** over 1–6 m stratigraphic distance, with interfingering and textural gradation involved in the transition. The deposit is ≈100 m thick.

Lower Palomas Formation

Nppwl **Western piedmont deposits, lower unit [cross section only] (early Pliocene)—**

*Short***—**

Sandy gravel interbedded with subequal(?) fine-grained sediment. Sandy gravel is in tabular to lenticular beds; <10% cross bedding. Fine-grained sediment is in medium to thick, tabular, massive beds; composed of light-brown to pink, silt to fine-grained sand with minor (trace to 25%) scattered medium to very coarse sand and trace-20% pebbles. 10-50% strongly cemented; sparse paleosols. Deposit is ≈40 m thick.

*Long***—**

Sandy gravel interbedded with subequal(?) fine-grained sediment. Sandy gravel is in very thin to medium, tabular to lenticular beds. There is <10% cross-stratification. Gravel are clast- to sand-supported and consist of pebbles with minor. Clasts are subrounded (mostly) to rounded, poorly sorted, and near Cuchillo Negro Creek is composed of ≈50% fine intermediate volcanics, 20-30% porphyritic intermediate volcanic rocks, 25-40% felsic volcanic rocks; <3% each of Paleozoic limestone and Kneeling Nun Tuff (visual estimation of clast%). Gravel matrix is a pinkish-gray to light-brown (7.5YR 6/2–3), fine- to very coarse-grained sand (mostly medium- to very coarse-grained) that is subrounded to subangular, poorly to moderately sorted, and composed predominately of volcanic lithic grains with subordinate feldspar and lesser quartz; matrix has 0-2% clay. Intervals with higher matrix clay (0.5-2%) are generally light reddish brown (5YR 6/4). Gravelly sediment is more cemented than the middle interval (10-50% strong cementation by calcium carbonate). Fine-grained sediment is in medium to thick, tabular, internally massive beds and composed of light-brown to brown to pink (7.5YR 6–7/3; 5/4) silt to fine-grained sand with minor (trace to 25%) scattered medium- to very coarse-grained sand and trace to 20% pebbles.

Moderately to well consolidated; sparse paleosols. Grades laterally eastward into unit **Npal1**. Deposit is ≈40 m thick.

Npplt Transition zone at base of western piedmont deposits [cross section only] (earliest Pliocene)— Light-reddish-brown (5YR 6/3–4) strata in medium to thick, tabular beds, and composed of: 1) siltstone and very fine- to fine-grained sandstone (about 50-70%); and 2) fine- to medium-grained sandstone (≈20%), and 3) coarse channel-fills (increasing up-section from 10 to 25%) composed of pebbly sand or sandy pebbles. Deposit is ≈30 m thick.

Npal1 Coarse axial-fuvial facies of the lower Palomas Formation, upper unit [cross section only] (earliest Pliocene)—

Short—

Whitish, coarse- to very coarse-grained sand with abundant conglomeratic tongues. Very coarse-grained sand and pebbles are subangular to subrounded and composed of felsic volcanic rocks, with sedimentary clasts increasing to the south. Coarse-grained sand is composed of quartz, 33–50% volcanic grains, 5–20% probable potassium feldspar, 1–5% granite, and 1% chert. Deposit is 45–50 m thick in the Getty West Elephant Butte No. 2.

Long—

The unit consist of slightly reddish-white (5–7.5YR 8/1) sand that is mainly coarse- (lower) to very coarse- (upper) grained, and has 15-50% conglomeratic tongues. Broken pebbles are up to 12 mm long and composed of felsic volcanic rocks, with sedimentary rocks becoming more abundant to the south. Pebble size and abundance increase down-section. Sand and pebbles are subangular to subrounded. The coarse sand is composed of quartz, 33–50% volcanic grains, up to 25% clear to greenish grains (likely Mesozoic sandstone), 5–20% orange-creamy feldspar (probably potassium feldspar), 1–5% granite, and 1% chert. Correlates to unit Tpal2 in Koning et al. (2018). 45–50 m thick in Getty West Elephant Butte No. 2.

Npal2 Coarse axial-fluvial facies of the lower Palomas Formation, lower unit (earliest Pliocene to latest Miocene)—Upward coarsening, slightly reddish white sand with pebbles. Sand is mostly coarse to very coarse and has 10–15% very fine to fine pebbles composed of felsic volcanic rocks, but sedimentary clasts become more common to the south. The sand is subrounded to subangular and composed of fine-grained felsic volcanics, 1–5% Mesozoic sandstone, and 1–3% quartz. The unit is 30 m thick in Getty West Elephant Butte No. 2.

Nppe Eastern piedmont deposits (latest Miocene to early Pliocene) —

Short—

Yellowish- to slightly greenish-brown, sandy conglomerate and conglomeratic sandstone. These strata are in very thin to medium-thick, tabular to lenticular beds, with ≈5–10% cross-stratification. Clasts are composed of 50% greenish sandstone, 10–45% light-gray limestone, and 1–5% reworked Permian strata. Minor pebbly, very fine- to fine-grained sand tongues. The deposit is up to 180 m thick.

Long—

Yellowish- to slightly greenish-brown, sandy conglomerate and conglomeratic sandstone and pebbly fine-grained sandstone. Conglomeratic strata are in very thin to medium-thick, tabular to lenticular beds, with ≈5–10% cross-stratification having very thin, typically planar or low-angle foresets. Gravel is sand- to clast-supported, subrounded to angular, and poorly to moderately sorted within a bed and consists of very fine to very coarse pebbles and ≈5–15% cobbles. Clasts are composed of 50% greenish sandstone (matching the Flying Eagle Canyon Formation and especially abundant in the finer pebble fraction), 10–45% light-gray limestone (upper Paleozoic source), 1–5% reddish very fine- to fine-grained sandstones and siltstones (inferred Permian strata source), and 0–1% granite. Gravel matrix consists of light-olive-brown to light-yellowish-brown (2.5Y 5-6/3 and 6/4) or yellowish-brown (10YR 5/4–6), fine- (lower) to very coarse- (upper) grained sand that is subrounded (minor subangular), poorly sorted, and a sediment-grain lithic arenite; medium sand is mostly quartz with minor clear feldspars; coarse to very coarse sand is composed of sedimentary lithics; 10–20% irregular to nodular (0.5–5 cm long) calcium carbonate cementation. Locally, beds are 1–3 m thick, matrix-supported, and internally massive (interpreted as debris flow deposits). Minor brown to light-brown (7.5YR 5–6/4), pebbly, very fine- to fine-grained sand with 10–25% scattered, medium to very coarse sand and an estimated 5% silt-clay; 10–50% calcium carbonate cementation in 0.5–5 cm wide nodules to irregular masses. This fine-grained sand is interbedded with minor, 20–25% sandy pebble beds (lenticular and up to 30 cm thick). Aside from the aforementioned nodules, strata are weakly to moderately cemented by calcium carbonate (weak to strong HCl effervescence). The deposit is well consolidated. The upper contact intertongues with axial-fluvial deposits (**QNpa**) over a few meters. The deposit is up to 180 m thick.

Nppes Southern fan deposits of the eastern piedmont (latest Miocene to early Pliocene)—

Short—

Sandy conglomerate and gravelly sandstone in thin to thick, relatively tabular beds that are internally massive. Gravel is mostly subangular, poorly sorted, and composed of reddish siltstone–very fine-grained sandstone (to north) and carbonate clasts (to south). Interfingers northward with **Nppe.** The sand is silty-clayey and very fine- to very coarse-grained. The deposit is well cemented and >45 m thick.

Long—

Sandy conglomerate to gravelly sandstone in thin to thick, tabular to broadly lenticular beds. Deposited in paleo-alluvial fans flanking the western Caballo Mountains and interfingers northward with unit **Nppe**. Beds are commonly massive and represent hyperconcentrated to debris flows. Gravel are sand- to clast-supported, angular to subangular (minor subrounded), very poorly to moderately sorted, and composed of reddish siltstone to very fine-grained sandstone (derived from Abo Formation and found to the north) and limestone and dolomite clasts (derived mainly from Pennsylvanian units and dominates near southern quadrangle border); to the south are 1–5% reddish, angular chert. The sand is silty-clayey and very fine- to very coarse-grained. The coarse and very coarse-grained sand contains high proportions of sedimentary lithic fragments and is poorly sorted and angular to subangular. The deposit is well cemented and at least 45 m thick.

Rincon Valley Formation

Nrpbf Distal piedmont and basin floor deposits [cross section only] (late Miocene)—

Short—

Clayey very fine- to fine-grained sand that likely becomes more conglomeratic to the west. In its basal portion, where penetrated by the Getty West Elephant Butte No. 2 well, the sand is mostly composed of rounded quartz grains and is subrounded to rounded and well sorted. The deposit is ≈107 m thick where penetrated by the well, but inferred to be ≈300 m to west.

Long—

Clayey very fine- to fine-grained sand that likely becomes more conglomeratic to the west. In its basal portion, where penetrated by the Getty West Elephant Butte No. 2 well, the sand is mostly composed of rounded quartz grains and is subrounded to rounded and well sorted. This quartz-rich, basal sand is inferred to reflect erosion of Yeso Group and Abo Formation rocks on the Mud Springs Mountains, the detritus of which was transported to the distal piedmont. Described using cuttings logs and down-hole geophysical logs from the Getty West Elephant Butte No. 2 well. The deposit has an apparent thickness of 107 m where penetrated by the well, but inferred to be ≈300 m thick west of the well.

Nrpd Playa-lacustrine and deltaic deposits (late Miocene)—

Short—
Interbedded clay, silt, and very fine- to fine-grained sand. Reddish-brown to brown clay and yellowish-brown silt are in very thin to medium, tabular beds and massive to horizontally laminated. Quartz-rich, light-colored sand tongues are very fine- to fine-grained and increase upsection, exhibiting intricate inter-stratification with clayey sand and silt micro-laminae. The deposit is >15 m thick.
Long—
Interbedded clay, silt, and very fine- to fine-grained sand. Clay and silt are in very thin to medium (minor thick), tabular beds. Clayey sediment is reddish-brown to brown (5–7.5YR 5/3–4, 4/4), minor yellowish-red (5YR 5/6), and massive to horizontal-planar laminated. Silt is light-yellowish-brown (2.5Y 6/3–4) to pale-brown (10YR 6/3) and locally indurated by calcium carbonate. Mixed silt-clay (mud) is reddish-brown to brown (5–7.5YR 5/4). Very sparse laterally extensive calcium carbonate marker beds inferred to represent lacustrine limestone. Sand tongues increase proportionally upsection and consist of very fine- (lower) to fine- (lower) grained sand that occurs in medium to thick beds that are well laminated (up to 5 mm thick and horizontal-planar, cross-stratified, wavy, or ripple-marked); clayey sand and silt micro-laminae are intricately interstratified with the sand laminae. Sand is pink to very-pale-brown (7.5–10YR 7/3) and dominated by quartz grains; fining-upward trends are commonly observed. No desiccation features are present. Contacts are generally sharp and planar. Basal sand contacts may be scoured. The unit is disconformably overlain by well-cemented **Nppe**, with a calcic paleosol immediately below the contact (pebble- to cobble-sized calcium carbonate nodules). The deposit is >15 m thick.

Nrp Playa-lacustrine deposits [cross section only] (late Miocene)—Reddish-brown to reddish clay in the Getty West Elephant Butte No. 2 well, where it has an apparent thickness of 217 m. Where exposed to near the Hot Springs fault, this clay occurs in a ≈7 m-thick tongue within eastern piedmont sediment and locally exhibits mm-scale, sand-filled fractures (desiccation cracks), slickenside faces and $CaCO_3$ nodules.

Nrpe Rincon Valley Formation, eastern piedmont deposits (late Miocene)—
Short—
Medium to thick, tabular to lenticular beds of sandstone and conglomeratic sandstone. Sandstone is fine- to medium-grained, with 15% coarse- to very coarse-grained sand composed of volcanic grains. Gravel is composed of plagioclase-phyric intermediate volcanic rock with 5% green siltstone to fine-grained sandstone. Gravel matrix is a light-yellowish-brown, muddy, very fine- to fine-grained sand. The unit is ≈350 m thick.
Long—
Medium to thick, tabular (mostly) to lenticular beds of well-cemented sandstone. Sand grains are fine (upper)- to medium- (upper) grained with 15% coarse- to very coarse-grained sand composed of volcanic grains. Overall, the sandstone is subrounded to subangular and low to moderately sorted. Sand is composed of quartz, subordinate feldspar, and 5–20% volcanic lithic grains. Locally, beds are matrix-supported and massive, with the gravel being angular to subangular and very fine to very coarse pebbles in size. The gravel clasts are composed of intermediate volcanic rock (plagioclase-phyric) with 5% green siltstone and very fine-grained sandstone. The gravel matrix is light-yellowish-brown (10YR 6.4), muddy very fine- (lower) to fine- (upper) grained sand that is massive and composed of quartz and feldspar with ≈15% mafic grains. ≈350 m thick.

INTRUSIVE IGNEOUS ROCKS PRE-DATING SANTA FE GROUP
NPEa Andesite Dikes (Miocene?)—
Gray, fine- to medium-grained, porphyritic andesite that weathers brown or dark-gray. Phenocrysts are mainly plagioclase. Dikes are up to 8 m thick and have steep dips.

PALEOGENE TO LATE CRETACEOUS STRATA

McRae Group

Note that we follow Lucas et al. (2019) in raising the McRae to Group status and within the McRae use the following as formation-rank terms: Double Canyon, Hall Lake, and José Creek.

Kmrd Double Canyon Formation (earliest Paleocene to latest Cretaceous)—

Short—

Light-colored succession of interbedded mudstone, siltstone, sandstone, and conglomerate. Fine-grained strata lack red colors and contain thin sandstone beds. Pebbly strata are commonly cross-stratified and clasts are composed of granitic and volcanic rocks, chert, and mudstone rip-ups. Sand is fine- to coarse-grained. Silicified logs and stumps are locally present. The deposit is >130 m thick.

Long—

Light-colored succession of interbedded mudstone, siltstone, sandstone, conglomerate, and minor bedded chert. We apply the name Double Canyon Formation to these strata that overlie the Hall Canyon Formation, following Lucas et al. (2019). Sandstone and pebbly sandstone are light-gray, light-brownish-gray, or greenish-gray; mudstone and siltstone are not reddish, as in the Hall Canyon Member, but typically olive colored to gray. Thin sandstone interbeds are common in the fine-grained strata. Amalgamated (multistory) channel-fill complexes are several meters thick and cross-bedded (commonly trough cross-stratified) or horizontal-planar laminated. Pebbly sandstone is generally in very thin to medium, tabular to lenticular beds that exhibit cross-stratification. Conglomerates are massive or trough cross-bedded. Pebbles are subangular to rounded. Clasts are composed of granitic rocks, volcanic rocks, chert of various colors, and mudstone rip-up clasts. Sand is fine- to coarse-grained, subangular to subrounded, moderately sorted, and composed of feldspar, quartz, and minor volcanic grains. The average composition of sandstone listed in Lucas et al. (2019) is $Q_{55}F_{19}L_{26}$. Lithic grains consist of volcanic rock fragments and volcanic chert grains, with less common granitic rock fragments. Large, silicified logs and stumps are locally present. A thickness of ≈130 m is preserved on this quadrangle, but thickness is greater to the north (Cikoski et al., 2017).

Kmrh Hall Lake Formation (Maastrichtian to late Campanian(?))—

Short—

Reddish-brown mudstones with subordinate, lenticular sandstone tongues and sparse conglomeratic beds. Mudstones exhibit blocky structure and contain calcic paleosols. Sandstones are massive, horizontally laminated, or cross-bedded. Sand is fine- to very coarse-grained. Volcanic gravel clasts dominate, but granite, chert, quartzite, and quartz increase upsection. The deposit is ≈700 m thick.

Long—

Reddish-brown mudstones interbedded with subordinate, lenticular sandstone tongues and sparse conglomeratic beds. We apply the term Hall Canyon Formation to these strata, which are overlain by the Double Canyon Formation and underlain by the José Creek Formation (*sensu* Lucas et al., 2019). Mudstones are mainly reddish-brown to maroon that erode to form low, hummocky landforms. These exhibit blocky structure and slickensides and contain calcisols and vertic calcisols (Buck and Mack, 1995). Sandstones are single- to multistory, up to 4–6 m thick, and extend laterally 20–150 m. These display various colors but are mostly reddish-gray to gray. Within the sandstone tongues are medium to thick, tabular to lenticular beds that are internally massive, horizontally laminated, or cross-bedded (tangential and lesser planar foresets). The sand is fine- to very coarse-grained, moderately to well-sorted, angular to subangular, and a lithic arenite to feldspathic litharenite. Hunter (1986) shows a sand composition of 43–66% lithic grains, 13–30% feldspar, and 15–27% quartz. Lucas et al. (2019) note that coarse-grained sandstones are dominated by quartz with lesser feldspars (plagioclase and potassium feldspars) and volcanic rock fragments, with the average composition being $Q_{45}F_{24}L_{31}$. Although lithic grains are mostly volcanic, metamorphic and plutonic rock fragments are more abundant relative to José Creek Member strata. Conglomeratic strata are up to ≈2 m thick and massive or trough cross-bedded. There is a basal conglomerate that contains cobbles as large as 30 cm, whose clast composition includes quartzite, rhyolite, granite, and intermediate volcanic rocks. In overlying strata, intermediate volcanic clasts dominate conglomerates, but red to pink granite, chert, quartzite, and quartz increase in proportion upsection (Lucas et al., 2019); intraformational conglomerates are also observed. Dinosaur fossils are most abundant in the lower part of the formation and include *Tyrannosaurus rex*, *Torosaurus* or *Triceratops*, ankylosaur, and *Alamosaurus* (Lucas et al., 2019; Lozinsky et al., 1984; Wolberg et al., 1986; Gillette et al., 1986). This unit has conformable upper and lower contacts and strata are ≈700 m thick.

Kmrj José Creek Formation (late Campanian)—

Short—

Grayish to brown sandstones with 35–50% olive to brownish-gray siltstones to mudstones; the latter contain interbeds of very fine- to fine-grained sandstone. Mudrocks are massive and have paleosols. Sandstones exhibit cross-bedding and horizontal laminations. Conglomeratic bodies increase and coarsen southwards and dominated by porphyritic andesite clasts. Contains petrified wood. The unit is 120–200 m thick.

Long—

Brown to greenish-gray to olive-gray sandstone, siltstones and mudstones, and intermediate-composition volcaniclastic conglomerates. Fine-grained strata are about subequal or up to two-thirds in proportion relative to sandstones and conglomeratic sandstones. We apply the term José Creek Formation to these strata, which are overlain by the Hall Canyon Formation and underlain by the Ash Canyon Formation (*sensu* Lucas et al., 2019). Mudstones and siltstones are mostly olive, dark-green, and brownish-gray. Mudstone and siltstone strata range from 1 to 15 m thick and commonly contain thin (<1 m thick) interbeds of very fine- to fine-grained sandstones that are massive (with variable root traces and burrows), horizontal-planar laminated, or ripple-marked. Mudrocks are massive and exhibit paleosols. Sandstones are grayish to brown and typically are in 2–9 m thick bodies that are laterally continuous over tens to hundreds of meters. Bedding within these bodies is lenticular to tabular and thin to thick. Cross-bedding, scour and fill features, horizontal-planar lamination, and lesser ripple marks are observed. Sand is mainly medium- to coarse-grained, subangular, moderately sorted, and composed of volcanic grains (55–80%) and plagioclase-dominated feldspar (20–40%) with 0–5% quartz (Hunter, 1986; Cikoski et al., 2017); however, near the base of the unit, the quartz content is higher (up to 80%), and there are many chert and potassium feldspar grains, reflecting erosion of the underlying Ash Canyon Formation or a conformable transition (Lucas et al., 2019). Conglomeratic sandstones are 1–10 m thick, extend laterally a few hundred meters to 1 km, and contain granules and pebbles composed mainly of intermediate rocks (i.e., porphyritic andesites) and intraformational siltstone, sandstones, and carbonate rocks. Less common clasts include mafic clasts and chert pebbles (the latter locally present near the base of the formation). Conglomerates are massive or trough cross-bedded. Conglomerates make up only 5% of the unit north of McRae Canyon, but the overall proportion and size of clasts in Jose Creek Formation conglomerates increase southward so that at the south end of Elephant Butte Lake, cobbles and boulders are abundant (Bushnell, 1953, 1955a, 1955b). Sparse, laterally continuous, thin (0.3–1 m thick) beds of siliceous tuffs are mainly observed in the upper half of the unit. Leaf fossils and petrified wood are observed throughout the José Creek Formation (Upchurch and Mack, 1998; Estrada-Ruiz et al., 2012a, 2012b, 2018). The unit is 120–200 m thick.

Terrestrial Strata Between McRae Group and Gallup Sandstone

Kac Ash Canyon Formation (Campanian)—

Short—
Ledge-forming, tan to brown, medium- to coarse-grained sandstone and pebbly conglomerate interbedded with subordinate olive-gray mudstone. Pebbles are subrounded and composed mainly of chert and quartz. Petrified wood is common. We follow Lucas et al. (2019) in elevating this unit to formation-rank status. The deposit is ≈360 m thick.
Long—
The Ash Canyon Formation (sensu Lucas et al., 2019) differs from the Flying Eagle Canyon Formation by having abundant resistant and ledge-forming, tan, medium-grained, quartzose sandstones that form multistory sheets. Sandstone intervals are typically several meters (up to 15 m) thick and laterally continuous over 100–800 m. Mudstone and siltstone intervals, similar to those described for the Flying Eagle Canyon Formation, are subordinate to these sandstones. Sandstones are light-gray to pale-yellow on fresh surfaces, weathering to light-brownish, yellowish, and pinkish-gray. There is extensive cross-stratification (with common trough forms and tangential foresets), but horizontal-planar laminations and massive beds are locally present. Grain size ranges from very fine- to very coarse-grained but is mostly medium-grained. Sand is mainly subrounded, moderately to well-sorted, and composed of quartz, <10% feldspar, and ≈5% lithic grains dominated by chert. Pebbly sandstone and pebble conglomerate are composed of rounded clasts of chert, quartz, quartzite, siltstone rip-ups, and 1–5% siliceous volcanic rocks (aphanitic and gray). Conglomerate is trough cross-bedded or rarely massive. These strata represent fluvial deposition by sand-dominated fluvial systems and are ≈360 m thick.

Kfe Flying Eagle Canyon Formation (Campanian to Coniacian)—
Short—
Ledge-forming, fine- to medium-grained, gray to brown sandstones interbedded with siltstones and mudstones, sensu Lucas et al. (2019). The sandstones are sheetlike, lenticular or ribbonlike and 2–8 m thick. The mudstones are gray to olive gray and interbedded with thin, very fine- to fine-grained sandstones that exhibit horizontal laminations, ripple marks, or are massive. Strata are 300–340 m thick.
Long—
The 300- to 340-m-thick Flying Eagle Canyon Formation (sensu Lucas et al., 2019) has a notably olive to brown color and consists of ledge-forming sandstones interbedded with slope-forming intervals of mudstone and thin sandstones. The ledge-forming sandstones are sheetlike to lenticular or ribbonlike and range from 2–8 m thick. These sandstones are fine- to medium-grained, typically single story, and gray, tan, or greenish-brown. Sand is subangular to subrounded, relatively well-sorted, and composed of quartz, a few percent lithic fragments, and 6% feldspars (Lucas et al., 2019). Their bases are sharp and erosional but exhibit gradational upper contacts. Within the sand bodies are trough cross-bedding and horizontal-planar lamination in addition to asymmetrical ripple cross-laminae and intraformational conglomerates (with mudstone rip-ups). The slope-forming mudstones are interbedded with thin (<1 m thick) sandstones that are very fine- to fine-grained and may exhibit horizontal laminations and ripple marks; these sandstones may also be massive with root traces. The mudstones are gray to olive-gray and weather into blocky fragments. The top contact is placed at the base of a laterally extensive, thick (>few meters), quartz-rich, resistant sandstone at the base of the sandstone-rich Ash Canyon Formation.

Marine, Nearshore, and Coastal-Margin Strata

Kgm Undivided Gallup Sandstone and D-Cross Tongue of the Mancos Shale [cross section only] (late Turonian)—Sandstone and shale lying above the Tres Hermanos Formation, as interpreted in the Getty West Elephant Butte No. 2 well. These strata correlate to the D-Cross Tongue of the Mancos Shale and the overlying Gallup Sandstone. The map unit may include lowest strata of Flying Eagle Canyon Formation (**Kfe**). Strata are 90–100 m thick.

Kg Gallup Sandstone (late Turonian)—

Short—

Light-colored, tabular-bedded sandstones that are mainly very fine- to fine-grained (minor fine- to medium-grained beds). In the lower part of the unit, fine-grained sandstones are interbedded with gray, silty shales. Sandstones are horizontally laminated, trough cross-bedded, ripple-laminated, bioturbated, or massive. Sparse bivalves, plant debris, and shark teeth are present. The unit is 40 m thick.

Long—

Three subunits are recognized by Seager and Mack (2003). The lower subunit (≈10 m thick) is characterized by two parasequences exhibiting interbedded very fine- to fine-grained sandstone and gray, silty shales, but there is a systematic up-section increase in the number and thickness of sandstone beds. Shale is absent in the upper part of the lower subunit, and there the sandstone is tan to light-brown and thin- to medium-bedded. These beds exhibit horizontal-planar lamination, hummocky cross-stratification, ripple marks, and numerous burrows (mostly horizontal). The middle subunit of the Gallup Sandstone is a 10 m thick, ledge-forming sandstone that is fine- to medium-grained, contains plant debris, and is thick-bedded to massive; this sandstone has sparse cross-bedding, horizontal-planar lamination, and ripple marks; locally dense *Ophiomorpha* burrows are present at the top of this sandstone. The upper subunit (≈20 m thick) has dark-gray, argillaceous sandstone at its base (with numerous burrows and oyster shells) capped by a sandstone channel fill that is trough cross-bedded and oyster-bearing. The upper part of the upper subunit consists of gray, thin-bedded, heavily bioturbated, very fine- to fine-grained sandstone capped by a sandstone that exhibits channel morphology and is cross-bedded. This capping sandstone is overlain by thin coal that marks the base of the Flying Eagle Canyon Formation. The lower and middle parts of the Gallup Sandstone are interpreted to represent delta front and distributary mouth bar environments, respectively. The dark, argillaceous sandstone is interpreted as a brackish bay on the delta, overlain by delta front sandstones; the two trough cross-stratified sandstones in the upper subunit may represent distributary channels or tidal channels. The entire unit is 40 m thick.

Kmd D-Cross Tongue of Mancos Shale (late Turonian)—

Short—

Shale in the lower 30 m transitioning upward to interbedded silty shale, siltstone, and sandstone. Shale is mostly grayish and, in its lower part, calcareous. Sandstone intervals are up to 8 m thick and trough cross-bedded (most common), horizontally laminated, planar cross-bedded, or massive. There are distinct limestone concretions. The unit is 50 m thick and its top contact is gradational.

Long—

Shale in the lower 30 m that transitions upward to interbedded shale, siltstone, and sandstone. Shale is dark-gray weathering to olive-gray; shale is calcareous in the lower part and becomes silty in the upper 60 m. Sandstone intervals are up to 8 m thick and trough cross-bedded (most common), horizontally laminated, planar cross-bedded, or massive. Distinct septarian concretions are composed of dark-gray, dolomitic and micritic limestone concretions that weather to rusty orange (0.2–1.2 m diameter). Ammonites and other marine fossils are present. The upper contact is gradational. The unit is 50 m thick.

Kth Tres Hermanos Formation (middle Turonian)—

Short—

A ≈75 m thick succession divided into a basal sandstone (Atarque Member), a medial carbonaceous mudstone-dominated interval (Carthage Member), and an upper sandstone (Fite Ranch Member). The Atarque Member is 13–14 m of sandstone and minor shale; sandstone is trough cross-bedded, horizontally laminated, or massive. The Carthage Member is composed of non-fissile mudstone and siltstone and is 50 m thick.

Long—

Relatively resistant, 75 m thick succession that can be subdivided into a basal sandstone (Atarque Member), a medial carbonaceous mudstone-dominated interval (Carthage Member), and an upper sandstone (Fite Ranch Member). The Atarque Member is 13–14 m of sandstone and minor shale. The sandstone is trough cross-bedded, horizontally laminated, or massive; it is very calcareous and weathers to large, rounded, concretionary forms. The sandstone is commonly fine- to medium-grained, subangular to subrounded, well-sorted, and composed of quartz and minor potassium feldspar, plagioclase, and chert; there are rare lithic grains composed of fine-grained volcanic and metamorphic fragments and opaque grains. The Carthage Member is 50 m thick and composed of non-fissile mudstone and siltstone; some mudstone layers are carbonaceous. The lower half contains minor, thin (<0.2 m thick) limestone beds. In the upper half, the mudstone is interbedded with sandstone intervals (up to 3 m thick) that are trough cross-bedded, planar cross-bedded, ripple-laminated, or massive to bioturbated; there are minor limestone concretions. The Fite Ranch Member consists of a few meters of bedded sandstone that is dominantly trough cross-bedded and subordinately massive, with an intervening thin mudstone bed.

Kmt Tokay Tongue of Mancos Shale (early Turonian to late Cenomanian)—

Short—

Dark-gray, calcareous shale and siltstone with some sandstone. Intercalated limestone is common ≈60 m above the base of the unit and assigned to the Bridge Creek Limestone. Silty shale and siltstone increase upsection above this stratum. Sandstones in the upper part are commonly hummocky cross-stratified or horizontally laminated. Contains numerous bentonite beds. Strata are ≈150–160 m thick.

Long—

Dark-gray, calcareous shale and siltstone with some sandstone and thin, intercalated limestone in 3- to 30-cm-thick beds; limestone is most common ≈60 m above the base of the unit and assigned to the Bridge Creek Limestone by Hook et al. (2012) and Mack et al. (2015). Lucas et al. (2019) designate a limestone-bearing unit at 12–25 m height as the Greenhorn Member of the Mancos Shale. Shale weathers greenish-gray or olive-gray and is silt-free to slightly silty in the lower and medial part. Silty shale and siltstone increase upsection above the medial limestone interval. The sandstones in the upper part are commonly hummocky cross-stratified or horizontally laminated; sandstone occurs mainly as thin beds (<0.2 m thick) and less commonly as 0.5–3 m thick beds. Sixty-four bentonite beds have been observed in the lower 60 m of the unit (Hook et al., 2012). Assignment of Tokay Tongue follows Hook and Cobban (2015). The upper contact is gradational. Strata are ≈150–160 m thick.

Kd Dakota Sandstone (middle Cenomanian)—

Short—

Medium-bedded, white to buff, medium- to coarse-grained sandstone with a 15–20 m thick medial, grayish, sandy shale. Sandstone is mostly medium-grained, subrounded, and a quartz arenite with minor chert grains; variably pebbly and cross-stratified to horizontal laminated. The upper sandstone unit is ≈5 m thick and contains burrows of *Ophiomorpha* and *Thalassinoides*. The unit is 30–40 m thick.

Long—

Medium-bedded, white to buff, medium- to coarse-grained sandstone at the top and bottom with a medial sandy shale. Sandstone is mostly medium-grained, subrounded (minor rounded), well-sorted, and a quartz arenite with minor chert grains. Locally, the sandstone is poorly to moderately sorted and contains clasts up to 5 mm. The lower sandstone is 5–7 m thick and trough cross-bedded to horizontally laminated; there is much fossil plant detritus and some pebbly conglomerate lenses. The medial unit is 15–20 m thick and dominated by sandy shale and gray mudstone, relatively thin sandstone beds, or lenses that exhibit cross-bedding (including ripple marks) or are bioturbated. The upper sandstone unit is ≈5 m thick and trough cross-bedded or horizontally laminated; it is extensively bioturbated and contains burrows of *Ophiomorpha* and *Thalassinoides.* The unit is 30–40 m thick.

PALEOZOIC STRATA

Permian Strata

Ps San Andres Formation (Permian; early Guadalupian to late Leonardian)—

Short—

About 30 m of thin- to medium-bedded limestone forming a hogback. This is overlain by ≈200 m of thin- to medium-bedded, fossiliferous, chert-poor limestone and dolomite interbedded with yellow to red, very fine- to medium-grained sandstone, along with local beds of gypsum. The upper contact is an unconformity. Correlates to the upper Yeso Formation of Seager (2015). Strata are ≈230 m thick.

Long—

30 m thick limestone conformably overlain by ≈200 m of limestone and dolomite interbedded with sandstone. The lower limestone consists of medium-bedded, fossiliferous, dark-gray to black, packstone limestone with a few dark-gray chert nodules, along with minor thin-bedded, dark-gray shale and lenticular sandstone. The limestone forms a prominent, almost continuous hogback. Overlying strata are composed of medium-bedded, fossiliferous, chert-poor limestone and dolomite (includes packstones, wackestones, and oolitic and fossiliferous grainstones) and yellow to red, very fine- to medium-grained sandstone; there are local beds of gypsum in this upper unit. The upper contact is a regional unconformity. Correlates to the upper Yeso Formation of Seager (2015). The unit is ≈230 m thick.

Py Yeso Group (Permian; Leonardian)—

Short—

The Yeso Group includes the Arroyo de Alamillo and Los Vallos Formations (sensu Lucas and Krainer, 2012). The Arroyo de Alamillo consists mainly of orange (minor white to light-green), very fine- to fine-grained, well-sorted sandstone with local ripple marks, salt casts, and burrows. The Los Vallos Formation contains interbedded dolomite, limestone, siltstone to very fine-grained sandstone, and gypsum. The unit is 180–210 m thick.

Long—

The Yeso Group consists of Arroyo de Alamillo Formation overlain by the Los Vallos Formation (sensu Lucas and Krainer, 2012). The Arroyo Alamillo Formation primarily consists of orange, very fine- to fine-grained, well-sorted sandstone. There are subordinate beds of medium-grained sandstone and siltstone. Orange sandstone exhibits millimeter- to centimeter-scale horizontal or low-angle lamination. Alteration of these beds with softer, bioturbated sandstones forms a steplike outcrop appearance. Shale and mudstone are sparse and restricted to the top of the Arroyo de Alamillo Formation. In the Arroyo de Alamillo Formation, there are several distinct beds of white to light-green, fine-grained sandstone with symmetrical ripple marks, salt casts, and burrows. The Los Vallos Formation consists of dolomite, limestone, siltstone to very fine-grained sandstone, and gypsum. There are three ledge-forming limestone/dolomite units, each ≈10–15 m thick within a sequence of interbedded, massive or thinly bedded gypsum, thin-bedded limestone, and red to yellow sandstone and siltstone (the latter similar to that seen in the Arroyo de Alamillo Member). Thinning and thickening of the unit and contortion of bedding are due to gypsum flowage. The upper contact is mapped at the base of a cliff-forming, dark-gray, lower limestone of the San Andres Formation. The unit is 180–210 m thick.

Pa Abo Formation (Permian; middle to late Wolfcampian)—

Short—

The unit consists of brick-red, reddish-brown, or purplish mudstone (blocky-textured), shale, siltstone, and fine-grained sandstone. Siltstones and very fine-grained sandstones are commonly in thin (<1 m) beds with ripple marks or horizontal laminae. Very fine- to fine-grained sandstones occupy paleochannels or form sheetlike bodies. Sparse limestones and thin (<0.5 m) beds of intraformational conglomerate. The unit is ≈150 m thick.

Long—

The unit consists of brick-red and reddish-brown mudstone, shale, siltstone, and fine-grained sandstone. Sparse limestone interbeds. Mudstone has a blocky texture and commonly displays slickensides; calcic nodules are locally present in some beds. Siltstones and very fine-grained sandstones are commonly in thin (<1 m) beds and exhibit ripple cross laminae or horizontal-planar laminae; upper parts of beds may have desiccation cracks or bioturbation features. Very fine- to fine-grained sandstones occupy paleochannels or are in sheet forms locally exhibiting small-scale trough cross-beds. In the lower part of the unit are sparse, thin (<0.5 m) beds of intraformational conglomerate that fill broad, shallow paleochannels relatively devoid of sedimentary structures or may exhibit small-scale trough cross-beds; clasts consist of shale, siltstone, and carbonate. The upper contact is conformable and placed at the change from brick-red mudstones to orangish and greenish siltstones and sandstones of the overlying Yeso Group. The unit is ≈150 m thick.

Pennsylvanian Strata

IPbb Bar B Formation (Pennsylvanian; late Virgilian to late Desmoinesian)—

Short—

The unit consists of interbedded limestone, dolomite, shale, and (in upper 50 m) conglomerate. Shale is more abundant than in the Gray Mesa Formation, is gray to purplish-gray, and forms slopes. Limestone is gray, tan, and orange and forms ledges 1–5 m thick; some beds locally have abundant marine fossils, burrow traces, and chert. The upper contact is at the top of the highest limestone bed. The unit is 119 m thick.

Long—

Interbedded limestone, dolomite, shale, and conglomerate. Shale is proportionally more abundant than in the Gray Mesa Formation, is gray to purplish-gray, and underlies slopes. Limestone is gray, tan, and orange, forms ledges 1–5 m thick, and is micritic. The tops of dolomitic beds may be brecciated, with red shale or siltstone between the clasts. Some beds locally contain abundant marine fossils, burrow traces, and chert. The upper 50 m consists of interbedded purplish and red siltstone, shale, limestone, and limestone-pebble conglomerate. The upper contact is placed at the top of the highest limestone bed in the Bar B Formation. The unit is 120 m thick.

IPgm Gray Mesa Formation (Pennsylvanian; Desmoinesian)—

Short—

Usage of Gray Mesa follows Lucas et al. (2012a). It consists of ledge-forming limestone (1–15 m thick beds) separated by thinner covered slopes. Limestones are commonly gray, bioturbated, fossiliferous packstones. Dark-gray or black chert is very common. Grainstones are less common. Covered intervals correspond to thin-bedded limestones and reddish, green, or gray shale. The unit is ≈190 m thick.

Long—

Usage of Gray Mesa follows Lucas et al. (2012a). It consists of ledge-forming, relatively thick-bedded limestone (1–15 m thick) separated by thinner covered slopes. Limestones are commonly gray (weathering gray to tan), bioturbated, fossiliferous packstones. Dark-gray or black chert is very common. Gray grainstones are less common and composed of intraclasts, bioclasts, or ooids. Covered intervals correspond to thin-bedded limestones and reddish, green, or gray shale. The unit is 190 m thick.

Ordovician Strata

Om Montoya Formation—Dark-brown, medium- to coarse-grained, basal sandstone overlain by thinly bedded to massive, gray dolomite with scattered brown chert nodules and lenses. The unit is 110 m thick.

Appendix 2. Paleoflow data

All paleoflow data were measured using a brunton compass and imbricated gravel clasts at a location corresponding to the FieldID field within the Station point feature class and the StationsID field in the Orienation feature class. Simple statistics calculated for data at each site (average, median, number, standard deviation) are given below the compiled measurements in this apppendix. On the map, the average bearing is plotted for each station in the OrientationPoints feature class.

In each data table below, direciton-corrected bearings is an intermediary value that allows calculations of averages that are approximately northwards. For example, 350° is -10° and 340° is -20°.

EB-50				
Bearing(°)	# of clasts	Bearing per clast(°)	Direction-corrected bearing per clast(°)	Notes
155	2	155		
		155		
137	2	137		
		137		
130	1	130		
122	1	122		
127	1	127		
131	1	131		
186	2	186		
		186		
210	2	210		
		210		
291	3	291		
		291		
		291		
138	1	138		
147	2	147		
		147		
192	1	192		
123	1	123		Values below are from an overlying
148	2	148		lenticular bed.
		148		
146	2	146		
		146		
315	1	315		
154	1	154		
128	1	128		
144	1	144		
117	2	117	128	
		117		
166	1	166	144	
127	1	127	117	
275	2	275	117	
		275	166	
141	2	141	127	
		141		
266	2	266	275	
		266		
260	2	260		

		260			
165	1	165			
167	2	167			
		167			
138	2	138			
		138			
150	2	150			
		150			
193	2	193			
		193			
263	2	263			
		263			
207	2	207			
		207			
158	2	158			
		158			
159	2	159			
		159			
146	1	146			
281	2	281			
		281			
121	3	121			
		121			
		121			
144	1	144			

Average(°)	**180**
Median(°)	**155**
Count	**64**
StDev(°)	**57**

EB-52				
Bearing(°)	# of clasts	Bearing per clast(°)	Direction-corrected bearing per clast(°)	Notes
49	1	49	49	Outcrop face trends 100 degrees.
46	1	46	46	
46	1	46	46	
3	1	3	3	
52	1	52	52	
94	1	94	94	
110	1	110	110	
98	1	98	98	
62	1	62	62	
59	2	59	59	
		59	59	
67	1	67	67	
60	2	60	60	
		60	60	
39	2	39	39	
		39	39	
60	1	60	60	
48	1	48	48	
55	1	55	55	
30	1	30	30	
20	1	20	20	
70	1	70	70	
62	1	62	62	
50	1	50	50	
359	2	359	-1	
		359	-1	
40	1	40	40	
58	2	58	58	
		58	58	
12	1	12	12	
172	1	172	172	
345	1	345	-15	
300	1	300	-60	
327	1	327	-33	
278	1	278	-82	
297	2	297	-63	
		297	-63	
277	1	277	-83	
267	1	267	-93	
18	1	18	18	
2	1	2	2	

347	1	347	-13	
52	1	52	52	
23	1	23	23	
54	1	54	54	
75	1	75	75	
127	1	127	127	
27	1	27	27	
48	1	48	48	
312	1	312	-48	
66	1	66	66	
22	2	22	22	
		22	22	
30	2	30	30	
		30	30	
58	1	58	58	
15	1	15	15	
43	1	43	43	
45	2	45	45	
		45	45	
332	2	332	-28	
		332	-28	
11	1	11	11	
16	2	16	16	
		16	16	
338	2	338	-22	
		338	-22	
1	1	1	1	
27	1	27	27	
30	1	30	30	
28	2	28	28	
		28	28	
31	1	31	31	
79	1	79	79	
310	1	310	-50	
343	2	343	-17	
		343	-17	
25	1	25	25	
20	2	20	20	
		20	20	
19	1	19	19	
8	1	8	8	
18	1	18	18	
36	1	36	36	
317	2	317	-43	
		317	-43	
30	1	30	30	
358	1	358	-2	

49	3	49	49	
		49	49	
		49	49	
		Average(°)	**25**	
		Median(°)	**30**	
		Count	**91**	
		StDev(°)	**45**	

EB-56B				
Bearing(°)	# of clasts	Bearing per clast(°)	Direction-corrected bearing per clast(°)	Notes
				Lower 2 ft of bed.
240	1	240		Outcrop face trends 230 to 240 degrees.
197	1	197		
258	1	258		
230	1	230		
207	1	207		
223	1	223		
256	1	256		
200	1	200		
221	1	221		
196	1	196		
243	2	243		
		243		
244	1	244		
213	3	213		
		213		
		213		
210	2	210		
		210		
220	2	220		
		220		
228	2	228		
		228		
238	1	238		
239	1	239		
235	1	235		
226	2	226		
		226		
206	1	206		
225	1	225		
249	1	249		
249	1	249		
100	2	100		
		100		
215	1	215		
300	1	300		
177	1	177		
148	1	148		
246	1	246		
230	2	230		
		230		

239	1	239		
225	1	225		
45	1	45		
39	3	39		
		39		
		39		
143	1	143		
253	1	253		
61	2	61		
		61		
10	1	10		
35	2	35		
		35		
239	1	239		
227	1	227		
227	1	227		
	Average(°)	**191**		
	Median(°)	**222**		
	Count	**56**		
	StDev(°)	**74**		

EB-56A

Bearing(°)	# of clasts	Bearing per clast(°)	Direction-corrected bearing per clast(°)	Notes
				Lower 4 ft of bed, where imbrication
184	1	184		is more obvious
173	1	173		
172	1	172		
201	1	201		
171	1	171		
182	1	182		
30	3	30		
		30		
		30		
172	1	172		
183	1	183		
196	2	196		
		196		
216	1	216		
165	1	165		
141	1	141		
141	1	141		
110	1	110		
201	1	201		
230	1	230		
227	1	227		
214	1	214		
216	1	216		
167	1	167		
156	1	156		
179	2	179		
		179		
200	1	200		
175	2	175		
		175		
183	2	183		
		183		
197	3	197		
		197		
		197		
166	1	166		
119	1	119		
203	1	203		
181	2	181		

		181		
95	1	95		
86	1	86		
203	1	203		
257	1	257		
237	1	237		
234	1	234		
159	1	159		
162	1	162		
215	1	215		
268	2	268		
		268		
318	3	318		
	3	318		
	3	318		

	Average(°)	**184**
	Median(°)	**183**
	Count	**54**
	StDev(°)	**60**

EB-60			
Bearing(°)	# of clasts	Bearing per clast(°)	Notes
141	1	141	Face trends 120 degrees. Good 3D exposure of clasts.
109	1	109	No clay films or clay in matrix, just gravel.
152	1	152	
137	1	137	
119	1	119	
102	1	102	
104	1	104	
103	1	103	
135	1	135	
145	1	145	
148	1	148	
118	2	118	
		118	
98	1	98	
120	1	120	
126	1	126	
105	1	105	
107	2	107	
		107	
139	2	139	
		139	
125	1	125	
165	1	165	
149	1	149	
117	1	117	
128	1	128	
149	1	149	
256	1	256	
271	2	271	
		271	
161	1	161	
137	1	137	
146	1	146	
118	1	118	
134	1	134	
148	1	148	
119	1	119	
129	1	129	
137	1	137	
	Average(°)	**139**	
	Median(°)	**134**	
	Count	**39**	

StDev(°)	**40**

EB-65				
Bearing(°)	# of clasts	Bearing per clast(°)	Bearing per clast(°)	Notes
154	2	154		Outcrop face trends about 120 degrees.
		154		
154	1	154		
149	2	149		
		149		
120	1	120		
205	2	205		
		205		
117	1	117		
162	1	162		
128	1	128		
109	1	109		
144	1	144		
118	1	118		
218	1	218		
294	1	294		
300	1	300		
275	1	275		
197	2	197		
		197		
258	1		258	New bed, about 2/3 way up exposure
258	1		258	
205	1		205	
206	2		206	
			206	
148	1		148	
229	1		229	
190	1		190	
226	1		226	
192	1		192	
219	1		219	
253	1		253	
258	1		258	
208	1		208	
136	1		136	
194	1		194	
168	1		168	
151	1		151	
	Average(°)	177	206	
	Median(°)	154	206	
	Count	20	18	
	StDev(°)	57	37	

EB-68A

Bearing(°)	# of clasts	Bearing per clast(°)	Notes
			Very consistent imbrication in the lower 2 ft of gravel.
200	5	200	Arroyo wall trends about 195 to 200 degrees.
		200	
		200	
		200	
		200	
192	2	192	
		192	
207	1	207	
220	3	220	
		220	
		220	
223	1	223	
212	1	212	
228	1	228	
198	2	198	
		198	
223	1	223	
184	2	184	
		184	
206	3	206	
		206	
		206	
215	1	215	
209	1	209	
198	2	198	
		198	
219	1	219	
224	2	242	
		242	
229	1	229	
223	1	223	
206	2	206	
		206	
220	2	220	
		220	
214	2	214	
		214	
200	2	200	
		200	

Average(°)	**210**
Median(°)	**206**
Count	**39**
StDev(°)	**14**

EB-68B

Bearing(°)	# of clasts	Bearing per clast(°)	Bearing per clast(°)	Notes
Base of Qppw				Good 3D exposure; outcrop face trends 310 degre
263	2	263		"+/-" 10 degrees in the measurements
		263		
241	2	241		
		241		
240	2	240		
		240		
240	1	240		
243	1	243		
179	1	179		
229	2	229		
		229		
234	1	234		
207	1	207		
241	2	241		
		241		
87	1	87		
200	2	200		
		200		
201	1	201		
264	2	264		
		264		
265	1	265		
249	1	249		
203	1	203		
193	1	193		
238	2	238		
		238		
201	1	201		
177	3	177		
		177		
		177		
310	1	310		
210	2	210		
		210		
250	1	250		
				Top of the bed, upper foot measurement
190	3		190	
			190	
			190	
184	1		184	
198	1		198	

216	1		216	
185	1		185	
195	1		195	
198	1		198	
181	1		181	
212	1		212	
217	1		217	
220	3		220	
			220	
			220	
262	1		262	
186	1		186	
194	1		194	
182	1		182	
193	1		193	
	Average(°)	**224**	**202**	
	Median(°)	**238**	**195**	
	Count	**35**	**20**	
	StDev(°)	**38**	**19**	

EB-72

Bearing(°)	# of clasts	Bearing per clast(°)	Notes
			Base of thick gravel section (Qppuc), good exposure, consistent
263	1	263	Outcrop face trends 230 degrees.
243	1	243	Good 3D exposure.
215	1	215	
202	1	202	
197	1	197	
107	2	107	
		107	
241	1	241	
190	1	190	
145	2	145	
		145	
120	4	120	
		120	
		120	
		120	
135	3	135	
		135	
		135	
145	2	145	
		145	
119	2	119	
		119	
233	2	233	
		233	
166	2	166	
		166	
161	1	161	
208	1	208	
156	1	156	
190	2	190	
		190	
148	3	148	
		148	
		148	
	Average(°)	**165**	
	Median(°)	**148**	
	Count	**34**	
	StDev(°)	**43**	

EB-84

Bearing(°)	# of clasts	Bearing per clast(°)	Direction-corrected bearing per clast(°)	Notes
				In Qpt.
195	2	195		Imbrication is consistent and obvious.
		195		
269	1	269		
250	2	250		
		250		
269	2	269		
		269		
244	2	244		
		244		
225	2	225		
		225		
149	1	149		
191	2	191		
		191		
208	2	208		
		208		
237	2	237		
		237		
240	2	240		
		240		
248	2	248		
		248		
249	2	249		
		249		
266	2	266		
		266		
238	2	238		
		238		
259	2	259		
		259		
266	2	266		
		266		
263	2	263		
		263		
258	2	258		
		258		
246	3	246		
		246		
		246		

230	2	230		
		230		
228	2	238		
		238		
275	2	275		
		275		
250	1	250		
244	2	244		
		244		
273	1	273		
269	1	269		
270	2	270		
		270		
218	1	218		
210	3	210		
		210		
		210		
238	2	238		
		238		
211	2	211		
		211		
	Average(°)	**240**		
	Median(°)	**244**		
	Count	**60**		
	StDev(°)	**26**		

EB-87

Bearing(°)	# of clasts	Bearing per clast(°)	Direction-corrected bearing per clast(°)	Notes
				Good exposure
87	1	87		"+/-" 15 degree measurement error.
78	1	78		50 ft thick gravel; measured 2/3 up Qppw.
44	1	44		Measuring over 4 m vertical distance
21	1	21		wihtin a 5 m horizontal distance.
132	1	132		Outcrop face trends about 190 degrees.
50	2	50		Most measurements are from clast imbri-
		50		cation paleoflows which are
54	2	54		perpendicular to the outcrop face.
		54		
112	1	112		
77	1	77		
74	1	74		
151	3	151		
		151		
		151		
151	2	151		
		151		
164	1	164		
122	2	122		
		122		
131	1	131		
98	1	98		
185	2	185		
		185		
170	1	170		
138	2	138		
		138		
140	1	140		
111	2	111		
		111		
125	2	125		
		125		
73	1	73		
85	2	85		
		85		
79	2	79		
		79		
85	1	85		
92	1	92		

128	1	128		
68	1	68		
129	1	129		
110	1	110		
183	1	183		
105	1	105		
101	1	101		
97	1	97		
81	3	81		
		81		
		81		
75	1	75		
150	2	150		
		150		
83	1	83		
83	1	83		
135	1	135		
163	1	163		
152	1	152		
128	1	128		
123	2	123		
		123		
186	1	186		
127	1	127		
125	2	125		
		125		
107	1	107		
87	1	87		
69	1	69		
74	1	74		
98	1	98		
87	1	87		
127	2	127		
		127		
99	1	99		
105	1	105		
58	1	58		
88	1	88		
46	2	46		
		46		
27	1	27		
41	3	41		
		41		
		41		
55	1	55		
77	1	77		
33	1	33		

44	1	44		
72	1	72		
88	1	88		
73	1	73		
30	1	30		
138	1	138		
	Average(°)	**101**		
	Median(°)	**98**		
	Count	**92**		
	StDev(°)	**40**		

EB-88A

Bearing(°)	# of clasts	Bearing per clast(°)	Direction-corrected bearing per clast(°)	Notes
				About 1% Kneeling Nun Tuff.
33	2	33		Outcrop face trends 110 NE; moderate
		33		clast imbricaiton. Paleoflow is mostly
94	1	94		towards me.
103	1	103		
96	1	96		
83	1	83		
72	1	72		
66	2	66		
		66		
109	2	109		
		109		
102	2	102		
		102		
75	1	75		
102	1	102		
102	2	102		
		102		
96	1	96		
82	1	82		
95	1	95		
95	3	95		
		95		
		95		
110	1	110		
85	2	85		
		85		
91	1	91		
88	1	88		
64	1	64		
75	1	75		
47	1	47		
49	1	49		
165	1	165		
197	1	197		
75	2	75		
		75		
52	1	52		
58	1	58		
50	1	52		

54	1	54		
72	1	72		
69	1	69		
143	1	143		
62	1	62		
88	1	88		
90	1	90		
83	2	83		
		83		
62	2	62		
		62		
180	1	180		
	Average(°)	**87**		
	Median(°)	**85**		
	Count	**51**		
	StDev(°)	**32**		

EB-90B

Bearing(°)	# of clasts	Bearing per clast(°)	Direction-corrected bearing per clast(°)	Notes
				Lower part of Qppw. Multiple-orienated
110	1	110		of gravel face. Face overall goes N-S.
135	1	135		Decently exposed.
116	1	116		
131	1	131		
112	1	112		
123	1	123		
146	1	146		
157	1	157		
170	1	170		
166	1	166		
183	1	183		
181	1	181		
144	1	144		
110	1	110		
160	1	160		
152	1	152		
164	1	164		
164	1	164		
157	1	157		
193	1	193		
182	1	182		
122	1	122		
139	1	139		
124	1	124		
7	2			Not used because it is clearly not consistent
				with the other measurements.
205	1	205		
196	1	196		
160	2	160		
		160		
171	1	171		
163	1	163		
131	1	131		
110	1	110		
143	2	143		
		143		
159	2	159		
		159		
144	2	144		

		144		
107	2	107		
		107		
145	2	145		
		145		
147	1	147		
151	1	151		
119	2	119		
		119		
	Average(°)	**147**		
	Median(°)	**146**		
	Count	**46**		
	StDev(°)	**25**		

EB-93

Bearing(°)	# of clasts	Bearing per clast(°)	Direction-corrected bearing per clast(°)	Notes
120	1	120		Measurement site is about 1/4 way up from bottor
139	1	139		
87	1	87		
196	1	196		
192	1	192		
122	1	122		
100	1	100		
142	2	142		
		142		
128	1	128		
121	1	121		
88	1	88		
130	1	130		
155	1	155		
138	1	138		
164	1	164		
183	1	183		
178	1	178		
190	2	190		
		190		
205	1	205		
138	1	138		
170	1	170		
161	1	161		
134	2	134		
		134		
187	1	187		
152	2	152		
		152		
237	1	237		
149	3	149		
		149		
		149		
189	1	189		
153	2	153		
		153		
270				
150	1	150		
170	2	170		
		170		

165	1	165		
172	1	172		
165	2	165		
		165		
133	1	133		
160	2	160		
		160		
	Average(°)	**155**		
	Median(°)	**153**		
	Count	**46**		
	Stand. Deviation	**29**		

EB-94b

Bearing(°)	# of clasts	Bearing per clast(°)	Direction-corrected bearing per clast(°)	Notes
				Clasts stick out of outcrop face. The face
100	2	100		trends about 120 degrees.
		100		
120	1	120		
123	1	123		
113	1	113		
111	2	111		
		111		
154	1	154		
130	1	130		
103	1	103		
110	1	110		
110	1	110		
84	1	84		
85	1	85		
82	1	82		
104	1	104		
79	1	79		
88	2	88		
		88		
	Average(°)	**105**		
	Median(°)	**104**		
	Count	**19**		
	StDev(°)	**18**		

EB-96d

Bearing(°)	# of clasts	Bearing per clast(°)	Direction-corrected bearing per clast(°)	Notes
				High-qulaity measurment from middle of
132	1	132		of felsic-rich interval.
130	1	130		
132	1	132		Plus or minus 20 degree error
124	1	124		Measured the lowest gravel.
168	1	168		
138	1	138		
113	1	113		
178	2	178		
		178		
179	1	179		
135	1	135		
177	1	177		
106	2	106		
		106		
132	1	132		
132	1	132		
133	1	133		
133	1	133		
140	1	140		
163	2	163		
		163		
150	1	150		
141	2	141		
		141		
153	1	153		
161	2	161		
		161		
149	1	149		
193	2	193		
		193		
137	1	137		
176	1	176		
140	1	140		
145	1	145		
136	2	136		
		136		
73	1	73		
107	1	107		
123	1	123		

167	1	167		
169	1	169		
137	1	137		
125	1	125		
128	1	128		
156	2	156		
		156		
172	2	172		
		172		
161	2	161		
		161		
136		136		
174	3	17		
		174		
		174		
153	1	153		
138	1	138		
113	1	113		
158	1	158		
135	1	135		
148	1	148		
135	1	135		
	Average(°)	**144**		
	Median(°)	**141**		
	Count	**61**		
	StDev(°)	**28**		

EB-101B

Bearing(°)	# of clasts	Bearing per clast(°)	Direction-corrected bearing per clast(°)	Notes
				3D view of outcrop and outcrop face trends
				130 degrees.
108	1	108		Error per clast is plus or minus 20 degrees
125	1	125		QNpf unit.
121	1	121		
84	1	84		
117	1	117		
126	1	126		
144	1	144		
145	1	145		
130	1	130		
135	2	135		
		135		
106	1	106		
115	1	115		
140	1	140		
125	1	125		
121	2	121		
		121		
127	1	127		
126	1	126		
113	1	113		
110	1	110		
125	1	125		
121	1	121		
136	3	136		
		136		
		136		
120	1	120		
188	1	188		
231	1	231		
144	1	144		
141	1	141		
140	1	140		
	Average(°)	**131**		
	Median(°)	**126**		
	Count	**32**		
	StDev(°)	**25**		

EB-109

Bearing(°)	# of clasts	Bearing per clast(°)	Direction-corrected bearing per clast(°)	Notes
				One Alamosa Creek marker clast
221	3	221		Nicely exposed; dominated by intermediate
		221		clasts even though at bottom of Qppw.
		221		Measuring top ~1 m of gravel.
183	3	183		
		183		
		183		
162	1	162		
100	1	100		
157	1	157		
129	1	129		
116	3	116		
		116		
		116		
250	3	250		
		250		
		250		
285	1	285		
154	2	154		
		154		
187	2	187		
		187		
161	1	161		
219	2	219		
		219		
198	2	198		
		198		
187	1	187		
201	2	201		
		201		
212	1	212		
184	1	184		
220	2	220		
		220		
97	1	97		
108	1	108		
239	2	239		
		239		
206	1	206		
162	1	162		

194	1	194		
185	2	185		
		185		
269	2	269		
		269		
203	1	203		
202	1	202		
193	1	193		
231	1	231		
291	1	291		
172	1	172		
125	1	125		
125	1	125		
178	1	178		
142	1	142		
155	1	155		
238	1	238		
250	1	250		
210	1	210		
230	1	230		
173	1	173		
169	1	169		
135	1	135		
207	1	207		
215	1	215		
228	2	228		
		228		
222	1	222		
232	2	232		
		232		
230	1	230		
	Average(°)	**194**		
	Median(°)	**200**		
	Count	**70**		
	StDev(°)	**45**		

EB-121

Bearing(°)	# of clasts	Bearing per clast(°)	Direction-corrected bearing per clast(°)	Notes
181	1	181		Individual clast measurements
181	1	181		that have +/- 20 degree error per measurement.
169	1	169		Relatively coarse cobble bed
260	1	260		
234	1	234		
219	1	219		
228	1	228		
233	1	233		
220	1	220		
254	1	254		
210	1	210		
225	1	225		
250	1	250		
212	1	212		
208	1	208		
247	1	247		
207	1	207		
207	1	207		
237	1	237		Moved 2 m to east.
165	1	165		
152	1	152		
190	2	190		
		190		
174	1	174		
174	1	174		
140	1	140		
183	1	183		
145	1	145		
260	1	260		
280	1	280		
280	1	280		
278	1	278		
	Average(°)	**212**		
	Median(°)	**211**		
	Count	**32**		
	StDev(°)	**39**		

EB-123A

Bearing(°)	# of clasts	Bearing per clast(°)	Direction-corrected bearing per clast(°)	Notes
29	1	389		From Nppe conglomerate bed.
39	1	399		
20	1	380		
5	1	365		
10	1	370		
0	1	360		
32	1	392		
312	1	312		
248	2	248		
		248		
276	1	276		
312	2	312		
		312		
298	1	298		
32	1	392		
41	1	401		
61	1	421		
276	1	276		
300	1	300		
299	2	299		
		299		
269	1	269		
238	1	238		
276	1	276		
294	1	294		
16	1	376		
104	1	104		
260	1	260		
282	1	282		
322	1	322		
309	1	309		
317	1	317		
334	1	334		
302	1	302		
311	1	311		
296	1	296		
291	1	291		
310	1	310		
290	1	290		
287	1	287		

243	1	243		
246	1	246		
297	1	297		
307	1	307		
306	1	306		
287	1	287		
309	2	309		
		309		
297	3	297		
		297		
		297		
	Average(°)	**308**		
	Median(°)	**300**		
	Count	**51**		
	StDev(°)	**53**		

EB-134A

Bearing(°)	# of clasts	Bearing per clast(°)	Direction-corrected bearing per clast(°)	Notes
288	1	288		
268	1	268		
242	1	242		
228	2	228		
		228		
235	2	235		
		235		
240	1	240		
241	1	241		
242	1	242		
89	1	89		
81	1	81		
78	1	78		
268	1	268		
98	1	98		
95	1	95		
96	1	96		
98	1	98		
265	2	265		
		265		
191	1	191		
204	1	204		
278	1	278		
281	2	281		
		281		
180	2	180		
		180		
166	1	166		
170	1	170		
155	1	155		
125	1	125		
136	1	136		
96	2	96		
		96		
240	1	240		
247	1	247		
158	1	158		
152	1	152		
253	1	253		
243	1	243		

233	1	233		
235	1	235		
260	1	260		
158	3		158	
			158	
			158	
138	1		138	
150	2		150	
			150	
171	1		171	
156	1		156	
167	1		167	
168	3		168	
			168	
			168	
146	3		146	
			146	
			146	
163	1		163	
180	1		180	
163	1		163	
164	2		164	
			164	
152	1		152	
143	1		143	
205	1		205	
220	1		220	
228	1		228	
203	2		203	
			203	
203	1		203	
219	1		219	
232	1		232	
235	1		235	
180	1		180	
210	1		210	
242	1		242	
226	1		226	
225	1		225	
219	1		219	
221	3		221	
			221	
			221	
232	2		232	
			232	
211	1		211	
210	2		210	

			210	
216	2		216	
			216	
219	1		219	
203	1		203	
250	1		250	
246	1		246	
225	1		225	
219	1		219	
221	3		221	
			221	
			221	
232	2		232	
			232	
211	1		211	
210	2		210	
			210	
216	2		216	
			216	
219	1		219	
203	1		203	
250	1		250	
246	1		246	
	Average(°)	**196**	**200**	
	Median(°)	**228**	**210**	
	Count	**43**	**67**	
	StDev(°)	**67**	**32**	

EB-135

Bearing(°)	# of clasts	Bearing per clast(°)	Direction-corrected bearing per clast(°)	Notes
273	1	273	273	
217	1	217	217	
273	1	273	273	
78	1	78	78	
80	1	80	80	
35	1	35	35	
35	1	35	35	
349	1	-11	-11	
328	1	-32	-32	
16	1	16	16	
118	2	118	118	
		118	118	
134	1	134	134	
39	1	39	39	
50	1	50	50	
68	1	68	68	
0	1	0	0	
65	1	65	65	
123	1	123	123	
26	1	26	26	
23	1	23	23	
352	1	-8	-8	
2	1	5	5	
19	1	19	19	
306	4	-54	-54	
		-54	-54	
		-54	-54	
		-54	-54	
345	2	-15	-15	
		-15	-15	
350	1	-10	-10	
69	1	69	69	
51	1	51	51	
70	1	70	70	
62	1	62	62	
12	2	12	12	
		12	12	
9	1	9	9	
354	1	-6	-6	
38	1	38	38	

Average(°)	**45**
Median(°)	**31**
Count	**40**
StDev(°)	**77**

EB-140B

Bearing(°)	# of clasts	Bearing per clast(°)	Direction-corrected bearing per clast(°)	Notes
				30 cm- thick channel fill
196	1	196		
188	1	188		
235	1	235		
145	1	145		
186	1	186		
194	1	194		
207	1	207		
185	1	185		
232	1	232		
198	1	198		
232	1	232		
240	1	240		
219	1	219		
212	1	212		
195	1	195		
168	1	168		
157	1	157		
144	1	144		
145	1	145		
170	3	170		
		170		
		170		
156	1	156		
182	1	182		
169	1	169		
217	1	217		
186	1	186		
205	2	205		
		205		
	Average(°)	**190**		
	Median(°)	**188**		
	Count	**29**		
	StDev(°)	**27**		

EB-140c

Bearing(°)	# of clasts	Bearing per clast(°)	Direction-corrected bearing per clast(°)	Notes
83	1	83		6 m to the east and
102	1	102		in the same channel fill as at EB-140b.
107	1	107		
124	1	124		
111	1	111		
184	1	184		
99	1	99		
109	1	109		
106	1	106		
148	1	148		
156	1	156		
146	1	146		
146	1	146		
124	2	124		
		124		
102	1	102		
118	1	118		
119	1	119		
149	2	149		
		149		
141	1	141		
140	1	140		
144	2	144		
		144		
130	1	130		
158	1	158		
117	1	117		
156	1	156		
173	1	173		
164	1	164		
155	1	155		
161	1	161		
136	1	136		
190	1	190		
164	2	164		
		164		
166	1	166		
171	1	171		
161	1	161		
	Average(°)	**140**		

Median(°)	**144**
Count	**39**
StDev(°)	**25**

EB-142

Bearing(°)	# of clasts	Bearing per clast(°)	Direction-corrected bearing per clast(°)	Notes
				E- W face with same indentations; medial
35	1	35		20 feet thick gravel tongue; gravel are mostly
41	2	41		felsic volcanic, no Alamosa marker clast.
		41		
53	2	53		
		53		2 plagioclase-phyric clasts with plag xtals
44	3	44		about ~1 cm long.
		44		
		44		
54	1	54		
54	1	54		
53	1	53		
53	1	53		
48	2	48		
		48		
28	2	28		
		28		
21	3	21		
		21		
		21		
28	1	28		
69	1	69		
70	2	70		
		70		
29	1	29		
49	1	49		
0	1	0		
58	1	58		
62	1	62		
32	1	32		
90	1	90		
52	1	52		
120	1	120		
76	1	76		
79	1	79		
98	1	98		
117	1	117		
15	1	15		
95	1	95		
98	1	98		

90	1	90		
71	1	71		
78	1	78		
74	2	74		
		74		
89	1	89		
64	1	64		
66	2	66		
		66		
37	2	37		
		37		
72	1	72		
58	1	58		
86	1	86		
53	1	53		
44	1	44		
89	1	89		
78	1	78		
38	2	38		
		38		
80	2	80		
		80		
90	1	90		
75	1	75		
25	1	25		
51	1	51		
82	2	82		
		82		
80	1	80		
71	2	71		
		71		
	Average(°)	**60**		
	Median](°)	**58**		
	Count	**70**		
	StDev(°)	**25**		

EB-143

Bearing(°)	# of clasts	Bearing per clast(°)	Direction-corrected bearing per clast(°)	Notes
				Unit Qppuc; trace Alamosa Creek porphyry
108	1	108		
113	1	113		
110	1	110		
91	1	91		
92	1	92		
103	3	103		
		103		
		103		
125	1	125		
170	2	170		
		170		
189	1	189		
73	2	73		
		73		
92	2	92		
		92		
112		112		
93	2	93		
		93		
103	1	103		
129	1	129		
190	1	190		
165	1	165		
165	1	165		
170	1	170		
152	1	152		
158	2	158		
		158		
150	2	150		
		150		
139	1	139		
135	1	135		
97	1	97		
192	1	192		
117	1	117		
110	1	110		
118	1	118		
115	2	115		
		115		

130	3	130		
		130		
		130		
119	1	119		
109	1	109		
112	1	112		
84	1	84		
130	1	130		
126	2	126		
		126		
114	2	114		
		114		
150	1	150		
	Average(°)	**125**		
	Median(°)	**118**		
	Count	**52**		
	StDev(°)	**30**		

EB-163

Bearing(°)	# of clasts	Bearing per clast(°)	Bearing per clast(°)	Notes
				Errors on each class is plus or minus 20
222	1	222		degrees. Measurements taken from middle
217	1	217		of Qtc3, working downwards.
141	1	141		
208	2	208		
		208		
193	1	193		
198	1	198		
191	2	191		
		191		
203	1	203		
197	1	197		
151	2	151		
		151		
115	1	115		
143	2	143		
		143		
154	2	154		
		154		
133	1	133		
175	2	175		
		175		
152	1	152		
146	1	146		
157	1	157		
180	1	180		
172	1	172		
234	1	234		
172	1	172		
186	1	186		
152	1	152		
141	2	141		
		141		
113	2	113		
		113		
146	2	146		
		146		
139	1	139		
148	1	148		
172	1	172		
181	2	181		
		181		

				Basal meter of deposit.
110	1		110	
110	1		110	
122	2		122	
			122	
106	1		106	
111	3		111	
			111	
			111	
225	1		225	
154	2		154	
			154	
163	4		163	
			163	
			163	
			163	
165	1		165	
128	1		128	
	Average(°)	**167**	**140**	
	Median(°)	**157**	**128**	
	Count	**41**	**17**	
	StDev(°)	**30**	**31**	

EB-171C

Bearing(°)	# of clasts	Bearing per clast(°)	Direction-corrected bearing per clast(°)	Notes
222	2	222	upper Nppe unit	
		222	lower part only part that is exposed well	
208	1	208		
237	2	237		
		237		
227	2	237		
		237		
223	1	223		
218	1	218		
244	1	244		
218	1	218		
237	2	237		
		237		
60	1	60		
20	1	20		
8	1	8		
214	1	214		
177	1	177		
198	1	198		
249	1	249		
205	1	205		
194	1	194		
207	2	207		
		207		
	Average(°)	**197**		
	Median(°)	**218**		
	Count	**24**		
	StDev(°)	**66**		

EB-171B

Bearing(°)	# of clasts	Bearing per clast(°)	Direction-corrected bearing per clast(°)	Notes
262	4	262		Middle of Nppe exposure. It has fine-grained
		262		sediment w/ pebble beds (30 cm thick).
		262		
		262		
264	4	264		
		264		
		264		
		264		
206	1	206		
213	1	213		
218	1	218		
219	1	219		
221	1	221		
207	1	207		
198	1	198		
202	1	202		
202	1	202		
243	1	243		
232	1	232		
228	1	228		
230	2	230		
		230		
228	1	228		
252	1	252		
260	1	260		
275	1	275		
241	1	241		
283	2	283		
		283		
268	1	268		
	Average(°)	**241**		
	Median(°)	**242**		
	Count	**30**		
	StDev(°)	**26**		

EB-171A

Bearing(°)	# of clasts	Bearing per clast(°)	Direction-corrected bearing per clast(°)	Notes
2	1	2	lowest exposure in quarry	
25	1	25	good clast imbercation, but not as consistent as middle unit	
347	2	347		
		347		
40	1	40		
44	1	44		
300	2	300		
		300		
167	1	167		
328	2	328		
		328		
265	2	265		
		265		
293	3	293		
		293		
		293		
291	1	291		
295	2	295		
		295		
235	2	235		
		235		
295	2	295		
		295		
323	2	323		
		323		
282	1	282		
295	1	295		
277	1	277		
293	3	293		2 m from base, this is 1 m higher than prior
		293		measurements.
		293		
277	1	277		
276	4	276		
		276		
		276		
		276		
277	1	277		
296	1	296		
258	1	258		
222	1	222		

237	1	237		
71	1		outcast	
283	1	283		
300	3	300		
		300		
		300		
279	1	279		
		279		
278	2	278		
		278		
273	2	273		
		273		
268	1	268		
267	1	267		
276	3	276		
		276		
		276		
305	1	305		
292	1	292		In general, clasts are more angular.
262	1	262		I estimate 15 degree error instead of 20 degree
246	1	246		
225	1	225		
230	2	230		On very bottom of interval.
		230		
192	1	192		
203	1	203		
	Average(°)	**262**		
	Median(°)	**277**		
	Count	**65**		
	StDev(°)	**68**		

EB-175

Bearing(°)	# of clasts	Bearing per clast(°)	Direction-corrected bearing per clast(°)	Notes
276	2	276		From unit Nppe
		276		Error for each clast is about 20 degrees
299	1	299		Outcrop trends 90 degrees. Measured imbrication
294	2	294		about 5 ft up from the base.
		294		
294	1	294		
286	1	286		
282	3	282		
		282		
		282		
274	3	274		
		274		
		274		
288	3	288		
		288		
		288		
288	2	288		
		288		
274	1	274		
306	1	306		
297	2	297		
		297		
293	2	293		
		293		
294	1	294		
290	2	290		
		290		
283	1	283		
277	1	277		
282	2	282		
		282		
122	2	122		
		122		
270	2	270		
		270		
268	1	268		
264	1	264		
264	1	264		
270	1	270		
268	1	268		

301	4	301		
		301		
		301		
		301		
329	1	329		
314	1	314		
282	1	282		
293	1	293		
295	1	295		
274	2	274		
		274		
304	1	304		
321	1	321		
302	2	302		
		302		
308	1	308		
299	1	299		
309	1	309		
299	3	299		
		299		
		299		
264	1	264		
298	2	298		
		298		
312	1	312		
298	3	298		
		298		
		298		
288	1	288		
282	1	282		
273	1	273		
265	2	265		
		265		
	Average(°)	**284**		
	Median(°)	**288**		
	Count	**73**		
	StDev(°)	**31**		

EB-182

Bearing(°)	# of clasts	Bearing per clast(°)	Direction-corrected bearing per clast(°)	Notes
302	1	302		Unit Nppe with good 3D perspective.
311	2	311		Measured lower 1-3 ft of exposure.
		311		Outcrop face trends about 300 degrees.
311	2	311		
		311		
307	2	307		
		307		
300	2	300		
		300		
297	1	297		
291	3	291		
		291		
		291		
253	1	253		
313	1	313		
307	1	307		
319	1	319		
272	2	272		
		272		
308	1	308		
303	1	303		
281	2	281		
		281		
297	1	297		
250	1	250		
251	1	251		
235	1	235		
258	1	258		
325	1	325		
291	1	291		
274	1	274		
233	1	233		
280	1	280		
328	1	328		
281	1	281		
273	1	273		
	Average(°)	**289**		
	Median(°)	**294**		
	Count	**36**		
	StDev(°)	**24**		

Table 1. Cuttings summary for the Getty No. 2 West Elephant Butte Federal

Map unit	Depth (cuttings ft)	Depth (wireline logs)	Description
	30 ft sample intervals	**0-350 ft 0-107 m**	Palomas Fm: Middle axial-fluvial facies: Elevation at suface: 4577 ft (1395 m).
QNpa	0-190		MEDIUM-COARSE SAND: 5YR 8/1, mU-cU (minor vcL-vcU) sand that is subrounded-subangular. Composition of: 35-45% quartz, 25-35% volcanic lithic grains, 15% orange Kspar, 5% granitic fragments, 1-10% chert, and trace biotite.
QNpa	220-280		COARSE SAND: mU-vcU sand and vf pebbles. Abundant cementation by calcium carbonate. The mU-cU sand is AA. Very corse sand and vf pebbles are volcanic in composition with 7-10% orange granite fragments.
QNpa	280-370 [280-310. 310-340, 340-370]		COARSE SAND: 5-7.5YR 8/1; slightly less red at top. Sand is mU-vcU and subangular-subrounded. Less granite fragments than at 0-190 ft. There are indications of local calcium carbonate cementation. Sand is composed of 50% quartz, 35-50% volcanic detritus, 10-15% orange Kspar, 5% chert, 1-3% granitic fragments.
		350-511 (107-156 m)	**Palomas Fm: Lower axial-fluvial facies (top at 1288 m elev)**
Npal2	370-460	350-	PEBBLY SAND: 5-7.5YR 8/1. Sand is cL-vcU (minor mU) and has 15-50% vf-f pebbles. Broken pebbles are up to 12 mm long and composed of felsic volcanic rocks. Pebble size and abundance increase down-section. Very coarse sand and pebbles are subangular-subrounded and composed of felsic volcanic rocks. The cU sand is composed of quartz, 33-45% volcanic grains, 5-20% orange-creamy feldspar (probably Kspar), 3-5% granite, and 1% chert. @400-430 ft: There are 0-10% orange granite. @425 ft: Shift in gamma ray curve.
Npal2	460-470		PEBBLY SAND: As above, but trace clear-green, quartz-rich sandstone clasts. Abundant calcium carbonate cementaton. 1-3% of very coarse sand is granitic.
Npal2	470-480		Red clay noted.
Npal2	480-490		PEBBLY SAND: As above, but trace clear-green, quartz-rich sandstone clasts. Abundant calcium carbonate cementaton. 1-3% of very coarse sand is granitic.
Npal2	490-520	-511	COARSE SAND: mU-cU (mnor vcL-vcU), 7.5YR 6-8/1, subangular-subrounded. Sand composed of subequal quartz and felsic volcanic grains with 10-25% clear-greenish, likely Mesozoic sandstone and 10% feldspar.

		511-616 (156 to 188 m)	**Transitional basal zone of Palomas – Rincon Valley formations (top at 1239 m)**
Npal1	520-550	511-	COARSE SAND WITH PEBBLES: 5YR 7/1-6/2, mU-vcU (mostly cL-vcU) with 10-15% vf-f, subrounded-broken pebbles composed of felsic volcanic rocks. Sand is subrounded-subangular and composed of fine-grained felsic volcanics, 1-5% Mesozoic sandstone, and 1-3% quartz. Much clay-cemented "balls" of fU-mU, quartz-rich sand [80-90% quartz sand vs 10-20% felsic volcanics. Interpretation: Arrival of Rio Grande during a time of coarse-grained detrital-shedding of San Mateo Mtns.
Npal1	550-580	-616	CLAYEY FINE-MEDIUM, QUARTZ-RICH SAND: 2.5-5YR 7/4 clay with 60-70% fU-mU, quart-rich sand and subordinate (~40%) felsic sand). 10% c-vc sand composed of felsic volcanic rocks and quartzite(?). Interpretation: Deltaic tongues of Rio Grande interbedded with playa-lake clays.
		616-1330 (188-405 m)	**RINCON VALLEY FORMATION: ALLUVIAL, BASIN FLOOR-PLAYA FACIES. OVERALL CLAYEY AND HIGH GAMMA RAY READINGS. (top at 1207 m elev)**
Nrp	580-610	616-	SANDY CLAY: 5YR 7/2; 20% fU-mU, quartz- and felsic-volcanic sand grains (slightly more quartz than volcanics). 5% vf-f pebbles composed of hard quartz-sandstone or possibly quartzite? Sand and pebbles are likely slough.
Nrp	610-640		SANDY CLAY: 5YR 7/2; 15% fU-mU, quartz- and felsic-volcanic sand grains. Clay alone is 5YR 6-7/4. Likely high component of slough.
Nrp	640-670		SANDY CLAY: 5YR 6-7/4; 15-20% fL-mU, quartz- and felsic-volcanic sand grains [subequal quartz and volcanic grains]. Probably sloughing.
Nrp	670-760		5YR 7/2-3 clay with up to subequal fL-mU sand coated by clay (not certain, but it seems like volcanic grains > quartz grains].
Nrp	760-1330	-1330	RED CLAY. Interpreted playa-lake environment.
Nrpbf		**1330-1680 ft (405-512 m)**	**RINCON VALLEY FORMATION: BASIN FLOOR AND DISTAL PIEDMONT). Top at 990 m elev).**
Nrpbf		1330-	Note: In driller logs, there is abundant quartz and feldspar grains mixed with clays down to 550 ft, but only trace sand (and mostly red clay) below 550 ft.
			USED EXCLUSIVELY DRILLER LOG BELOW HERE.
Nrpbf	1330-1610		CLAYEY FINE SAND: Clayey very fine- to fine-grained sand. Sand mostly composed of rounded quartz grains (from Cretaceous?).
Nrpbf	1610-1680	-1680	SANDSTONE: Sand is clear-white, very fine-grained, subrounded-rounded, well sorted.

			CRETACEOUS (top at 883 m elev)
		1680-1762	GALLUP SANDSTONE
		1762-1939	D-CROSS TONGUE OF MANCOS SHALE
		1939-2110	CARTHAGE AND FITE RANCH MBRS OF TRES HERMANSO FORMATION: Coal-rich near base.
		2110-2158	ATARQUE MEMBER OF TRES HERMANOS FORMATION: Very fine-grained, quartz sand.
		2158-2540	MANCOS SHALE: Gray shale.
		2540-2700	DAKOTA SANDSTONE: Coarse, multi-colored sand grains present.
			PERMIAN
		2700-3310	SAN ANDRES FM: Limestone-dominated
		3310-3350	GLORIETA SANDSTONE: Very fine- fine-grained sand.
		3350-4210	YESO FM: @3380 ft: Orange sandstone underlain by dolomite. LOCAL SILLS PRESENT.
		4210-5030	ABO FORMATION: Reddish mudstones and fineg-rained sandstones.
		5030-5175	BURSUM FM: Top placed at highest prominent limestone bed.
			PENNSYLVANIAN
		5175? -6728	BAR B, GREY MESA, AND RED HOUSE FORMATIONS: Top contact pick is questionable.
			ORDOVICIAN
		6728-7457	ORDIVICIAN STRATA: Very low gamma and very high resistivity – carbonate-dominated.
			PROTEROZOIC
		7457-XX	Top of Proterozoic rocks.

Table 2. Rattlesnake Island Ar-Ar data

Sample ID	UTM location (NAD 83, Easting (m)	Northing (m)	Age (Ma) (preferred method indicated)	MSWD	Steps	Stratigraphic position	Description
EB-20	296001	3674796	**2.468 ± 0.014 (plateau)**	1.46	7	Dike in maar breccia, south side of maar.	Black, fine-grained blasalt with trace olivine phenos up to 1.5 mm long; relatively unaltered. One possible quartz pebble xenolith (elongated).
EB-23	295933	3674922	**2.447 ± 0.057 Ma (Inverse Isochron)**	1.08	7	2 m-wide, NW-trending dike apparently intruding maar breccia, NW side of maar.	Black, fine-grained basalt with trace olivine phenos up to 2 mm long; relatively unaltered.

Note: Ages are from groundmass concentrate; errort report at 2-sigma uncertainty; MSWD - Mean Square Weighted Deviation